5-9-2015

Analysis of Settlement-Induced Bending Moments in Battered Piles within a Levee Embankment

Jehu Brick Johnson

Analysis of settlement-induced bending moments in battered piles within a levee embankment

By

Jehu B. Johnson

A Thesis
Submitted to the Faculty of
Mississippi State University
in Partial Fulfillment of the Requirements
for the Degree of Master of Science
in Civil Engineering
in the Department of Civil and Environmental Engineering

Mississippi State, Mississippi

May 2015

Analysis of settlement-induced bending moments in battered piles within a levee embankment

By

Jehu B. Johnson

Approved:

_____

Farshid Vahedifard
(Major Professor)

_____

Philip M. Gullett
(Committee Member)

_____

Richard J. Varuso
(Committee Member)

_____

James L. Martin
(Graduate Coordinator)

_____

Jason M. Keith
Interim Dean
Bagley College of Engineering

Name: Jehu B. Johnson

Date of Degree: May 8, 2015

Institution: Mississippi State University

Major Field: Civil Engineering

Major Professor: Farshid Vahedifard

Title of Study: Analysis of settlement-induced bending moments in battered piles within a levee embankment

Pages in Study: 125

Candidate for Degree of Master of Science

Settlement-Induced Bending Moments (SIBM) are an important design condition that must be considered whenever battered piles are placed in settling soils. The objective of this research was to investigate various parameters which can affect SIBM in battered piles within a levee embankment. The results from the current study were compared and verified against those obtained from centrifuge testing and alternative numerical simulations. A series of centrifuge testing as well as finite difference numerical simulations in Fast Langrangian Analysis of Continua (FLAC) were conducted. Different parameters which may affect the bending moments were investigated including pile connection fixity, batter, and stiffness of the pile as well as the magnitude of settlement. The simulations show that these parameters can have large impacts on the magnitude and location of the bending moments. Findings of this research can be used to validate or identify the need for adjustment of the current modeling/design approach.

DEDICATION

I dedicate this thesis to my beautiful wife Justina, who has always been a great source of encouragement and help.

ACKNOWLEDGEMENTS

There are many people who greatly contributed to this research and who deserve enormous amounts of credit. This research was a collaborative effort and could not have been done on my own.

I want to thank Richard Varuso, Ph.D., P.E. for giving me this assignment and helping guide the research from the beginning. Dr. Varuso has always been a great friend and inspiration and I am very thankful for all the knowledge he has given me over the years.

I want to thank the staff of RPI who worked on this project, specifically Tarek Abdoun, PhD, P.E., Panagiota "Yota" Kokkali, and Anthony Tessari, Ph.D. They put in a great effort to make the centrifuge tests a success and their expertise was greatly appreciated in all aspects of this work.

I want to thank Professor George Filz, PhD, P.E., and Alex Reeb from Virginia Tech for their invaluable help. Alex taught me most of what I know about FLAC and without his patient effort I would not have been able to do this research.

I want to thank Professor Farshid Vahedifard, PhD, P.E. for his extreme patience with me and his direction and advice. He helped direct this thesis into the finished product that it is.

I want to thank Mark Woodward, P.E., for encouraging me to get my Master's degree and for being an excellent supervisor over the years. I also want to thank Richard

Pinner, P.E., for always asking me questions that help me expand my horizon and think about issues in a new way.

Finally, I want to thank all my friends and family who encouraged me throughout the process and who helped me when they could, especially Daniel Polk and Charles Johnson.

If I missed someone, I apologize. The list of people who have helped me on this journey is too long to be able to remember all the time.

TABLE OF CONTENTS

LIST OF TABLES

LIST OF FIGURES

CHAPTER I

INTRODUCTION AND SCOPE

1.1 Introduction and Background

After Hurricane Katrina, the United States Army Corps of Engineers (USACE) New Orleans District (MVN) has extensively used concrete T-walls with battered piles in the new Hurricane Storm Damage and Risk Reduction System (HSDRRS). There are significant cost savings using battered piles versus vertical piles in the south Louisiana area due to the lack of lateral resistance with vertical piles. However, if the battered piles are placed in highly compressive soils with increased overburden then bending moments caused by downdrag on the piles may develop and can overstress the piles, especially in conjunction with loading events. MVN has utilized a method developed by the USACE St. Paul District and Virginia Polytechnic Institute with p-y springs to estimate these bending moments by means of the LPILE program (referred to hereafter as the USACE Limit Equilibrium (LE) method). However, the development of the USACE LE method was based mainly on numerical models, and the resulting bending moment has uncertainty when the procedure is applied to project conditions that deviate substantially from the conditions used to calibrate the USACE LE method. In addition, the location of the maximum bending moment is not well known. Depending on certain factors such as the estimated future consolidation, wall dimensions, pile batter, and pile/wall connection, this assumption would cause the piles to exceed the allowable design capacity. In order

to account for this assumption, modifications or remedial actions could be necessary and very costly. A refinement was deemed to be needed to more accurately capture the magnitude of the bending moment induced by the settling soils. Therefore, USACE St. Paul District contracted with a private engineering company to develop a Fast Langrangian Analysis of Continua (FLAC) finite difference numerical model to simulate the conditions of the specific reach and see if the bending moments exceeded allowable limits. However, there would be no real world validation of these analyses and it was thought that the model may give out moments that do not correspond with actual conditions.

To solve the issue of no physical verification, the MVN partnered with Rensselaer Polytechnic Institute (RPI) and Virginia Tech (VT) to develop a new design procedure that more accurately represents the field conditions. RPI has conducted centrifuge tests in the past for USACE to investigate the effects of flood loading on T-walls (Tessari 2012), and the findings and numerical modeling from these tests were incorporated into USACE T-wall design procedures (Varuso 2010). A testing program was jointly developed to perform centrifuge tests and then perform FLAC 2-D numerical models on the centrifuge tests. RPI performed a centrifuge test that generally modeled the conditions at a specific reach, namely a T-wall placed atop a levee embankment with a soft clay foundation. Personnel from MVN and Virginia Tech developed and evaluated numerical models for the centrifuge testing. MVN used the same design philosophy as the private engineering firm and Virginia Tech developed its own model and method. This was done to provide an additional level of verification.

1.2 Objectives

Settlement Induced Bending Moments (SIBM) are an important design condition that must be taken into consideration whenever battered piles are placed in settling soils. The objective of this research is to investigate various parameters which can affect SIBM in battered piles within a levee embankment. This will result in validation or need for adjustment of the numerical modeling philosophy and a comparison of different modeling techniques. There is also a need to see the differences between fixed and pinned connections at the base and how they affect the bending moments. This will have important impacts on how walls should be designed in the future.

1.3 Scope and Contributions

A series of numerical simulations was conducted using the MVN FLAC model and the effects of various parameters such as pile connection fixity, batter angle, and stiffness of the pile on SIBM are investigated. The results from the MVN FLAC model were compared against the results from the centrifuge testing, the Virginia Tech FLAC model and also against the USACE LE Method.

This thesis will focus on simulating only the centrifuge run that mimics the conditions at a specific reach which is a T-wall placed atop a levee embankment. Several other centrifuge runs were conducted for different configurations but the analysis of those runs is outside the scope of this thesis. The thesis will focus on the differences between the two modeling approaches compared to the centrifuge test results and some further interpretation using the two models with different conditions such the pile fixity connections at the base, stiffer pile elements, and different pile batters.

The thesis will give an overview of the centrifuge testing including the data from the modeled centrifuge run and how the centrifuge testing was developed, a discussion of the FLAC modeling performed, a parametric study investigating several important design considerations, and then a comparison of the current USACE LE Method with the FLAC modeling results.

Significant contributions to this thesis were made by RPI and Virginia Tech. RPI performed the centrifuge testing and reduced the raw data from the tests for use in the models. Virginia Tech created the additional FLAC model that is used in this thesis. They also contributed to the coding and knowledge base of the FLAC model used as the basis of this thesis.

Disclaimer: All opinions and positions expressed in this thesis are the author's and may not necessarily represent the USACE position.

CHAPTER II

CENTRIFUGE TESTING

2.1 Overview of Centrifuge Modeling

The use of centrifuges in geotechnical modeling and testing has grown exponentially in the past several decades. Significant advances in sensor technologies, event simulation capabilities, and sophistication of analysis software have allowed centrifuge testing to become an efficient and viable method for the investigation of geotechnical engineering problems. When coupled with a matched numerical analysis, the combination allows for simulation interpolation while maintaining that the results follow trends established through physical methods. Most of the information discussed in this chapter came from RPI personnel. Further discussion of the centrifuge tests will occur in a forthcoming dissertation from RPI.

The principles of centrifuge modeling have been discussed and thoroughly verified through numerous trials (Taylor, 1994; Garnier and Gaudin, 2007). The principal concept of operation is that the centrifuge creates a stress profile that is representative of field conditions. Reproducing real-world stress is essential because confining stress fundamentally influences soil behavior. The term model refers to the actual properties of the elements being tested on the centrifuge while prototype is used to describe what it represents at a given g-level.

Centrifuge modeling has a long and storied history beginning in the 19th century. In 1869, Edouard Phillips of France published a paper in which he recognized the significance of gravity-based scaling relationships that could be used to model similar stress conditions found in the field (Taylor, 1994). In the last thirty years, advances in sensor technologies, data acquisition, and digital control systems have made centrifuge modeling a viable option for comprehensive testing of multifaceted geotechnical problems. Today, centrifuge modeling has become an international research field with many machines found in facilities worldwide. Due to its size and technical capabilities, the geotechnical centrifuge at RPI is ideal for performing intricate parametric studies.

2.2 Geotechnical Centrifuge and Facility

The Geotechnical Centrifuge Research Facility at RPI was commissioned in 1989 and jointly financed by the Multidisciplinary Center for Earthquake Engineering Research (MCEER) at SUNY Buffalo, the National Science Foundation (NSF), the State of New York (NYS), and Rensselaer Polytechnic Institute (RPI). The current centrifuge at RPI, model 665-1, is comprised of the following: a) large 10.8 ft^2 area swinging basket; b) centrifuge booms; c) balance counterweights; d) hydraulic, water and air rotary joints; e) electrical and optical slip-rings; f) electric motor drive system; and g) in-flight imbalance readings and automatic control. The current performance specifications of the centrifuge are 150 g-tons at a nominal radius of 8.86 ft, a maximum payload of 1.5 tons, and a maximum g-level of 160g.

2.3 Data Acquisition

Data acquisition on the geotechnical centrifuge is accomplished through the combination of robust hardware and powerful software. The centrifuge had five distinct data acquisition systems: traditional sensors, high-speed camera, on-board cameras, tactile sensors, and bender elements. Each of the systems has a set of unique properties that require separate systems and software. However, all of them may be used in parallel for a single test (Tessari et al., 2010). The following sections detail the available systems, with more attention given to those applicable to the research contained within this thesis.

2.3.1 Traditional Data Acquisition System

The traditional data acquisition system (DAQ) is comprised of several components: the PCI eXtensions for Instrumentation (PXI) controller; one or more Signal Conditioning eXtensions for Instrumentation SCXIs; several sensor-specific conditioning cards and accessories; and custom LabVIEW-based software. The term traditional is used to identify sensors that measure a unit versus time. For example, an accelerometer measures acceleration as a function of time. Typical sensors that interface with the traditional DAQ include: accelerometers, pore-water pressure sensors, strain gages, linear variable differential transformers (LVDTs), and laser displacement transducers.

2.3.2 Advanced Data Acquisition

In addition to the aforementioned traditional instrumentation, there are several advanced sensors and technologies available for use in the RPI Centrifuge Facility. These include the high-speed camera, on-board cameras, and motion tracking system; tactile

pressure sensors; and bender elements. These have innate properties that prevent them from interfacing with the traditional DAQ system.

2.3.3 Video and Motion Tracking

The centrifuge is capable of handling up to eight on-board cameras and one overhead high-speed camera. The on-board cameras are 700 by 480 pixels in resolution and record at 24 frames per second. They are small and can be mounted using a variety of accessories to provide a desired view. The cameras are recorded using software that was originally developed for home security. The feeds are recorded in 15-minute segments, although this can be less if stopped manually. The segments can be stitched together during post-processing if necessary. The majority of the video recorded during experimentation utilizes the on-board camera system.

2.3.4 Bender Elements

Bender elements are piezoelectric transducers that are used to generate and measure mechanical waves in soil. They enable direct and in-situ measurements of compression wave and shear wave velocities. They have been adapted for use on the geotechnical centrifuge at RPI (Tessari, 2007). Specialized hardware and software allows researchers to rapidly collect, verify, and analyze data (Tessari et al., 2010).

2.4 In-flight Simulation and Testing

2.4.1 In-flight T-Bar Testing

T-Bar testing was used to determine the in-situ undrained shear strength for various cohesive soils in the centrifuge. It is an example of a full flow penetrometer test, which can utilize a bar, sphere, or plate. The centrifuge-based T-bar was developed at the

University of Western Australia (Stewart and Randolph, 1991). Numerical analyses regarding their mode of failure have been performed (Randolph and Andersen, 2006). Furthermore, the interpretation of data for clay similar to that present in the T-Wall project has been described and analyzed extensively (White et al., 2010).

The T-Bar penetrometer is preferential to the Cone Penetration Test (CPT) in soft cohesive soils. While the CPT also produces a continuous profile of the soil, it relies on empirically derived correction factors that are dependent on advanced knowledge of the soil loading history (Almeida and Parry, 1984). The T-bar, a type of full flow penetrometer, instead makes use of the plasticity solution for a cylinder moving laterally through a cohesive soil (Randolph and Houlsby, 1984). The analysis requires full closure of the soil as the bar penetrates. The presence of a gap in the soil will produce incorrect results. This cannot be avoided at shallow depths before the bar has fully penetrated the soil. However, correction factors for the shallow failure method have been developed for soft clays (White et al., 2010). The general equation for determining the shear strength based on the T-bar load cell reading is:

$$S_u = \frac{P}{N_{T-Bar} d} \tag{2.1}$$

where S_u is the undrained shear strength, P is the force per unit length acting on the cylinder, d is the diameter of the cylinder, and $N_{T\text{-}Bar}$ is the bar factor.

2.4.2 Method of Analysis

Equation 2.1 is the result of the plasticity solution acting on an infinitely long cylinder. The bar factor, $N_{T\text{-}Bar}$, is a function of the surface roughness. The upper and lower bounds for this factor are shown below. Researchers have performed many

analyses and found that 10.5 is a good approximation for T-Bars similar to the one in use at RPI (Randolph and Houlsby, 1984; Stewart and Randolph, 1991). The RPI T-bar is abraded on the surface of the cylinder in order to increase the roughness. The sides of the cylinder, however, are machined smooth in order to reduce friction during penetration.

During the course of operation, the T-bar will make contact with the soil, produce a shallow failure mechanism, a deep failure mechanism, and then reverse these during the pull out. Another benefit of using the T-bar over a CPT is that useful data can be collected while removing the probe from the soil. When the probe first hits the surface, it is important to note that this is not the zero depth point. The point of zero depth occurs when the center of the cylinder is parallel with the clay surface. The probe will encounter two different failure mechanisms: the shallow mechanism characterized by heave and the deep mechanism defined by clay flowing around the cylinder. This flow-round mechanism corresponds to approach embodied by the equation below. The transition between these two zones is apparent, as illustrated by Figure 2.1.

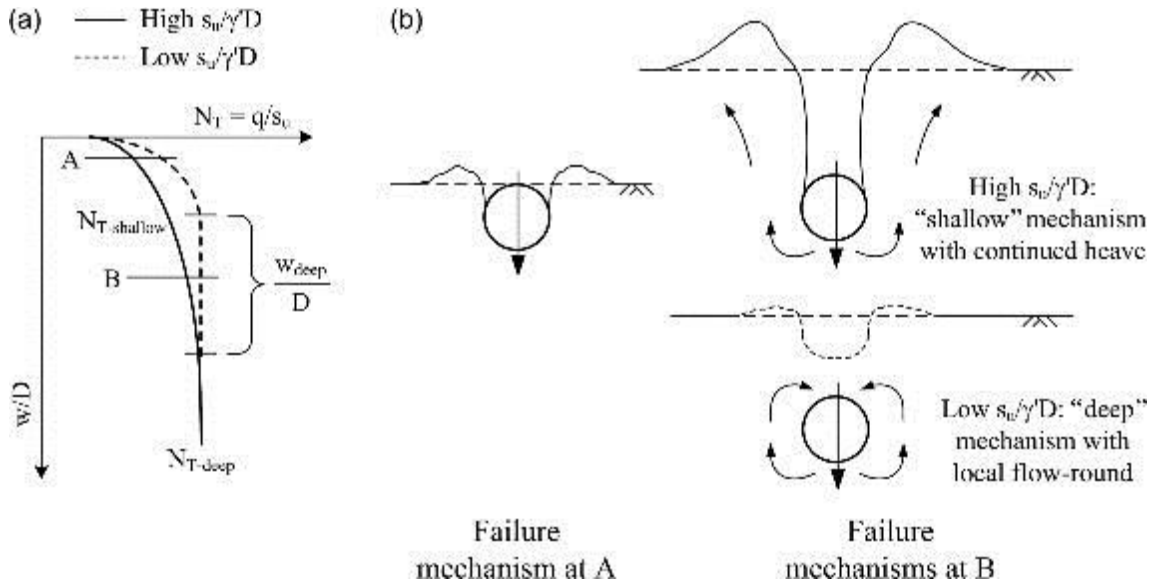

Figure 2.1 Behavior For T-Bar Penetration

Notes: Picture from White et al., 2010

White et al. (2010) provides a method for determining the depth at which this transition occurs. Assuming the shear strength from the pocket penetrometer is valid, we can derive this depth as a function of the bar diameter:

$$w_{deep} = 2.58\left(\frac{S_u}{\gamma' D}\right)^{0.46} + 0.24\left(\frac{S_u}{\gamma' D}\right)^{-0.63} \quad (2.2)$$

w_{deep} = depth of transition zone divided by bar diameter (unitless)

D = diameter of the cylinder

S_u = undrained shear strength

γ' = the effective unit weight of the soil

The average mid-depth clay shear strength is 334 psf, the 70g scaled diameter is 1.15 feet, and the effective unit weight is 37.5 pcf. Inserting these numbers into the equation above, w_{deep} is approximately 6.56. Therefore, the first representative shear

strength data is expected at a depth close to 7.5 prototype feet. The data above this point will rely on failure criteria that are different.

2.5 Overview and Objectives of Centrifuge Tests

The purpose of the tests were to: (1) gain insight into the mechanisms and magnitudes of downdrag-induced bending moments that develop in batter piles supporting T-wall structures in the New Orleans area and (2) provide reliable data sets that can be used to validate numerical models, which can then be used to develop an integrated design procedure for pile supported T-walls. Although the centrifuge model tests can disclose critically important underlying mechanisms and trends for conditions of interest to projects in the New Orleans area, the centrifuge model tests were different enough from real conditions that they cannot be used to directly develop design procedures. Instead, they will serve as the basis for validating numerical models that can then be used to investigate a wide range of realistic soil, T-wall, and flood loading conditions to develop a generally applicable T-wall design procedure. Therefore, readers should note that several compromises have been made due to the inherent constraints of the centrifuge while still providing the necessary information about critically important underlying mechanisms in the field and to calibrate the numerical model.

The centrifuge models were split into eight distinct trials with an initial calibration run. The calibration trial has been used to identify soil characteristics via in-situ methods and obtain information about the consolidation behavior of the clay layer. Furthermore, any unforeseen issues that arose during the construction and testing phase were addressed prior to the actual experimental runs. The calibration trial, also referred to as 'Run 0', was constructed and tested using the same methods as in subsequent runs. The models were

built in an existing container in order to meet the temporal demands of the project. Two identical containers were used to prepare models in pairs to expedite the testing program and efficiency of the centrifuge-based consolidation phase. Soil characterization included in-flight T-bar testing, CPT, and in-flight measurement of the clay shear wave velocity using bender elements. Post experiment soil characterization included 1-g penetrometer testing and water content sampling.

2.5.1 Pile Description, Selection and Scaling Constraints

One of the challenges in designing the centrifuge model was in the selection and fixation of the pile itself. Piles in the field are driven but this would be difficult to replicate in the centrifuge due to the difficulties working in such a small scale environment. First, custom containers would need to be constructed to allow enough vertical height capacity for the scaled length of pile. Second, driving the piles would necessitate a pile guide, which could itself damage the instrumented piles as they are installed. The second option was to drill out the soil and install the piles with unconsolidated slurry. This would add significant uncertainty to the overall consolidation process since the slurry itself would have to reach equilibrium prior to load testing. This would also impact the soil-pile contact conditions, which is an important parameter for studying the downdrag forces and would be a challenge to model numerically. Therefore, a method was introduced that allows use of existing containers and simulated correct soil consolidation near the soil-pile boundary. The piles are installed and pin connected to the bottom of the container prior to consolidation. They are free to move in the horizontal and vertical direction at the top during the initial consolidation phase and rotate into place so that they can be connected to the T-wall base. A stopper is used to ensure that the

piles will not move past the desired final location. The initial inclinations of the piles were varied in Run 0, and their responses during consolidation were monitored in order to determine the optimal initial inclination. This is defined at the inclination at which the pile makes contact with the stopper at the end of the consolidation phase. Since the piles are inserted in the model prior to consolidation, the combination of a pin support at the tip and stopper at the cap will allow the soil beneath it to consolidate normally without generating significant prestresses in the piles, as would occur if they were placed at their final position at the start. The testing g-level (70g) was iteratively selected in order to account for pile length, time of consolidation, and critical pile properties. The optimum point, which satisfied all criteria, results in scale model piles that are slightly larger than 0.197 in. in width. Furthermore, 30 (two row configuration) or 45 (three rows) piles are necessary to fill the width of the model container at this scale, which provides as representative section. Manufacturing exact scale replicas of typical H-piles would require significant lead time, vastly increase the per-test costs, and would be provided without any quality assurance from the machine shop. Several off-the-shelf components have been examined and the final design uses a commercially available brass rectangular tube. It is readily available and the manufacturer provides several quality control assurances. The width, flexural rigidity, and axial stiffness are all comparable to an HP14x73, as shown in Table 2.1. Two pile lengths are used in the testing program depending on the T-wall elevation. All piles extend through 70 feet of kaolinite clay. Although typical piles lengths may be much larger in the field, the maximum effect of downdrag has been estimated to occur at depths shallower than 70 feet.

Table 2.1 Properties of Field and Prototype Piles

Battered Pile Properties	Field	Model	Prototype
Material	Steel (HP14x73)	Brass	Brass
Modulus of Elasticity, E (psi)	2.90E+07	1.49E+07	1.49E+07
Width (ft)	1.22	1.04E-02	7.28E-01
Effective Width (ft)	1.22	1.90E-02	1.33
Length (ft)	1.13	2.08E-02	1.46
Thickness (in)	5.05E-01	1.40E-02	9.80E-01
Area Moment of Inertia, I (in^4)	7.29E+02	7.42E-05	1.79E+03
Area, A (ft^2)	1.49E-01	6.75E-05	3.30E-01
Bending Stiffness, EI ($lbs\text{-}ft^2$)	1.47E+08	7.68	1.85E+08
Axial Stiffness, EA (lbs)	6.21E+08	1.01E+03	7.15E+08

The piles were produced with an aluminum insert in both ends. This allows the pinned end to be drilled and attached to the base plate without producing a local bearing failure. Furthermore, the end that is attached to the T-Wall superstructure achieves its fixation through compression and requires additional local stiffness. The inserts have been sized such that the stiffening does not affect the pile in the clay layer. It would have been difficult to produce pinned connections at the T-Wall given the physical dimensions necessary for a three-row arrangement so a fixed connection was produced. Figures 2.2 and 2.3 show the model T-Wall with some of the piles connected. For this centrifuge test the piles were symmetrical with respect to the axis of the wall. The T-Wall base is split

into sections such that the piles can be clamped in position for both the two and three row arrangements. The three row arrangements were used in other centrifuge testing not included in this thesis.

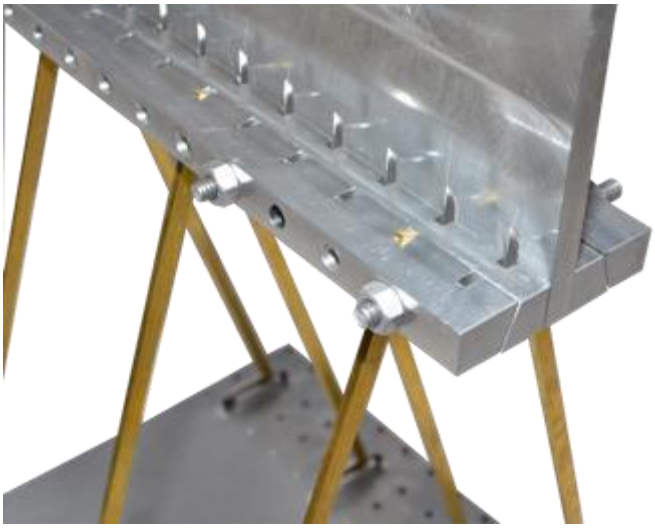

Figure 2.2 Model T-Wall Structure

Notes: Top View

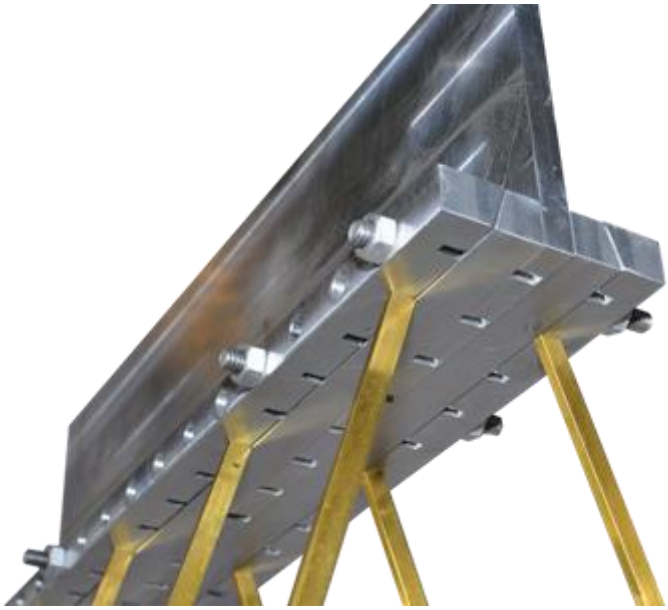

Figure 2.3 Model T-Wall Structure

Notes: Bottom View. Photo courtesy of RPI.

2.5.2 Model Description and Construction

The model geometry constructed for the calibration test (Run 0) is shown in Figure 2.4 in prototype units. The thickness of the clay layer is 70 ft prototype, and a pile configuration shorter than the one used in centrifuge Run 2 was used. A drainage layer was built at the bottom of the container. A drain was installed at the base of the box in combination with a vertical pipe attachment in order to maintain the same piezometric head level at the top and the bottom of the clay layer. The base plate for the piles was embedded in the sand layer. Since it has a unit weight similar to concrete, the model T-Wall was constructed out of machined aluminum. This increases the robustness of the system and repeatability of testing. Since the goals of the project center around determining the behavior of the piles in order to calibrate a numerical model, this approximation is justified.

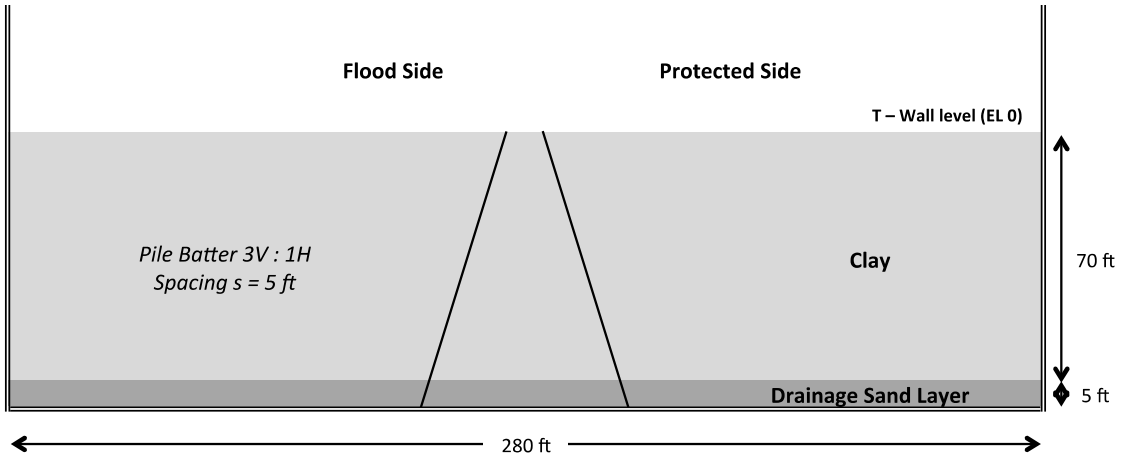

Figure 2.4 Model Configuration for Run 0

2.5.2.1 Container Preparation and Pile Installation

The container was prepared, cleaned and sealed. The drain that maintains the proper piezometric head for the sand base layer was installed. The walls of the container were sprayed with a silicone-based lubricant that reduces friction at the boundaries. The base plate, the piles and the pile stopper were inserted in the container. The bender element columns were installed in the container and the bender elements were fixed at the desired locations. Figures 2.5 and 2.6 show the test container for Run 0 with the piles and bender elements installed.

2.5.2.2 Construction of the drainage layer

After the base plate and the piles were inserted in the container, the drainage layer was constructed and saturated. The drainage layer consists of Nevada 120 Sand that was dry pluviated to a relative density $D_r = 60\%$.

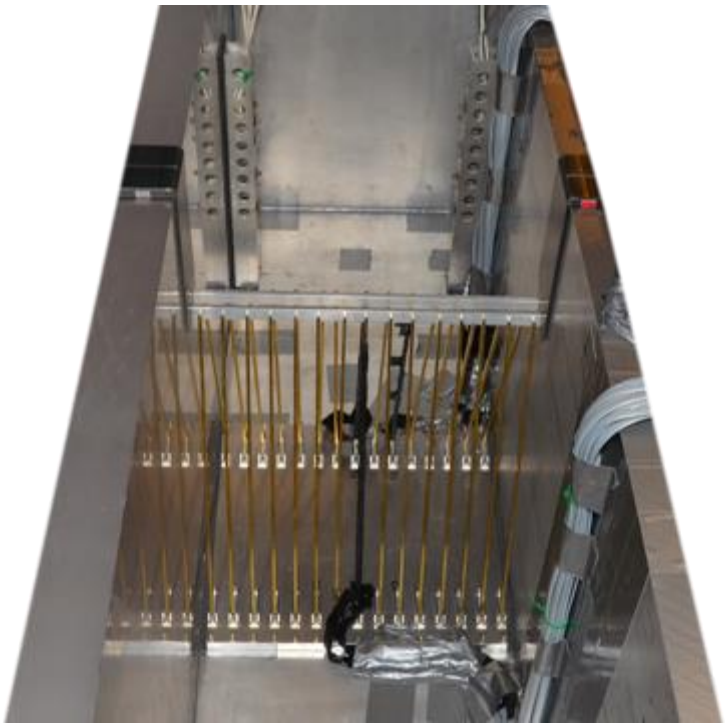

Figure 2.5 Piles Installed in Container

Notes: Photo courtesy of RPI

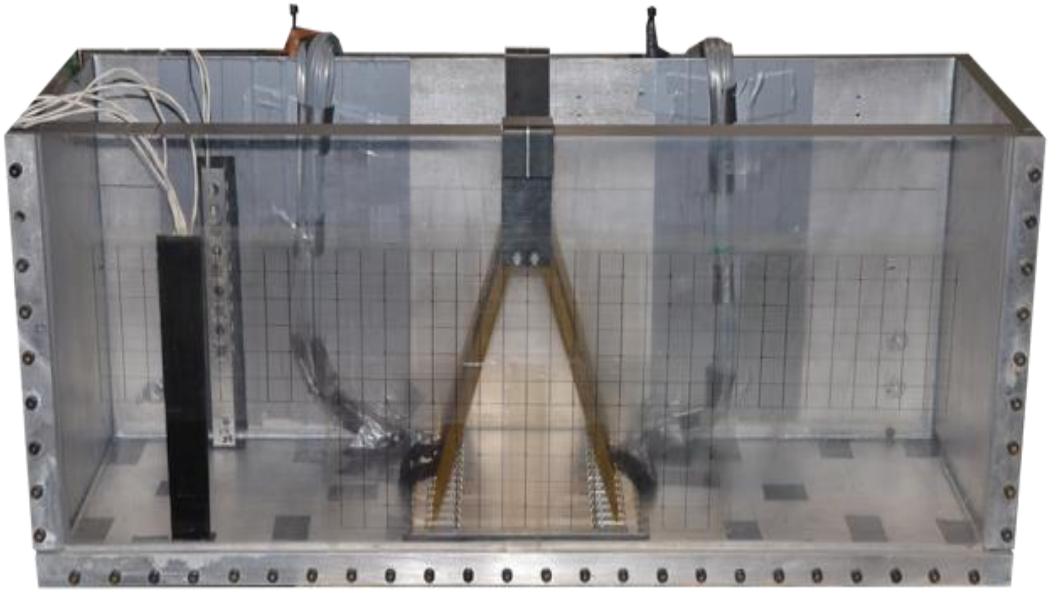

Figure 2.6 Empty Model Box

Notes: Run 0 Piles (Center) and Bender Element Columns (Left). Photo courtesy of RPI

2.5.2.3 Construction of the Clay Layer

After the piles were aligned at the initial inclination and the drainage layer was installed, the clay layer was built. As previously discussed, the initial inclination of the piles was varied parametrically (5 to 15 degrees) in order to identify the optimal initial pile position for subsequent runs. Kaolinite clay (BASF ASP 600) was mixed at 70% initial water content and installed in the container. The clay was installed in the container by hand in small disks and the boundaries between the discs were carefully integrated by gentle massaging of the clay. The soil has the properties listed in Table 2.2. The clay layer was built 26.6 prototype feet higher than the zero elevation mark (EL0) to account for the consolidation settlement. Excess material was removed after the initial consolidation phase carefully as to mitigate disturbance to the soil below. During the construction of the clay layer, pore pressure transducers and tracking targets were installed. The initial depth of the pore pressure transducers accounted for the consolidation settlement.

Table 2.2 Kaolinite ASP 600 Properties.

Liquid Limit	61
Plastic Limit	29
Density (w = 50%)	.058 lb/in^3
c_v	6.2x10^{-4} in^2/s

2.5.2.4 Construction of the Surcharge Layer

The sand surcharge for the initial consolidation phase is built on top of the clay layer (ca. 8 ft prototype). A geotextile is inserted between the surcharge and clay to prevent infiltration. The sand is dry pluviated to a relative density of 60%. Figures 2.7 and 2.8 show the model container at the end of the construction of the clay layer and while constructing the surcharge layer. Field installations will utilize surcharge embankment material that is similar to the foundation soil. This would be nearly impossible to replicate in the centrifuge for the cases where the T-wall rests on an existing embankment. Additional clay soil would need to be consolidated outside of the production model and installed in it after the consolidation phase. Since the piles were battered, this embankment would need to be further divided into segments to fit between the pile foundation system. It would be difficult to characterize the soil-pile interface in this instance. In order to facilitate both the construction of the models and the ability to model the geometry numerically, sand was selected for the surcharge material. The sand surcharge consists of Nevada 120 Sand that was dry pluviated to a relative density D_r = 60%. The sand fill was very dry with only air moisture in it and no compactive effort was used. Based on the pluviation process, a very uniform fill was placed. It results in soil properties as described in Table 2.3 (Tessari 2012).

Table 2.3 Nevada 120 Sand Properties.

Unit Weight	100 pcf
Void Ratio	0.77
Relative Density	60%
Fines Content	<5%
D_{50}	.0059 in

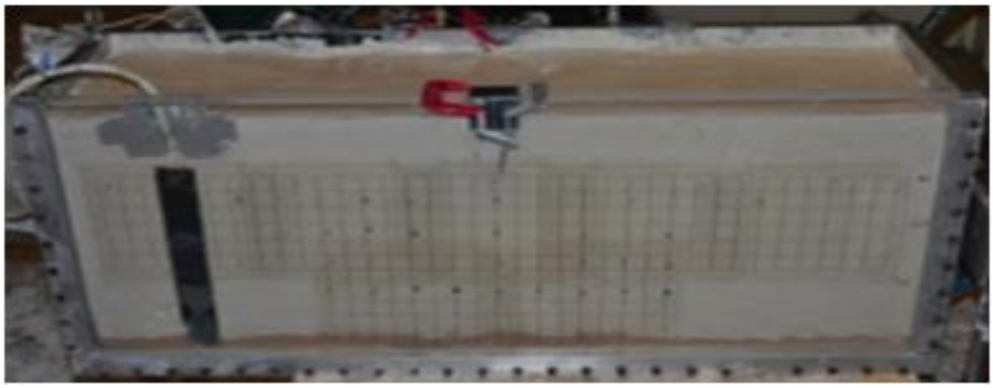

Figure 2.7 Construction of the Clay Layer

Figure 2.8 Consolidation Surcharge Layer

Notes: Photos courtesy of RPI

2.5.3 Instrumentation

2.5.3.1 Strain Gages

Four battered piles were instrumented with numerous strain gages in the production runs. Two of them were installed on the flood side and two on the protected side. In the calibration trial only two instrumented piles were used, one on each side. The width of the gage matches the width of the pile. The layout of the strain gages for the two different pile configurations in model scale is depicted in Figure 2.9.

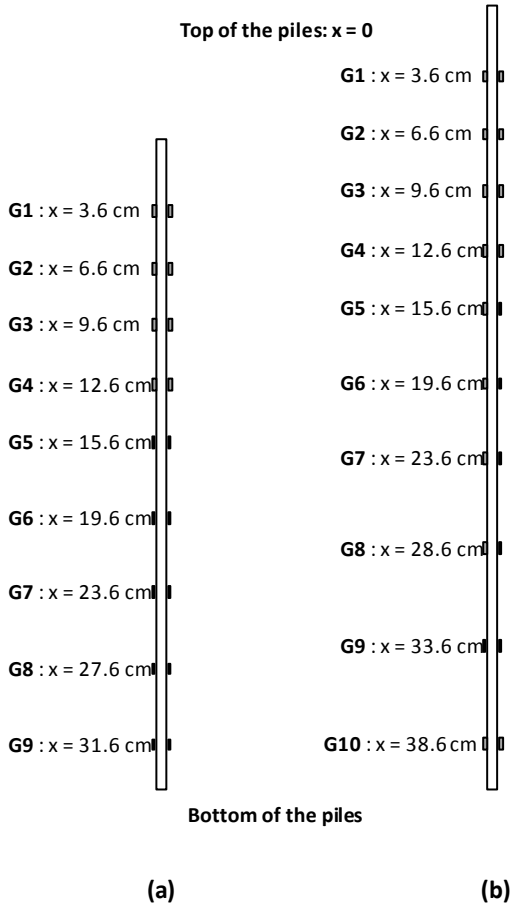

Figure 2.9 Layout of Strain Gages on Piles

Notes: (a) Short Pile Configuration, (b) Long Pile Configuration (Model Dimensions)

2.5.3.2 Pore Pressure Transducers

Pore pressure transducers were installed during the clay construction phase at various locations in the free field and around the piles to monitor the excess pore pressure dissipation during the clay consolidation phase and the fill loading. The sensors produce data with accuracy to a hundredth of a kilopascal. The sensors were submerged in water for 24 hours prior to model construction. The sensors contain a ceramic filter that prevents clay infiltration but allows transmission of water pressure. If the filter were not present, the clay would load the sensors directly and it would read soil pressure. The sensors are extremely small yet they are rugged and robust. The sensors are calibrated to relate the change in strain of the diaphragm to a known pressure.

2.5.3.3 Soil displacement tracking targets

Displacement tracking targets were installed in the clay stratum in order to measure the soil displacement. The motion of the targets was captured using the on-board camera system and tracked using specialized software. The targets were installed during construction at the transparent boundary of the container. These are small square targets with a 0.39 in. tail. The targets were installed using a transparent square grid on the acrylic side of the container. The sidewalls of the box were thinly coated in a silicone-based lubricant prior to construction so that friction is minimized and boundary effects are avoided. Vacuum grease was also applied to the head of the target to form a .039 in mound. The target was then pressed against the acrylic such that the vacuum grease spreads out uniformly around it. The grease prevents clay from moving in front of the target during consolidation.

2.5.3.4 Bender elements

The shear wave velocity profile of the clay layer was determined using bender elements. Bender elements are piezoelectric transducers that are used to generate and detect mechanical waves in a soil medium. This is accomplished by measuring the time difference between generation and detection of a wave. The bender elements were fixed on columns at the two sides of the box at the desired locations. A column with receivers was installed at the aluminum side of the box while the transmitters are placed at the Plexiglas window. Rubber was placed at the interfaces to minimize ambient vibrations and attenuate transmission through the container. After significant consolidation, reflections from the boundary of the container obscured readings of the true first shear wave arrival. Subsequent tests utilized a wave attenuating rubber at the two far boundaries of the container to reduce the p-wave reflections in the soil-container system. The bender element system uses specialized software with a built-in stacking algorithm that produces clear data with a high signal-to-noise ratio.

2.6 Testing Sequence

The testing sequence for the runs includes the clay consolidation phase, in-situ testing, and the loading stages. The calibration trial was conducted in order to obtain information about the soil characteristics; therefore the testing sequence is different. Details of the testing sequence for Run 0 are given below.

2.6.1 Clay Consolidation

The calculated consolidation time to reach 90% consolidation is sixteen hours using 1-D Terzaghi theory. The actual testing protocol called for the consolidation phase

to be stopped once the pore pressure transducer at the midpoint of the clay layer read an excess pore pressure equivalent to the surcharge load pressure. Thus, when the surcharge is completely removed, the clay would be normally consolidated at the mid-depth and overconsolidated at the drainage boundaries. This step was completed in one day. Bender elements readings were collected every hour and all other sensors were recorded for the duration.

2.6.2 In-flight Soil Characterization

The surcharge was removed from the model after consolidation, as the T-Bar cannot penetrate through it or the separation geotextile. The Z-Loading system was installed on the centrifuge basket and T-Bar testing was performed. The T-Bar is a full-flow penetrometer that is capable of generating undrained shear strength profiles for purely cohesive media. While a CPT could also be used in this test, it would require several correction factors to produce the true undrained shear strength profile. Despite its limitations, the CPT was used in a few runs to verify the readings developed by the full flow penetrometer.

2.6.3 Post Experiment Soil Characterization

Handheld penetrometer readings were taken after the box was removed from the centrifuge during the deconstruction to ensure consistency of the foundation material. Water content samples were collected during the excavation of the model. The T-Bar readings, water contents, handheld penetrometer, and bender element data were compiled into a database.

2.7 Run 0: Calibration Trial

The calibration trial, also known as Run 0, was tested in June 2013. The clay model was consolidated for 16 model hours (8.95 prototype years) under double drainage conditions through a sand layer placed at the bottom of the model and the geotextile and sand layer at the top. At the end of consolidation the excess clay material above EL 0 was removed. The location of the piles with the respect to the stopper (i.e. the desired final location) was inspected and the surface was prepared for testing with the T-bar.

The consolidation settlement at the surface of the clay layer was measured with a LVDT placed on the flood side far enough from the piles to be considered free field. Figure 2.10 shows the total settlement measured including spinning up to 70g and spinning down to 1g after 16 hours of consolidation (approximately 9 years prototype). Figure 2.11 illustrates the final location of the piles with respect to the stopper after the excess clay was removed. The initial distance from the stopper varied from 0.39-2.86 model in. As shown in Figure 2.11, most of the protected side piles reached the stopper at some point during consolidation, while the flood side piles that were initially positioned further away from the stopper were not subjected to adequate lateral movement to reach the resting position. After careful consideration and in order to be consistent with all future runs, it was decided to place the piles 0.79 model in away from the stopper. That distance corresponds to the spacing between the two rows of piles in the three-pile arrangement that was tested later that year.

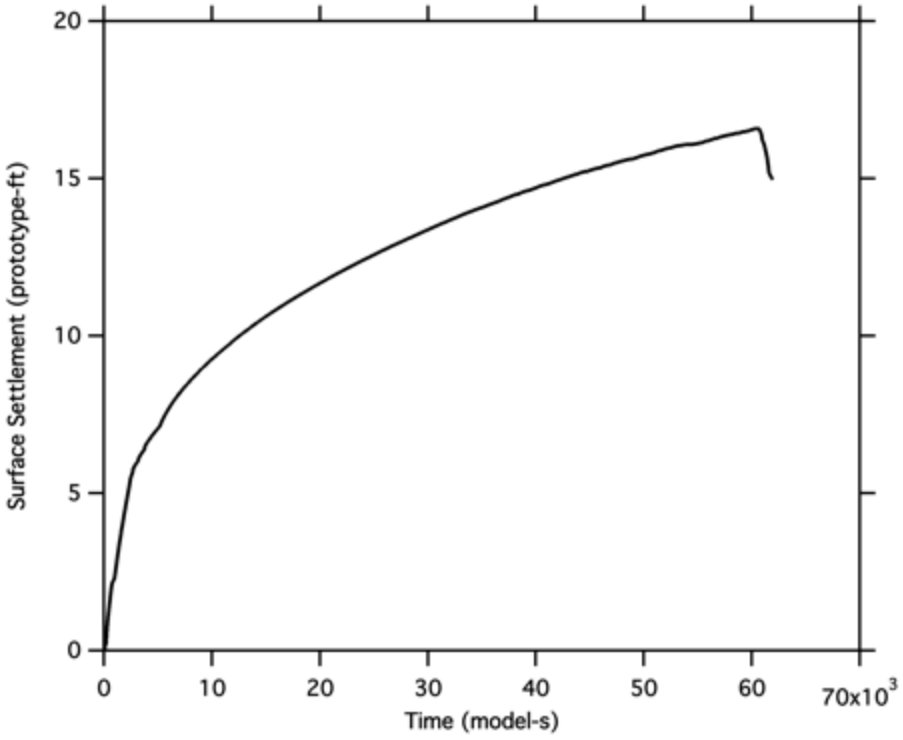

Figure 2.10 Consolidation Settlement at Surface Run 0

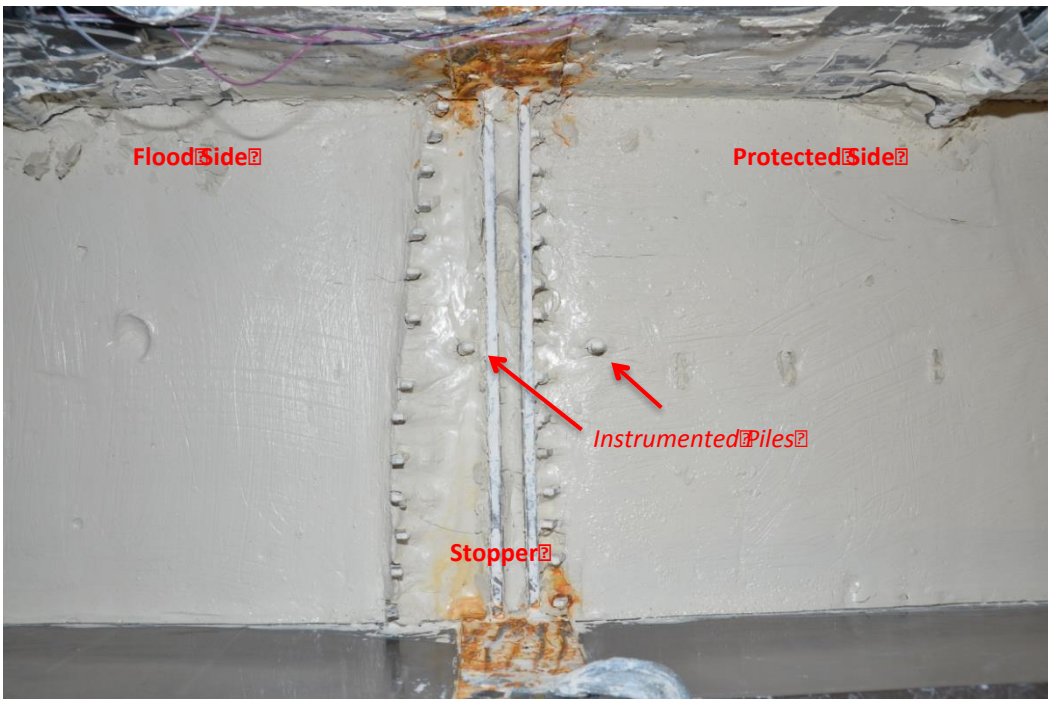

Figure 2.11 Pile Location Run 0 Consolidation

As shown in the same photo, none of the center piles that were instrumented with strain gages reached the stopper. Therefore, the strain levels on the piles were not representative of the actual pile final location. To avoid confusion, the bending moments on the piles at this stage are not presented in this section.

The T-Bar testing was performed at the end of the 16-hour consolidation phase. The model was spun up to 70g and allowed enough time to reach equilibrium. The T-Bar was moved to a dummy location and pushed into the soil such that the strain gage area was submerged and left in this position for a few minutes. This allowed the T-Bar to reach thermal equilibrium with the soil and prevented error due to thermal expansion or contraction. The T-Bar was moved to two different testing locations and pushed into the

soil at a rate of .122 in/s (equivalent to 8.54 in/s at the prototype scale). Figure 2.12 shows the undrained shear strength profiles obtained from Push 1 and Push 2.

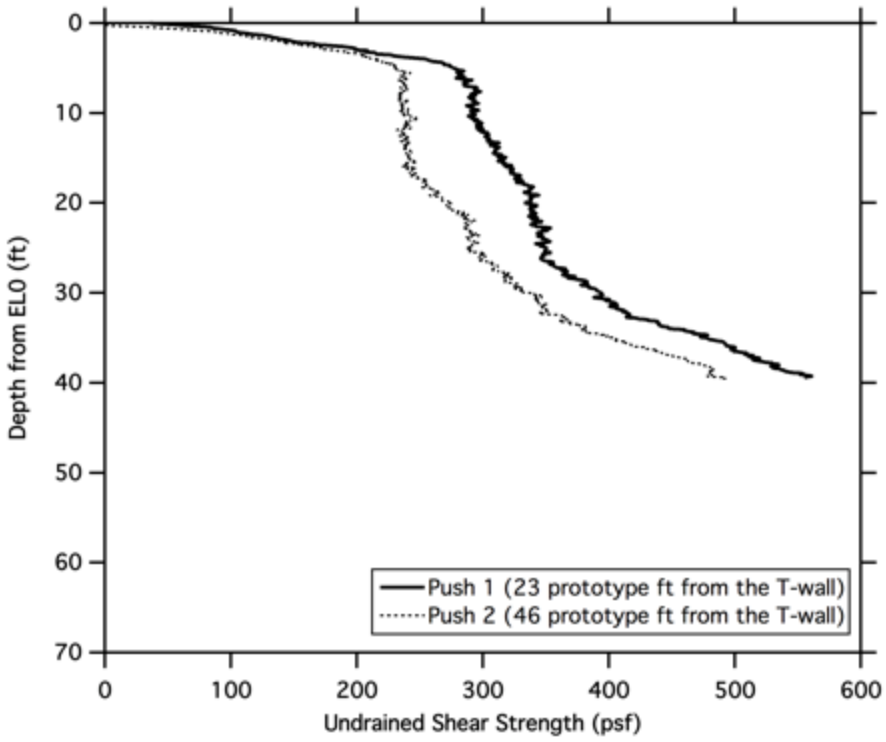

Figure 2.12 Undrained Shear Strength Profiles

Figure 2.13 contains information about the shear wave velocity profile as obtained from the bender elements during the consolidation phase. Readings were taken every model hour. The data shown in the graph correspond to the end of 4 hours (2.2 prototype years), 8 hours (4.4 prototype years), 12 hours (6.6 prototype years) and the end of consolidation (8.8 prototype years).

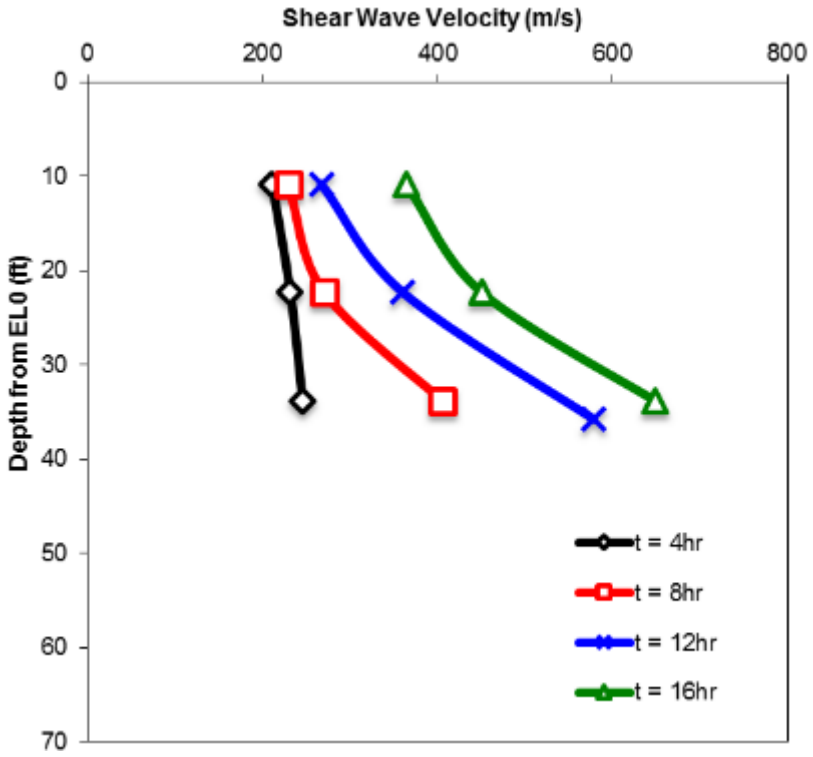

Figure 2.13 Shear Wave Velocity R0

As shown in Figure 2.13, the clay layer at 35 ft depth becomes significantly stiffer than the upper 35 ft during the last hours of consolidation, indicating overconsolidation of the bottom half with respect to the upper half of the clay layer. The undrained shear strength profiles lead to the same conclusion. Considering the above observations it was decided that the following modifications were applied to the consolidation testing phase for the subsequent Runs 1 and 2:

- The initial consolidation phase was broken down to four four-hour increments with half hour intervals at 1g. This would allow the research team to inspect the model and perform the drainage change after the first

interval, as described below, while maintaining symmetry in the testing protocol.

- During the first four hours the drain at the bottom of the container should remain closed so that single drainage would be taking place. The drain should be opened at the end of the four hours so that the remaining twelve model hours of consolidation take place under double drainage conditions. This was performed in order to slow down rapid early consolidation in the lower soil region, which would allow the piles to move toward the final position with less pre-stress generation.
- The consolidation surcharge would be reduced to 3 prototype feet of sand and additional initial clay material would be added. This ensures that both pile length configurations end consolidation with soil above the top of the piles.

Finally, it was noticed that at the end of the continuous 16 hours consolidation phase the temperature of the centrifuge room had increased and it was suspected that the change in temperature could affect the performance of some sensors such as the strain gages and the pore pressure transducers. The modified consolidation sequence for Runs 1 and 2 should serve as a way to keep the centrifuge room at a reasonable temperature level and avoid any overheating problems. Additionally, a thermocouple would be installed in the clay layer in order to monitor the temperature changes throughout the test and potentially correcting for the thermal drift of the sensors.

2.8 Run 1: T-Wall on Grade with Symmetrical Broad Lateral Extent Fill

After the calibration Run 0, the centrifuge experimentation resumed with Run 1, which was constructed, consolidated and tested during July of 2013. The model contained the short pile configuration and the loading conditions consisted of a symmetrical fill of broad lateral extend. Figure 2.14 illustrates the Run 1 configuration in prototype units.

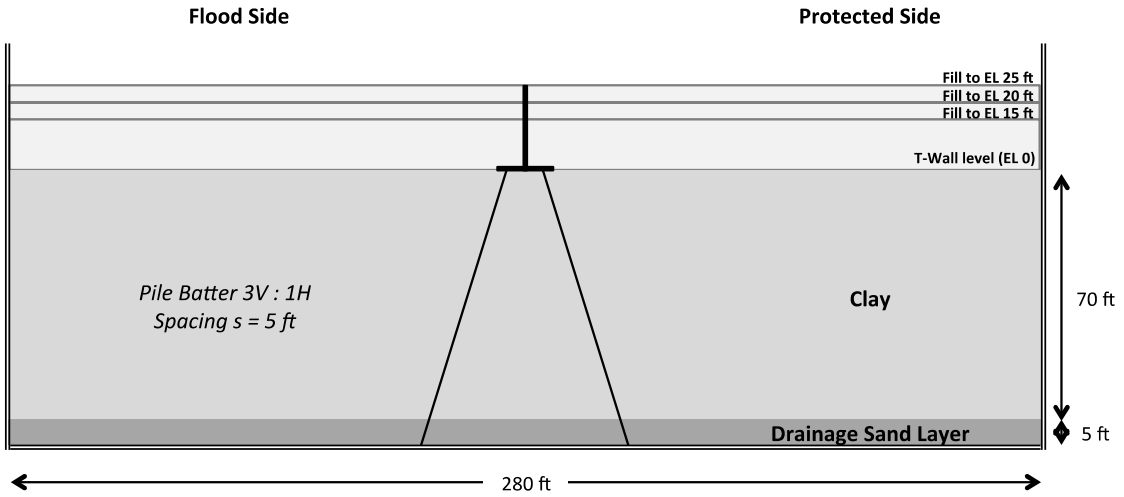

Figure 2.14 Model Configuration for Run 1

The construction of the Run 1 model (and all subsequent runs) was performed as described for the calibration trial. The testing program was broken into five phases: initial consolidation, nulling, 15 prototype-ft fill loading, 20 ft fill loading, and 25 ft fill loading. As explained in the previous section, the initial consolidation phase was broken down to four parts of four model hours. At the end of consolidation, the surcharge was removed as well as the excess clay material and the T-wall was installed. Furthermore, the in-situ undrained shear strength for the foundation soil was acquired both before and after the loading phases using a T-Bar and CPT.

Prior to the fill loading increments, the model was spun up to 70g and held for approximately 1 model hour (0.56 prototype years). This was performed in order to establish a baseline reading for the sensors, to which loading data could be compared. The first two fill loading increments were held at g-level for 1.5 prototype years. The last loading stage in Run 1 was consolidated for nearly 5 times as long at 6.7 prototype years. This established the long-term high-stress behavior of the system.

Similar to Run 0, pore pressure transducers were installed in the clay model to monitor the pore water pressure during the consolidation and the fill loading phases. Strain gages were installed along two piles (one on the flood side and one on the protected side) in order to obtain the bending moment profiles with depth. The settlement of the clay surface was recorded through LDVTs and shear wave velocity measurements were taken throughout the test. Figure 2.15 illustrates the sensor layout for Run 1.

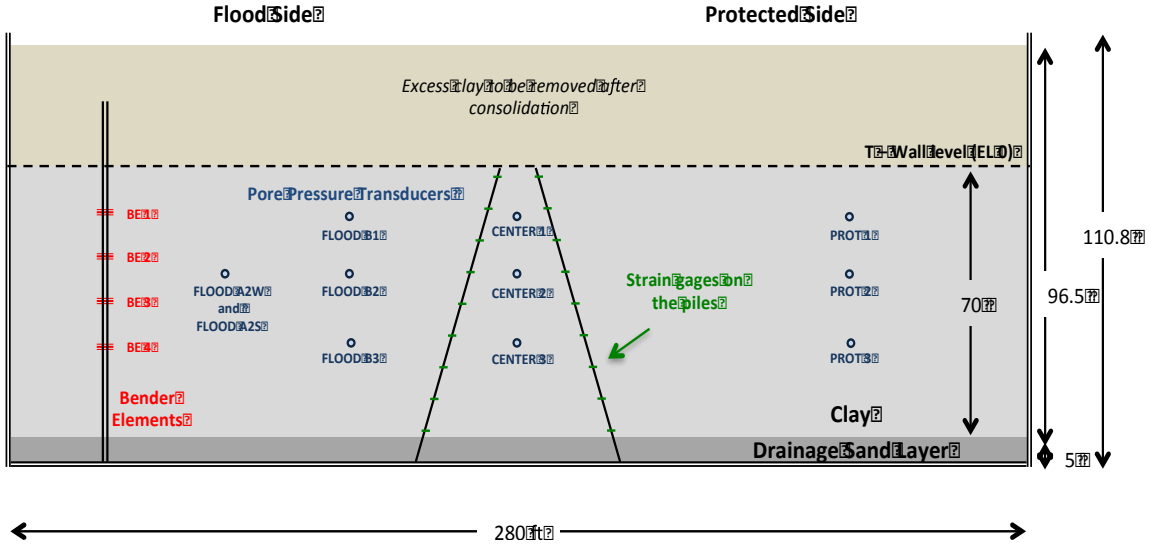

Figure 2.15 Run 1 Sensor Layout

The strain gages were installed as pairs on opposing sides of the piles (sides A and B) in order to be able to measure both axial force and bending moment. The Figure 2.16 shows how the strain gage readings on the opposing sides A and B were used to separate the bending from the axial strain component.

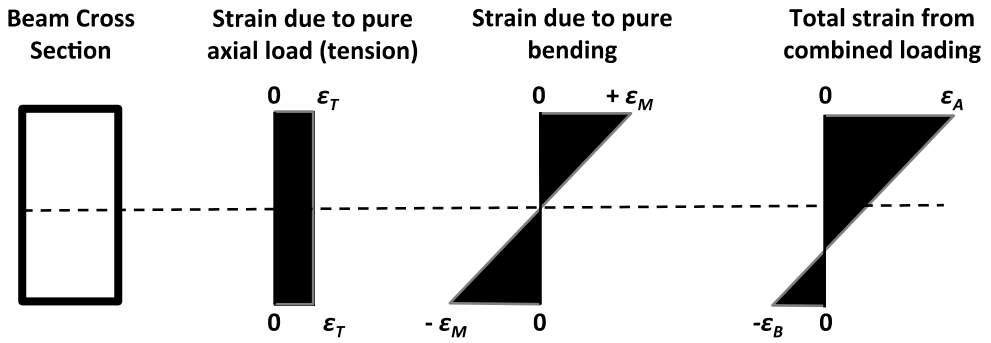

$$\varepsilon_M = (\varepsilon_A - (-\varepsilon_B))/2$$

$$\varepsilon_T = (\varepsilon_A + (-\varepsilon_B))/2$$

Figure 2.16 Strain Readings Schematic

The following formulas were used to calculate the bending moment and axial load:

$$M = \frac{\varepsilon_{dif}\, EI}{2c} \tag{2.3}$$

ε_{dif} = ***differential*** strain gage reading as shown above, c = distance from center of beam to edge, E = Young's modulus, I = Second area moment of inertia.

$$P = \varepsilon_{avg}\, E\, A \tag{2.4}$$

ε_{avg} = ***average*** strain gage reading as shown above, E = Young's modulus, A = pile cross sectional area.

The above equations can uncouple the axial loads from the pure on-axis bending component provided that this is the only loading combination. In reality, however, the piles were subjected to some unintended off-axis lateral bending as well. During several post-calibration tests on the pile strain gages at 1g it was observed that the strain gages on the pile strong axis (on-axis) were sensitive to off-axis lateral loading. While the effect of the off axis lateral loading on the piles is cancelled when using the differential strain gage reading for the bending calculations, it is still present in the average strain reading used for the axial loading calculations. Uncoupling the small axial components of this complicated loading combination has proven to be very challenging and cannot be accomplished for this set of readings. The axial loading plots provided in the appendix are not incorrect; however they reflect the combined loading (including off-axis bending) rather than the pure axial loads.

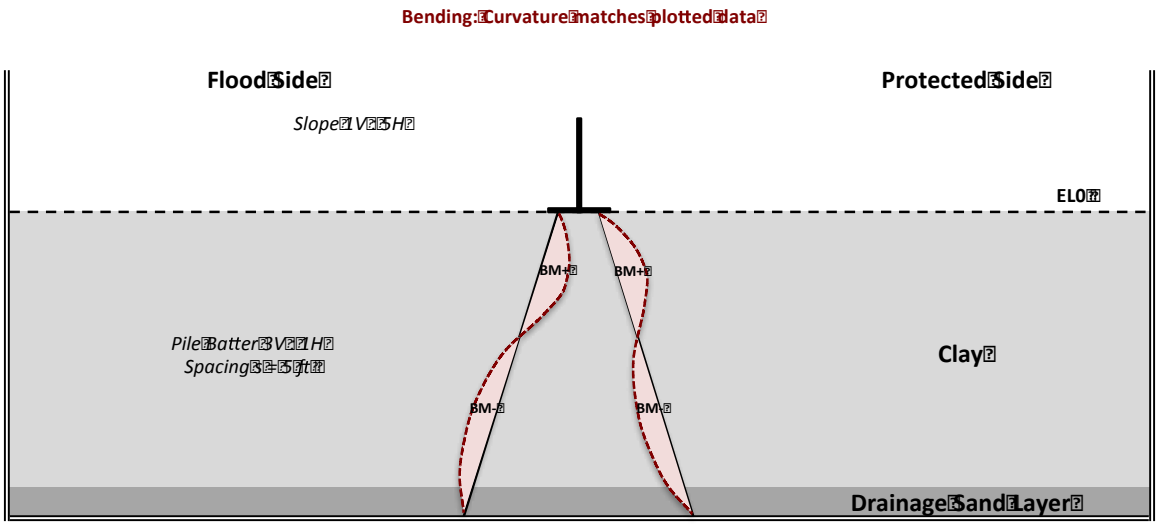

Figure 2.17 Bending Moment Sign Convention

2.8.1 Soil Testing

Soil testing was performed at four locations during Run 1: two locations were tested at the completion of the 16-hour consolidation process and two at the conclusion of the 25 ft of fill material loading phase. T-bar testing was performed as described before. CPT testing was performed along with the T-Bar in order to glean additional information about the soil below the depth limited by the length of the T-Bar. CPTs can be used to identify the undrained shear strength profiles for clay. The CPT is 250 mm in length, which is 75 mm more than the T-Bar. While the data from the CPT will most likely be skewed, it can be scaled to generate some information about the soil strength below the end depth of the T-Bar. The data obtained form Run 1 soil testing is shown in Figure 2.18. The T-Bar has been extended for future tests in order to obtain information regarding deep soil.

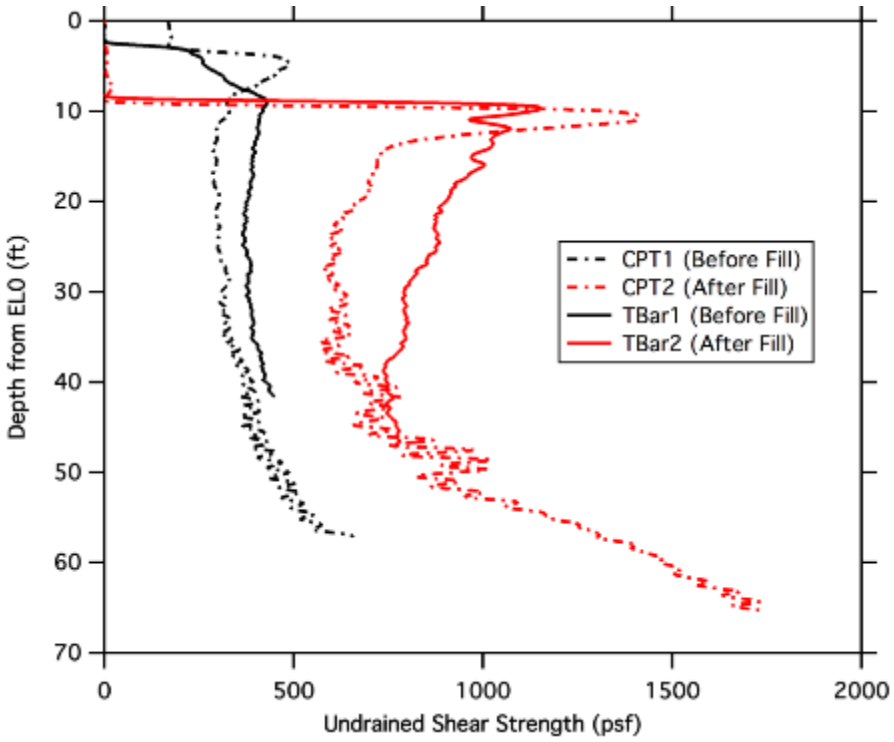

Figure 2.18 USS Profiles

The results from the T-Bar testing on Run 0 and Run 1 are shown in the Figure 2.19. As expected, due to the initial drainage differences between the tests, the deeper soil is weaker in Run 1. This is also observed via the shear wave velocity data shown in Figure 2.20. The LVDT mounted in the container during consolidation of Run 1 is shown in Figure 2.21. The consolidation settlement measured at the surface is 16 prototype-feet for Run 1 and was 16.6 prototype-feet for the calibration trial.

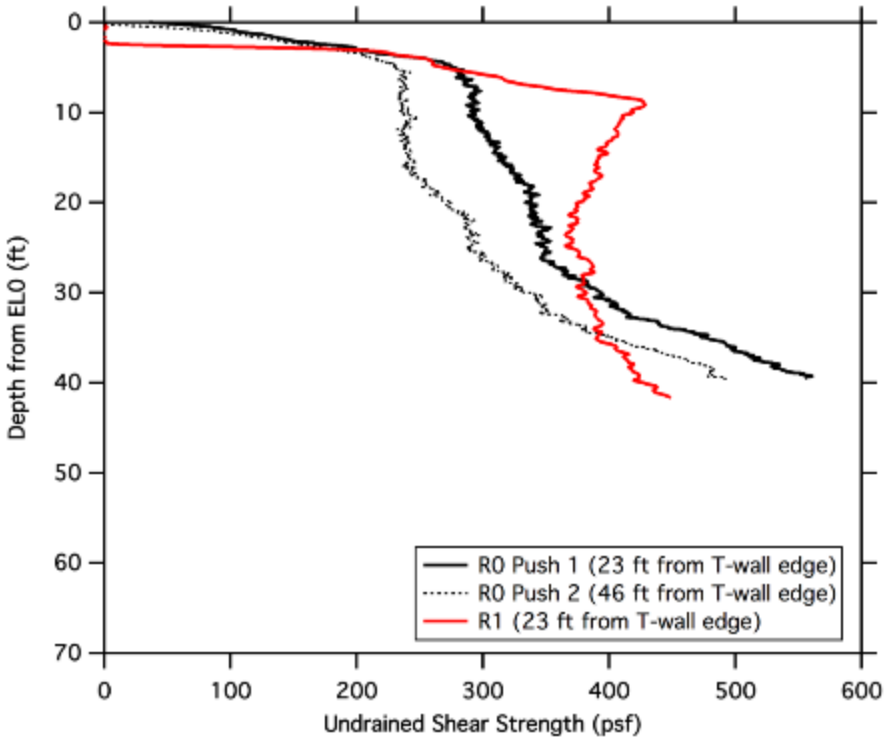

Figure 2.19 USS Profiles Runs 0 & 1

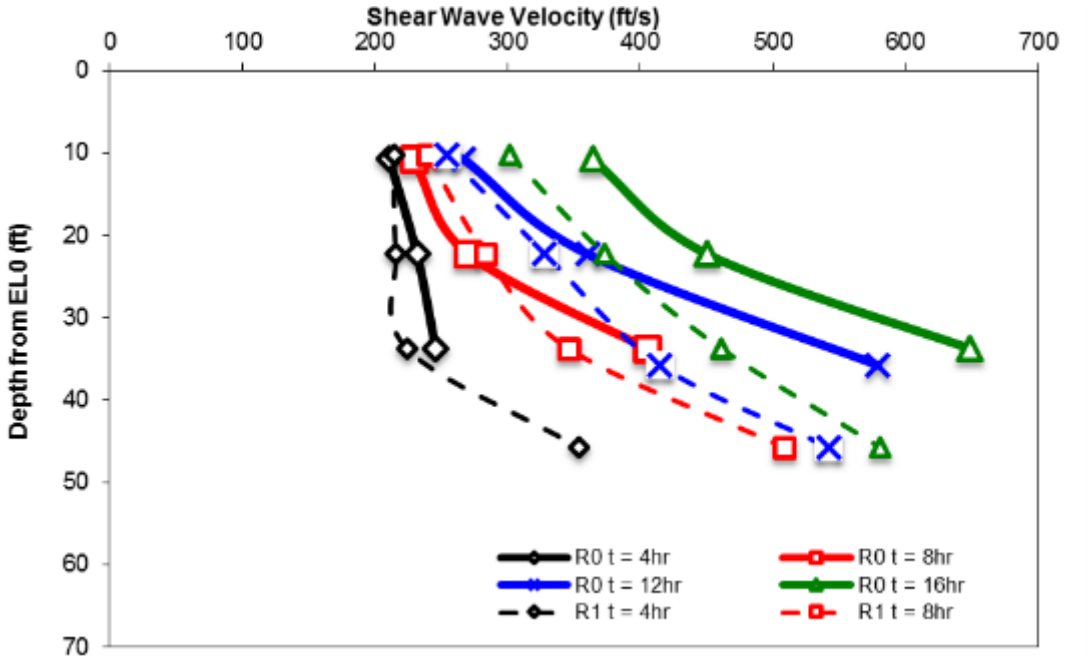

Figure 2.20 Shear Wave Velocity Profile

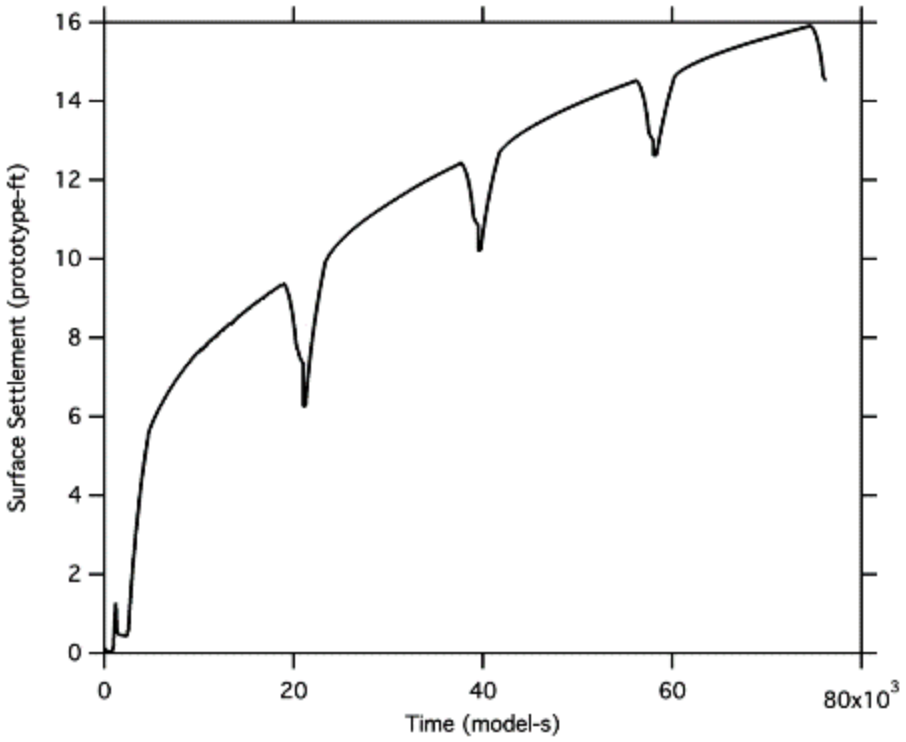

Figure 2.21 Consolidation Surface Settlement

Notes: 25 Ft Distance from the T-Wall

Figures 2.22 and 2.23 shows the shear wave velocity profiles as obtained from the bender elements at the end of the nulling phase and at the end of each fill loading phase of Run 1. An additional comparison of the shear wave velocity profiles at the end of consolidation and at the end of the nulling phase is provided in Figure 2.23.

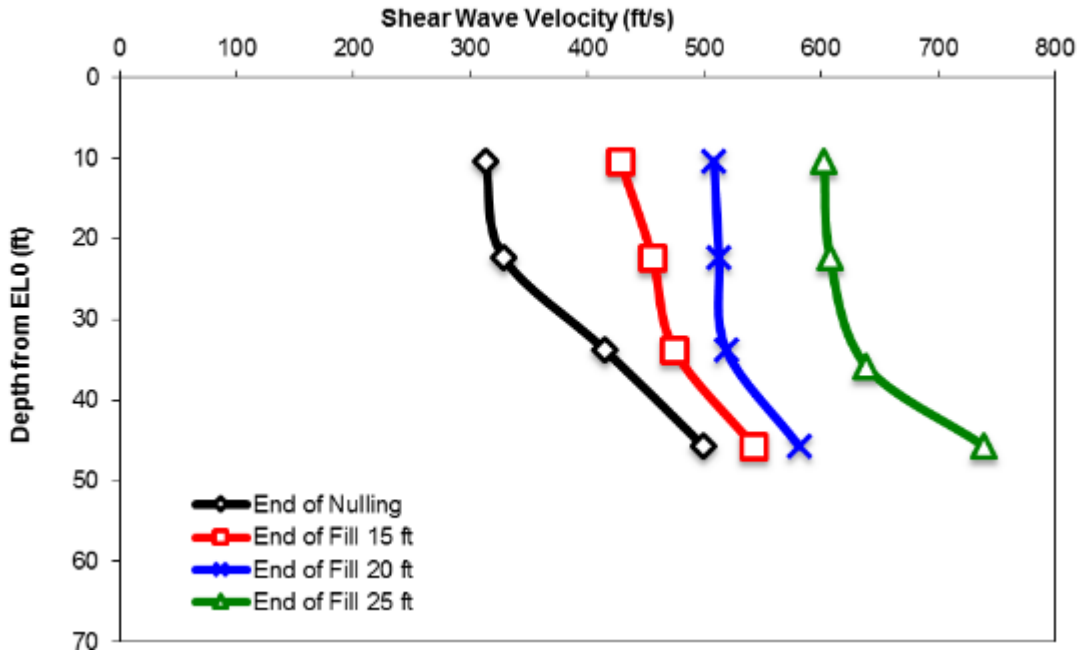

Figure 2.22 Shear Wave Velocity R1

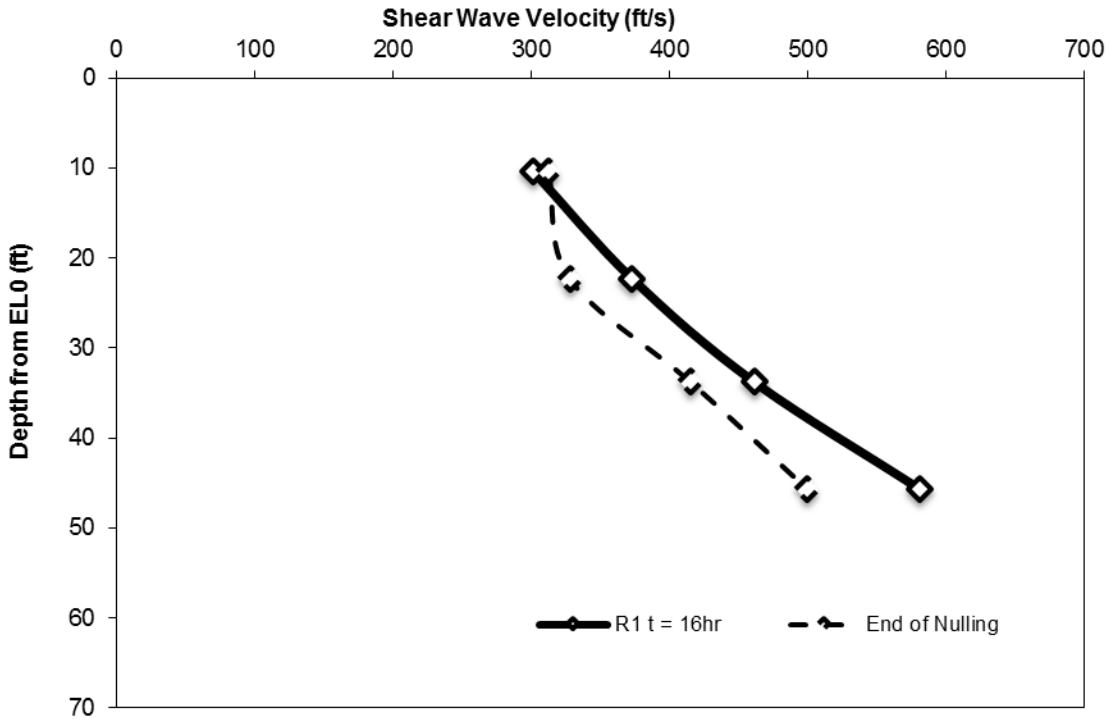

Figure 2.23 Shear Wave Velocity Comparison R1

2.9 Run 2: T-Wall on 15' Embankment with Symmetrical Limited Extent Fill

Run 2 was constructed, consolidated and tested during July and August of 2013. The model contained the long pile configuration and the loading conditions consisted of a symmetrical fill of limited lateral extend. Figure 2.24 illustrates the Run 2 configuration in prototype units.

The construction of the Run 2 model was performed as described for the calibration trial and Run 1. The testing program was broken into four phases: initial consolidation, nulling, 15 prototype-ft fill loading, and 25 ft fill loading. Similar to Run 1, the initial consolidation phase was broken down to four parts of four model hours. At the end of consolidation, the surcharge was removed as well as the excess clay material and the T-wall was installed. The two fill loading increments of this run were held at g-

level for 6.7 prototype years in order to establish the long-term high-stress behavior of the system. The list of actions performed during Run 2 is provided in Table 2.4.

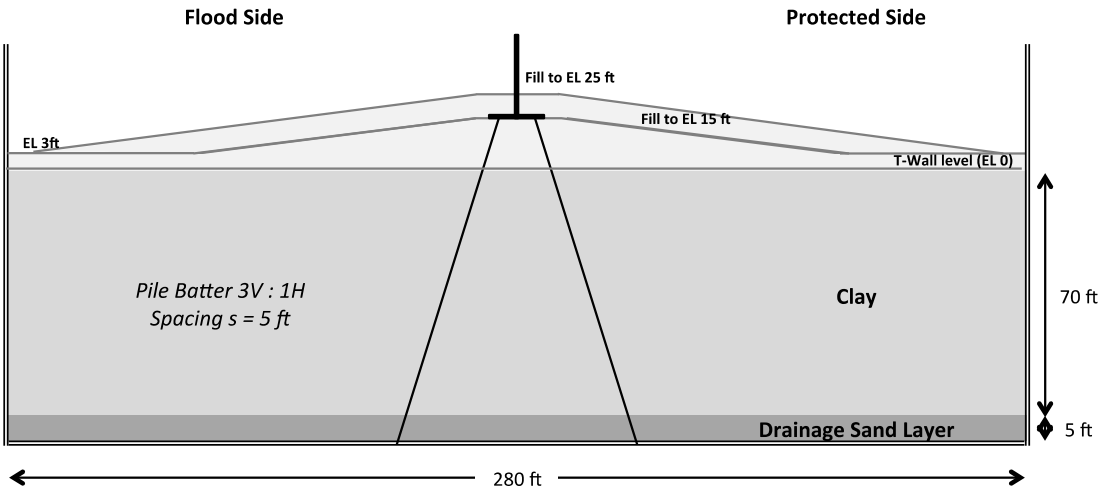

Figure 2.24 Model configuration for Run 2

Table 2.4 Summary of Actions Performed Run 2

Date	Action	Description
7/23/13	Model Layout	Check all sensors, layout, and mark container
7/24/13 7/25/13 7/26/13	Model Construction	Model soil overlain by 3 prototype-ft of Nevada 120 Sand at 100 pcf dry density
7/27/13	Consolidation (Phase I)	Consolidation part 1-3 completed 4 as 4 hour segments at 70 with 1 hour 1g intervals
7/28/13	Consolidation (Phase I)	Consolidation part 4 completed
7/28/13 7/29/13	Surface Preparation	Cut excess Kaolinite to match EL. 0 and install T-Wall
7/29/13	Nulling (Phase II)	Spin up to 70 to establish null loading conditions
7/30/13	15 ft Load (Phase III)	Install 15 prototype-ft of sand surcharge and spin at 70g for 12 hours (6.7 prototype-years)
7/31/13	25 ft Load (Phase IV)	Install 15 prototype-ft of sand surcharge and spin at 70g for 12 hours (6.7 prototype-years)
8/1/13	Post Test Evaluation	Model deconstruction, water contents and final sensor locations

The instrumentation utilized in Run 2 is identical to that present in Run 1 with one exception. The surface settlement was recorded at two points for fill loading phases of this run.

2.9.1 Consistency of Runs 1 and 2 via Shear Wave Velocity Testing

In order to ensure that inter-experiment comparisons are valid, the initial conditions must be tested and verified for consistency between tests. Figures 2.25 and 2.26 show the shear wave velocity profiles for Run 1 and Run 2. They show that the

behavior during consolidation and the final result were nearly identical for both runs. Therefore, the initial soil conditions were nearly the same and comparisons between the two experimental runs can be made.

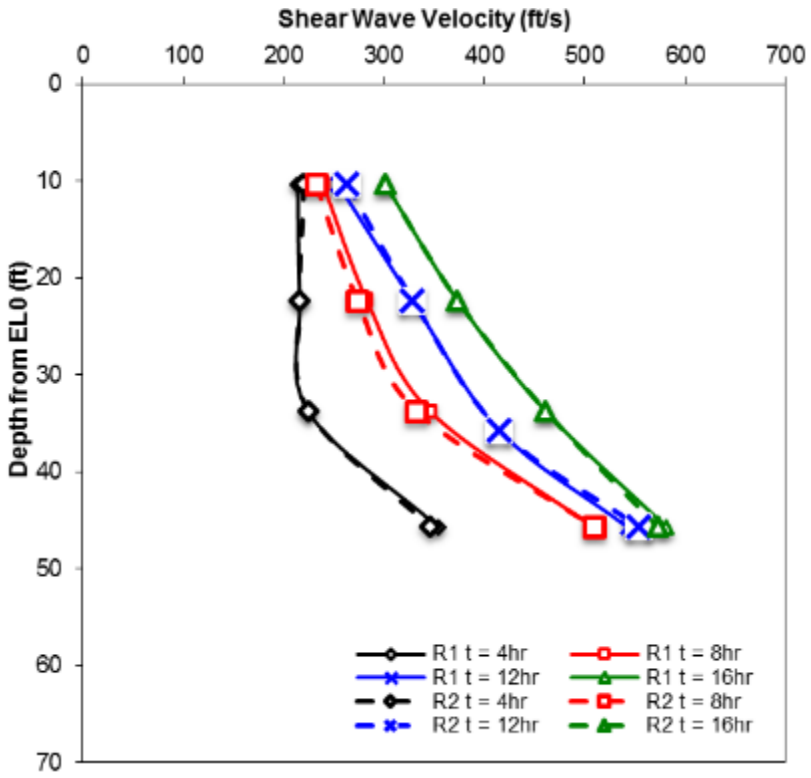

Figure 2.25 Consolidation Shear Wave Velocity Profiles

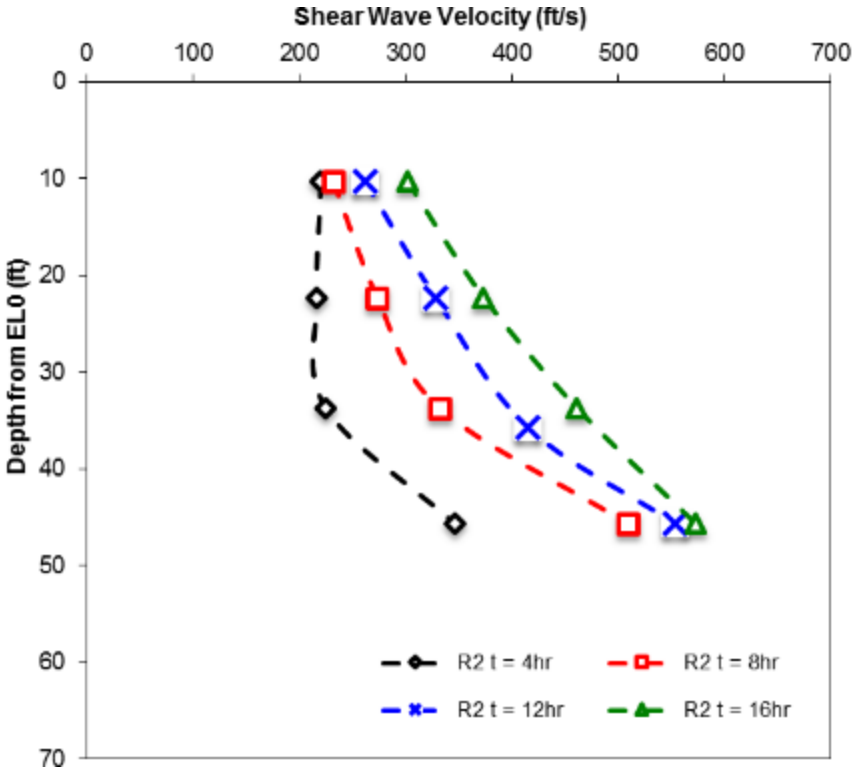

Figure 2.26 Shear Wave Velocity Profiles

2.9.2 Run 2 Data

The bending moments developed in the flood and protected side piles are shown in Figures 2.27- 2.32. Two different scenarios are depicted: 1) where the strain developed in the nulling case is included and 2) where the data is plotted with the null case subtracted. Note that in these figures, the depth is plotted relative to EL0 and the base of the T-Wall rests at -15 ft. Similar to Run 1, the maximum bending moments occur at the interface between the pile and wall. Within the soil mass, the maximum bending moment is at a depth of approximately 12 prototype feet.

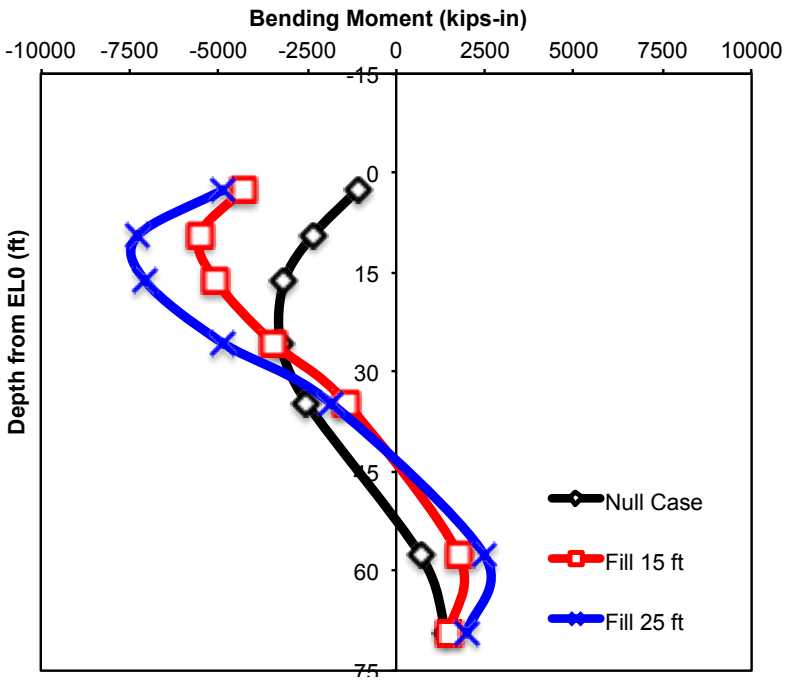

Figure 2.27 Protected Side Pile Moments

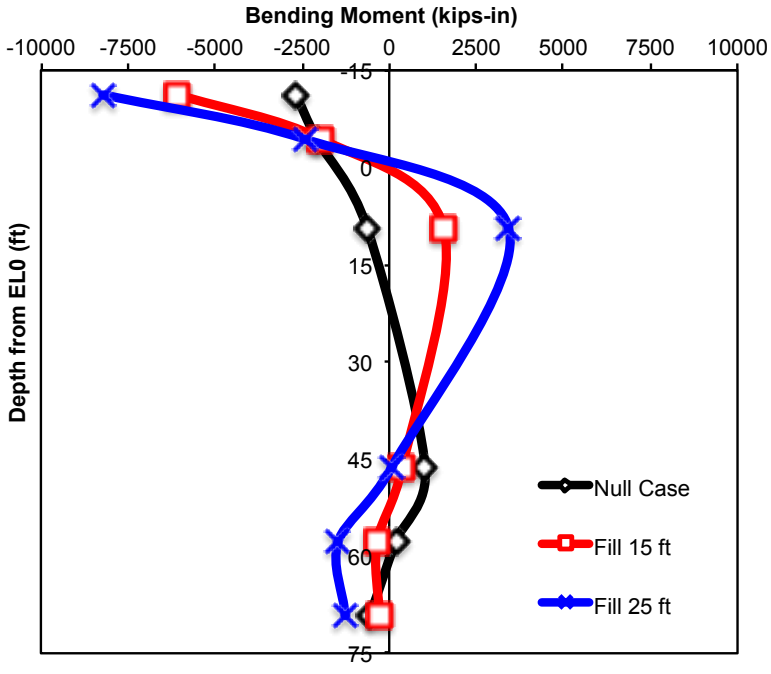

Figure 2.28 Flood Side Pile Moments

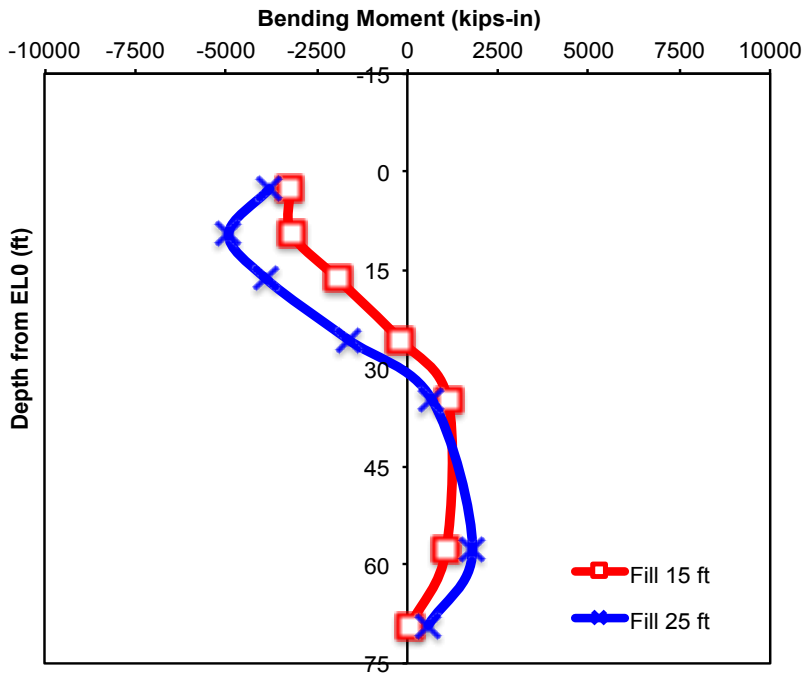

Figure 2.29 Protected Side Pile Moments

Notes: With Respect to the Null Case

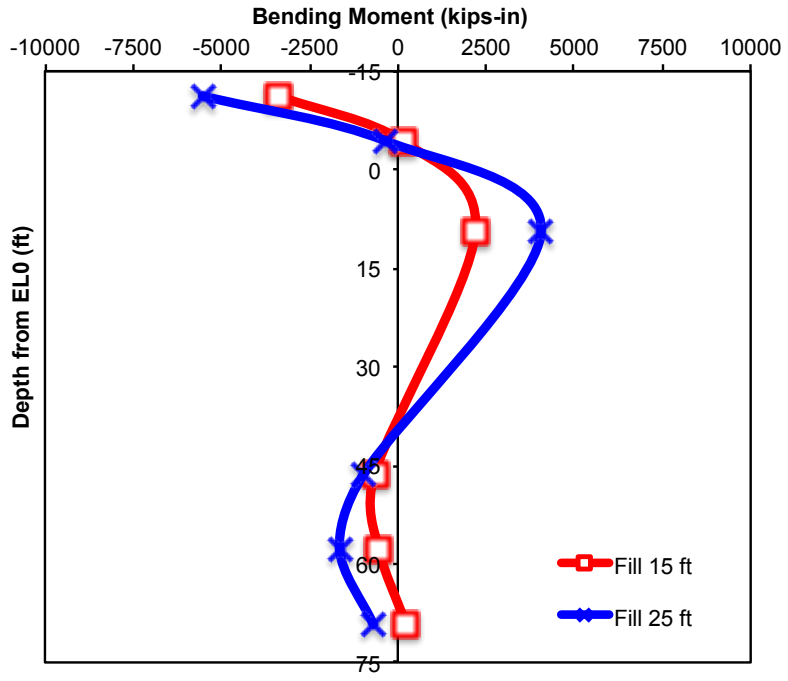

Figure 2.30 Flood Side Pile Moments

Notes: With Respect to the Null Case

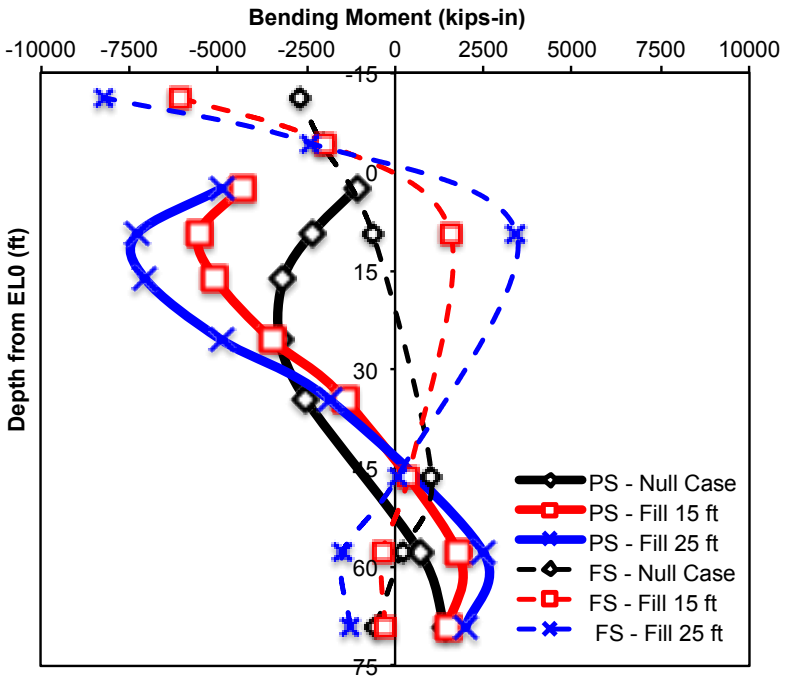

Figure 2.31 Pile Bending Moments

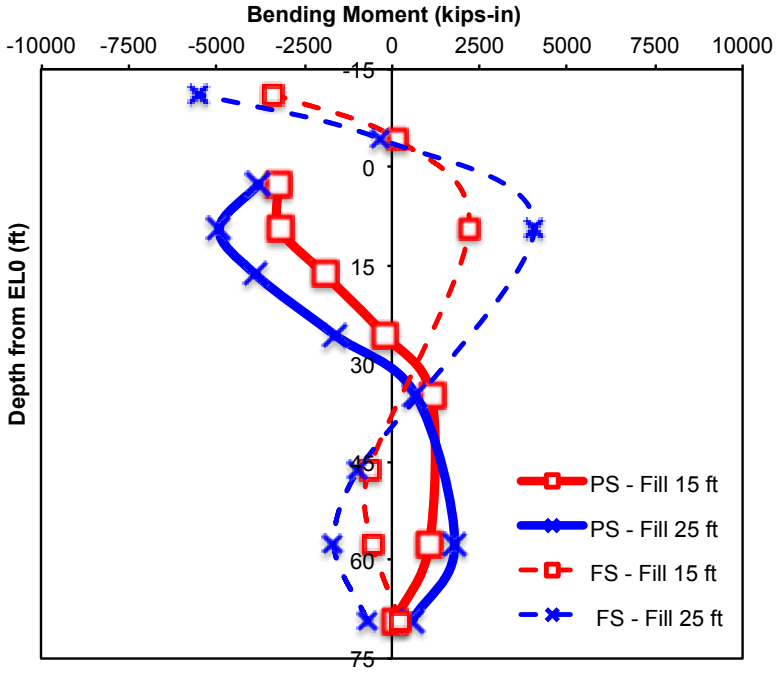

Figure 2.32 Pile Bending Moments

Notes: With Respect to the Null Case

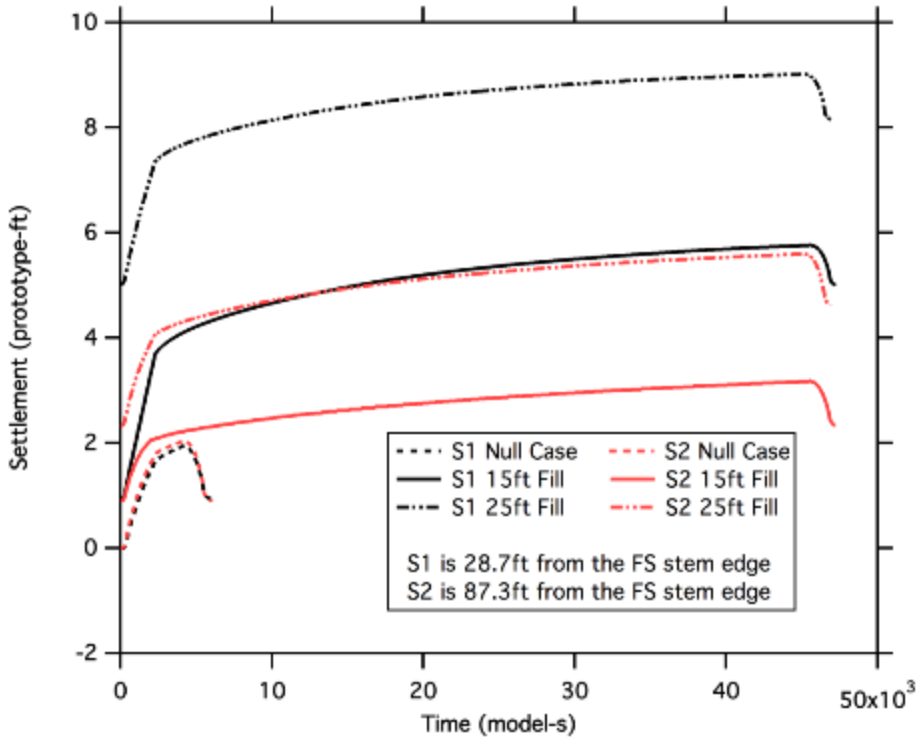

Figure 2.33 Settlement Readings

Figure 2.33 shows the surface settlement during the fill loading phases of Run 2 at two different locations: close to the wall and at a location far enough to be considered free field. As expected and also shown in Figure 2.34, the settlement around the wall where the fill loading was increased reaches higher levels.

The Figures 2.35 and 2.36 show the shear wave velocity profiles for the fill loading of Run 2 and then a comparison versus Run 1. The differences in the extent of the fill loading between Run 1 and 2 are apparent in the final loading stage. The bender elements were placed away from the T-Wall and experienced less overburden in the case of limited lateral extent fill geometry. Figure 2.37 shows a comparison of the post-

experiment water contents sampled from three zones in the model: under the T-Wall, on the protected side, and on the flood side.

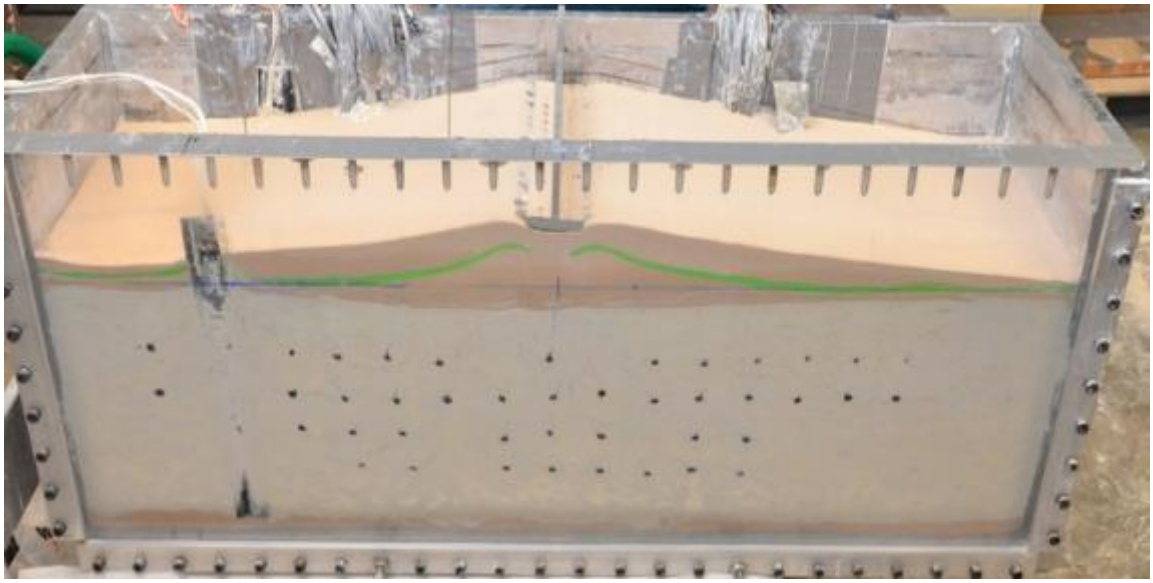

Figure 2.34 Model at the End of the Test

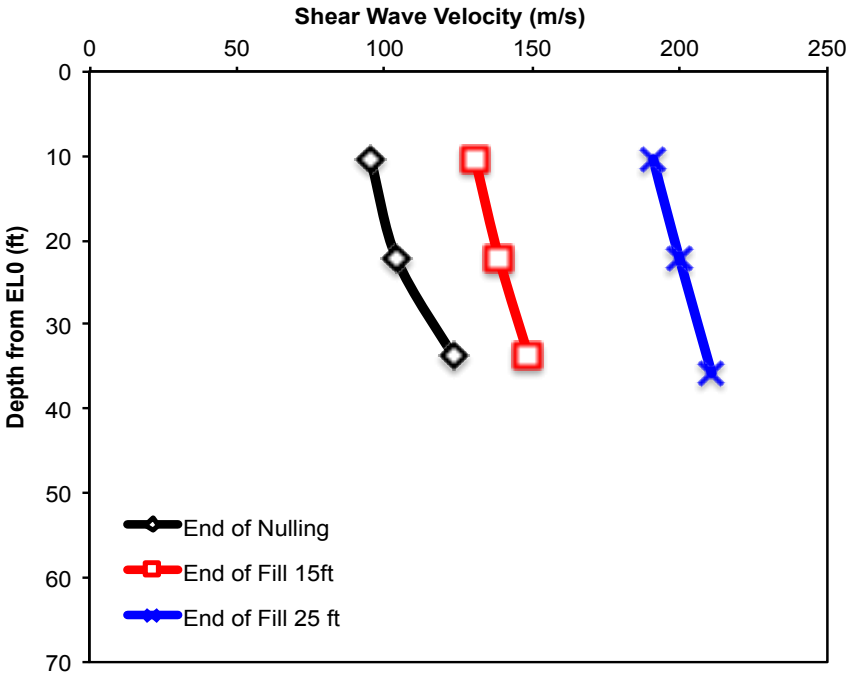

Figure 2.35 Shear Wave Velocity Profiles

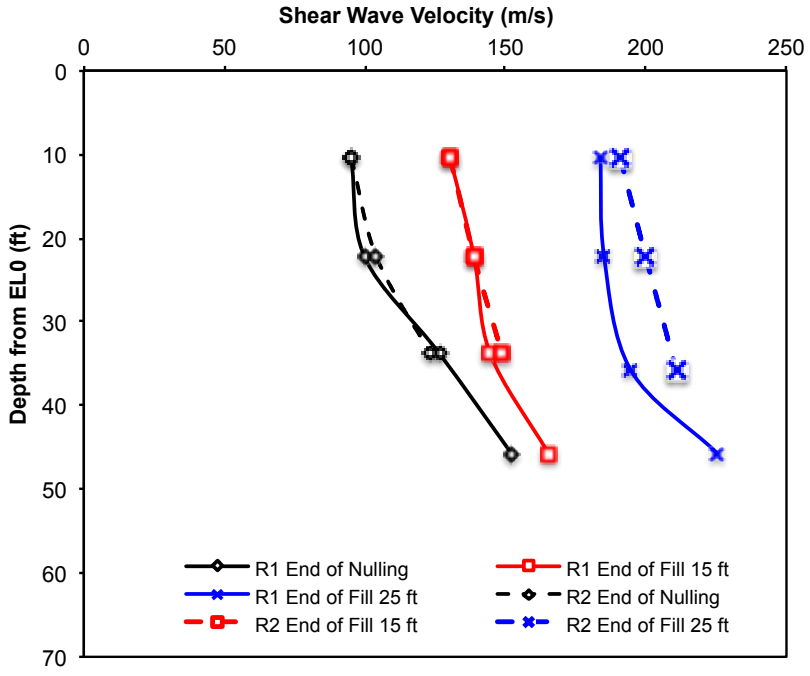

Figure 2.36 Shear Wave Velocity Profiles

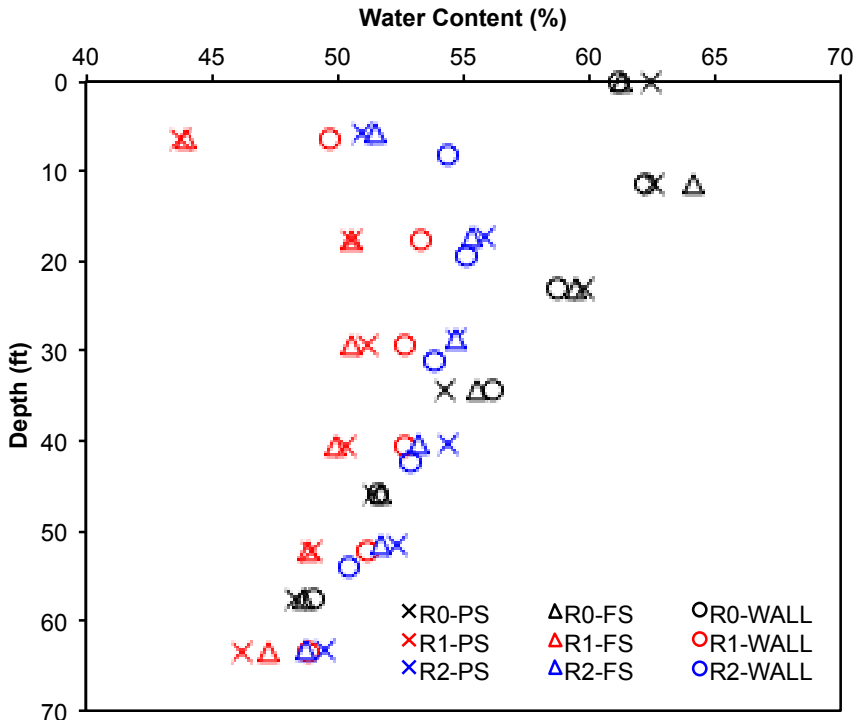

Figure 2.37 Post-Experiment water contents

CHAPTER III

MVN FLAC MODELING

3.1 Summary of MVN FLAC Model

Numerical modeling is an analysis tool that can be used to analyze complex problems. FLAC is a two-dimensional finite difference numerical modeling program developed by Itasca that has been tailored towards the analysis of geotechnical engineering problems (FLAC 2011). Version 7 was used for this thesis. FLAC has been extensively used by USACE and other geotechnical personnel on many other projects (e.g., Reeb et al. 2014, McGuire et al. 2012) which is one of the reasons it was chosen for this research.

The private engineering firm developed FLAC models for the analysis of pile-supported T-walls for a specific reach. In order to provide validation for these analyses, the Run 2 centrifuge test has been modeled using a modified FLAC modeling approach (hereafter referred to as the MVN model).

Due to the differences between the centrifuge test and the specific reach conditions, some changes to the model code had to be made. The soil parameters, fixity at the T-wall base, deletion of the sheet pile cutoff, and a pinned connection at the bottoms of the piles were the main differences between the firm's model and the USACE model. The USACE model included the main elements of the firm's model which were the method to calculate the normal and shear pile-soil coupling springs and the method of

an uncoupled approach to stepping down the pore water pressures. The firm's model also included interface elements but use of interface elements prevents rezoning while running the model. For the specific reach, the settlement was low enough that rezoning was not required, while for this modeling effort, rezoning was required for the larger settlements. The interface elements did not have any assigned bond properties therefore not using them should have zero impact on the results.

This chapter presents an overview of the Run 2 MVN FLAC analyses, including descriptions of the input parameters obtained from the centrifuge testing, and comparisons of the Run 2 MVN FLAC model and centrifuge test results.

3.2 Description of MVN Model

The MVN model was set up to have the same dimensions as the centrifuge test. The minimum zone width and height was 1-ft with a maximum width and height of 3-ft. The minimum zone widths were carried for 102 ft on either side of the center of the model and minimum zone height was carried to a depth of 87 feet from the top of the T-wall (El. -47). These zones transitioned into the maximum zones at a change ratio of 1.1. This resulted in a total number of zones of approximately 16,600. The minimum zones were used in the areas where the highest strains were expected to occur and also the area of greatest interest. The larger zones were used for parts of the model to decrease the total run time of the model and where greater accuracy was not needed. Figure 3.1 shows the undeformed model with the T-walls installed in the 15' fill increment. The T-wall and the embankment are not connected in the grid which allows separation to occur without the use of interface elements. Mohr-Coulomb models were used for the soil

conditions. The FLAC model is divided into 43 steps and takes approximately 2 days to run.

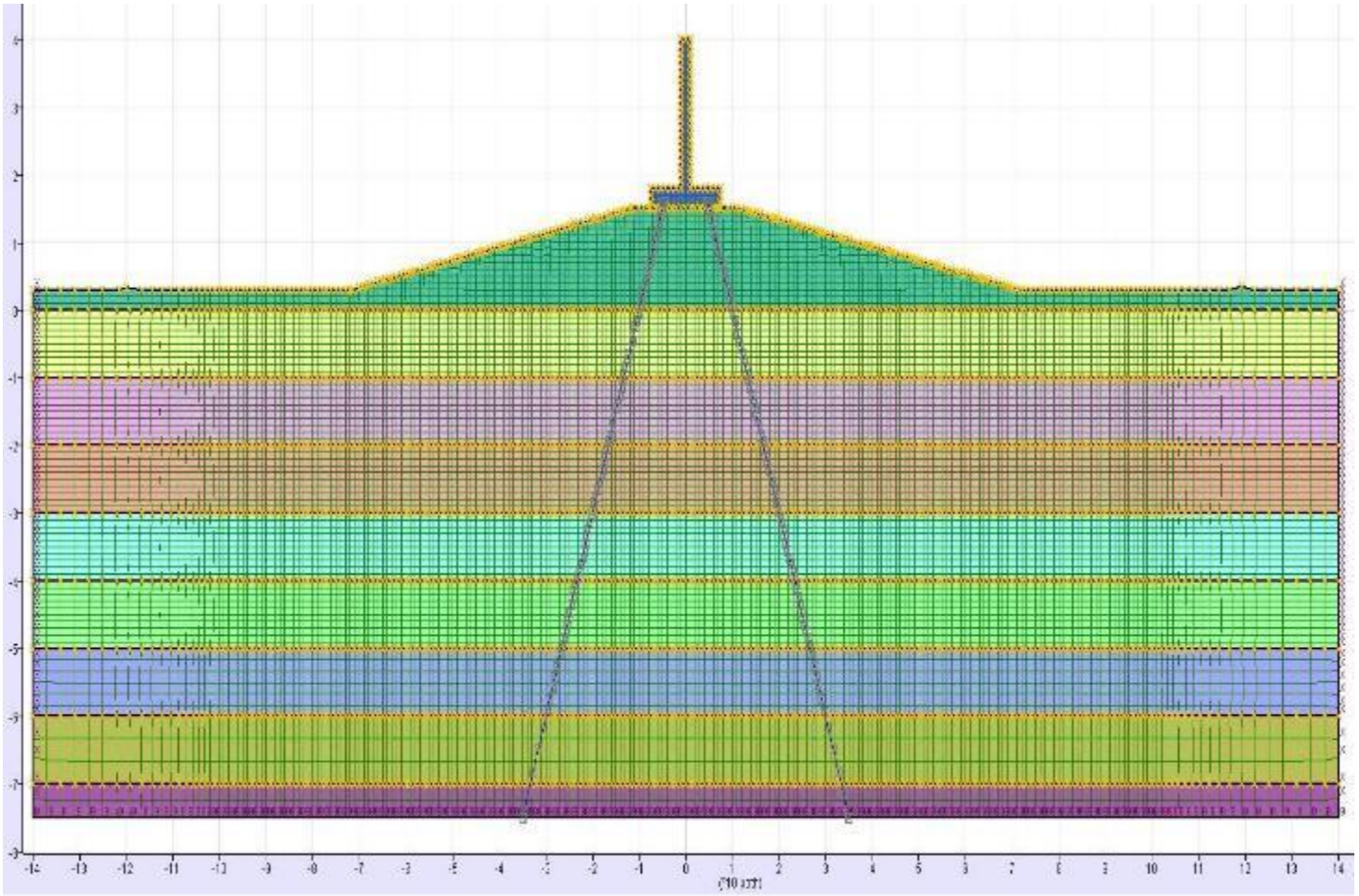

Figure 3.1 Undeformed model

Notes: 15’ fill increment installed. Axis units are in ft.

The MVN FLAC model begins at the "nulling" phase of the centrifuge test. Pore pressures were measured in the centrifuge during consolidation and during the "nulling" phase. Therefore, the preconsolidation pressure profile and the initial pore pressure profile (i.e., hydrostatic pore pressure plus excess pore pressure profile from the "nulling" phase) could be determined based on soil unit weights, elevations, and the pore pressure measurements from the centrifuge. In the MVN FLAC model, the initial stresses and pore pressures were set so that the model is in equilibrium with level ground at El 0 ft. A flat ground "branch" was modeled to show what the stresses should be for a no loading condition and confirm that the model is in equilibrium. The flat ground branch is solved but the stress state is restored to the initial assigned stress state. The preconsolidation pressure profile and the initial excess pore pressure distribution are specified in Table 3.2. The porewater pressures were linearly interpolated between points. The foundation soil properties are given in Tables 3.1 and 3.3. Unit weights, friction angles, compression properties and void ratios were based on discussions with RPI personnel.

The 15 ft placement modeling steps were performed in three iterations in order to develop a better estimate of the drained modulus values for the clay foundation soils. For the first iteration, the modulus values were set based on the initial stresses for level ground at El 0 ft, hand-calculated final stresses based on the height of the sand fill to El 15 ft fill increment without stress distribution, preconsolidation pressures, and the compressibility parameters from Table 3.1. For the second and third iterations, the same procedure is used to set modulus values, but the final stresses from the previous iteration were used instead of the hand-calculated final stresses. This iterative process follows the same approach as the VT modeling approach.

The piles were represented by pile elements instead of zones, and these were connected to the soil grid with pile-soil coupling springs. There were more pile elements near the top and middle of the pile compared to the bottom, as greater accuracy in the results was desired at the top and middle of the pile. The normal pile-soil coupling spring responses were based on the non-linear p-y curves developed by Matlock (1970) for clays and a modified version of Reese (FHWA 1993) for sands. The axial shear pile-soil coupling spring capacities were based on the procedure shown in FHWA (1993). The pile-soil springs were all based on effective stress strength properties, except that the normal pile-soil springs in clay were based on the undrained strength, consistent with the procedures described by Matlock (1970). The piles were pinned at the bottom of the FLAC grid and a fixed connection is modeled at the top of the piles, where they connect to the T-wall. This matches the centrifuge test. To model the fixed condition, the pile was connected to the grid of the T-wall and the pile segment in the T-wall was assigned a much higher value of Young's modulus. This resulted in an extra stiffening of the pile in the T-wall and ensured a fixed connection in the model. The pile and T-wall properties are given in Table 3.4.

Since the piles extend from the bottom of the model to the base of the T-wall at El 15 ft, all of the sand fill to El 15 ft needs to be placed before allowing the clay foundation soils to consolidate under the sand fill load. However, rapidly applying a large load to a material that is not linear elastic in FLAC will shock the model and lock in dynamic stresses and displacements. Therefore, in order to minimize inertial effects and to better simulate the slow consolidation of the clay foundation soils, the density of the sand fill to

El 15 ft is slowly incrementally increased from a low initial value to the final actual value while the model is solved.

To calculate the excess porewater pressure that would be generated during the 15ft and 25 ft fill placement, the fill was placed and the model solved in small strain mode. The stresses generated by this were then compared to the vertical effective stresses in a flat ground case or the 15ft fill case as needed and the difference in vertical effective stress was determined to be the excess porewater pressure that would be generated by the fill placement. These porewater pressures were then used for the consolidation analysis. The porewater pressures were then input in the model and large strain was turned on for the consolidation analysis.

Fill increments were consolidated using an uncoupled sequence. An uncoupled approach has flow steps and mechanical steps occur independently of each other. Flow steps occur for a set "age" and after this age is reached mechanical steps were taken to bring the model into equilibrium. The advantage of an uncoupled model is a significant increase in model speed compared to a fully coupled model. The model is stopped when the porewater pressure is reached in zones that match the final porewater pressure. The porewater pressure is updated as fill settles below the groundwater table at El. 0 to ensure that the correct unit weights were being applied in the model. To ensure that the correct final porewater pressure is obtained across the entire model, the final porewater pressure profile from the centrifuge test is then imposed and the model is solved for the final stresses and bending moments in the piles. The final pore pressure distribution after consolidation in the centrifuge under the 25-ft fill increment is about the same as after

consolidation under the 15-ft fill increment, as indicated in Table 3.5 which matches the centrifuge test.

The sand fill to El 25 ft was simulated using equivalent forces. This was done to avoid excessive "stretching" of soil zones which would cause bad geometry errors and also to be able to place additional fill underneath the T-wall base. Forces were placed under the T-wall base to simulate the fill that came through the T-wall base during the centrifuge test. Simulating the new fill with soil zones would have been extremely difficult and was not considered to have much added benefit.

These fill placement modeling steps were performed in three iterations in order to develop a better estimate of the drained modulus values for the clay foundation soils. For the first iteration, the modulus values were set based on the model stresses after consolidation under the sand fill to El 15 ft, hand-calculated final stresses based on the height of the sand fill to El 25 ft fill increment without stress distribution, preconsolidation pressures, and the compressibility parameters from Table 3.1. For the subsequent iterations, the same procedure is used to set modulus values, but the final stresses from the previous iteration were used instead of the hand-calculated final stresses. This process results in an enhanced accuracy related to issues that depend on the stress states.

The final order of steps is listed below:

1. Model geometry was created without piles. Properties were then assigned to all the soil zones and the T-wall.
2. A flat ground branch "nulls" the embankment and the T-wall and was solved with the final stresses recorded.

3. An original branch begins and the piles were placed in the model. The pile properties were reassigned due to coding issues as noted earlier.
4. The embankment's density is slowly applied in mechanical steps to avoid shocking the model. This is done in small strain mode. When the embankments density reaches the final density the model is then solved and the stresses recorded.
5. Recorded stresses from the previous step were compared to the stresses from the flat ground case. The difference in the vertical effective stress was considered the porewater pressure that would be generated by the fill being placed.
6. The porewater was placed in the model.
7. The model then began an uncoupled consolidation analysis. At the beginning of this model, an artificially high strength was applied to the soil embankment to keep the model stable. This strength was stepped down as the porewater dissipates. A preset porewater pressure was checked as the model cycles and if certain zones hit this pressure the model was stopped. A final porewater pressure profile was imposed on the model and then the model was allowed to solve.
8. The final stresses from the consolidation step are recorded and the model was reset.
9. The final stresses from the previous iteration were used to calculate modulus values.
10. Steps 4-9 were then repeated until 3 iterations were completed.

11. After the 3rd iteration for the 15 ft. increment is performed, equivalent forces representing the 25 ft. increment were slowly added in a manner similar to the way the 15 ft. increment was applied.
12. Recorded stresses from the previous step were compared to the stresses from the 15 ft. increment. The difference in the vertical effective stress was considered the porewater pressure that would be generated by the fill being placed.
13. The porewater was placed in the model.
14. The model then began an uncoupled consolidation analysis. At the beginning of this model, an artificially high strength was applied to the soil embankment to keep the model stable. This strength was stepped down as the porewater dissipates. A preset porewater pressure was checked as the model cycles and if certain zones hit this pressure the model was stopped. A final porewater pressure profile was imposed on the model and then the model was allowed to solve.
15. The final stresses from the consolidation step were recorded and the model was reset.
16. The final stresses from the previous iteration were used to calculate modulus values.
17. Steps 11-16 were then repeated until 3 iterations were completed.
18. Final stresses and bending moments were extracted from the model for both the 15 ft. increment and the 25 ft. increment.

3.3 MVN FLAC Model Input Parameters

There are three main categories of input parameters to the MVN FLAC model which are the physical dimensions of the model, the soil material properties, and the initial and final pore pressure distribution. These parameters were obtained from laboratory tests or centrifuge testing, or they were estimated. These parameters match the parameters used in the VT FLAC model. This was done so that a true comparison of modeling techniques could be performed. The parameters where chosen carefully as these can have large impacts on the computed stresses and bending moments (Dong et al. N.D.)

1. Model configuration and dimensions – Figure 3.2 shows the Run 2 cross section and configuration. The pile dimensions are listed in Table 3.4. In the Run 2 centrifuge test and FLAC model, the sand fill loading is placed based on mass as determined from the undeformed cross section show in Figure 3.1.
2. Material properties – Tables 3.1 and 3.3 list the soil material properties, and Table 3.4 lists the structural material properties. Many of the clay soil property values were measured in the laboratory or during centrifuge testing as described in the table footnotes.
3. Pore pressures – Table 3.2 specifies the preconsolidation pressure profile and initial excess pore pressure distribution, and Table 3.5 specifies the final pore pressure distribution after consolidation under the 15-ft or 25-ft sand fill increments. As described in the Table 3.2 footnotes, the preconsolidation pressure profile was estimated based on soil unit weights,

elevations, and the pore pressure measurements from the centrifuge after initial consolidation under the surcharge load.

Since the foundation soil is generally underconsolidated (with respect to level ground at El 0 ft) after initial consolidation under the surcharge load, excess pore pressures are present in the foundation soil during the "nulling" phase. The MVN FLAC model begins at the "nulling" phase of the centrifuge test, and so the values of excess pore pressure from Table 3.2 are used initially in the FLAC model.

Additional details of the input parameters are provided in Figure 3.2 and Tables 3.1 to 3.5.

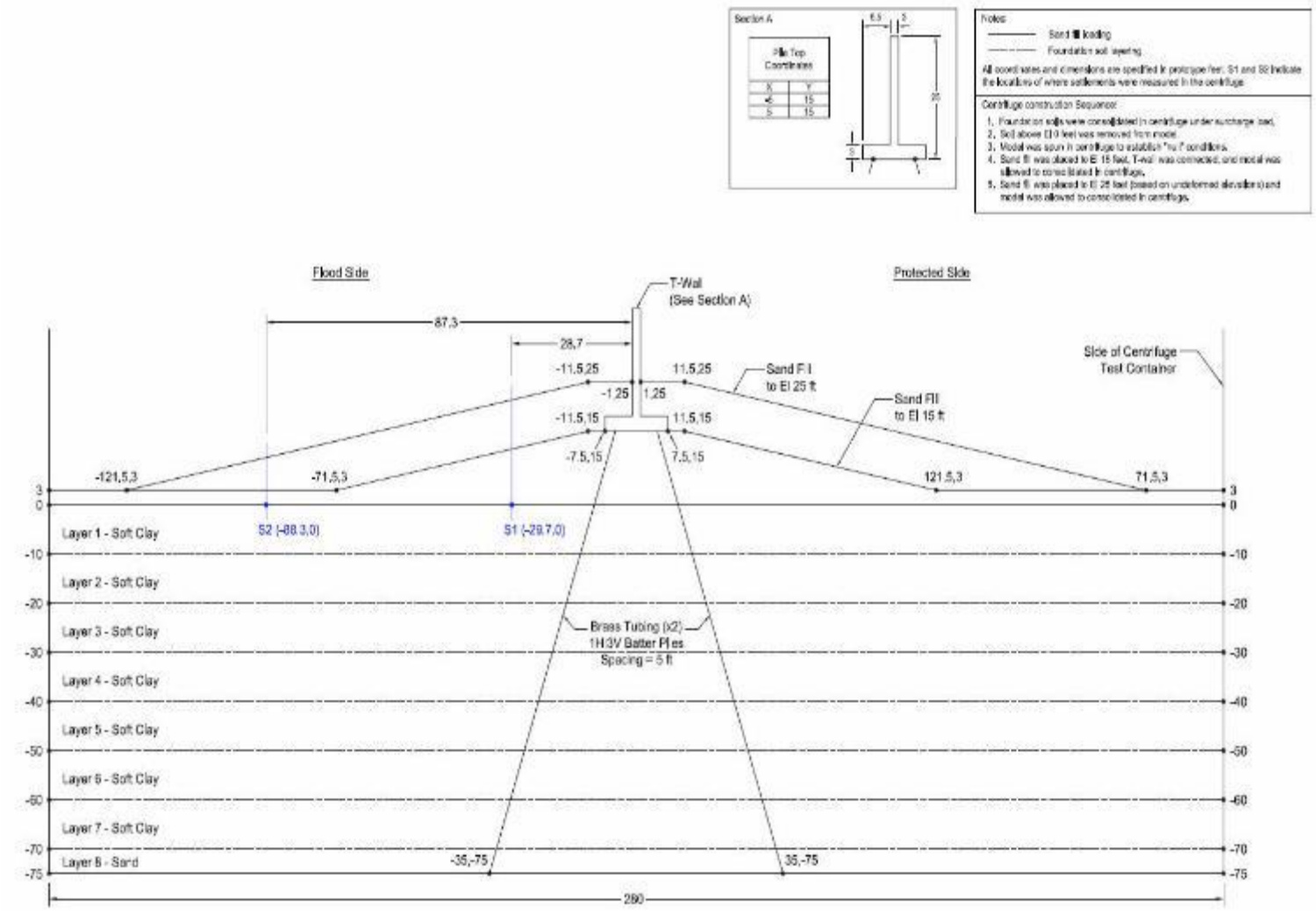

Figure 3.2 General Cross-section

Table 3.1 Soil Stratigraphy and Properties

Layer	*Top El (ft)*	*Bottom El (ft)*	*Unit Weight, γ_m or γ_{sat} (pcf)[1]*	*ϕ' (deg)[2]*	*c' (psf)[2]*	*Su_{top}[3] (psf)*	*Su_{botom}[3] (psf)*	*Comp. Ratio, $C_{c\varepsilon}$[4]*	*Recomp. Ratio, $C_{r\varepsilon}$[4]*	*Void Ratio[5]*
Sand Fill	*Varies*	*0*	*100*	*36*	*0*	-	-	-	-	*0.001*
1 – Soft Clay	*0*	*-10*	*98*	*20*	*0*	*380*	*325*	*0.162*	*0.0198*	*1.89*
2 – Soft Clay	*-10*	*-20*	*98*	*20*	*0*	*325*	*300*	*0.162*	*0.0198*	*1.89*
3 – Soft Clay	*-20*	*-30*	*98*	*20*	*0*	*300*	*310*	*0.162*	*0.0198*	*1.89*
4 – Soft Clay	*-30*	*-40*	*98*	*20*	*0*	*310*	*365*	*0.162*	*0.0198*	*1.89*
5 – Soft Clay	*-40*	*-50*	*98*	*20*	*0*	*365*	*470*	*0.162*	*0.0198*	*1.89*
6 – Soft Clay	*-50*	*-60*	*98*	*20*	*0*	*470*	*630*	*0.162*	*0.0198*	*1.89*
7 – Soft Clay	*-60*	*-70*	*98*	*20*	*0*	*630*	*810*	*0.162*	*0.0198*	*1.89*
8 – Sand	*-70*	*-75*	*100*	*36*	*0*	-	-	-	-	*0.77*

Notes:
[1]The water table is at El 0 ft throughout the fill loading phases of the analysis. Unit weights are estimated based on discussions with RPI.
[2]The effective stress strength parameters for the sand and CU triaxial test results for the clay, which were used to estimate effective stress strength parameters for the clay, are provided in Tessari (2012).
[3]The undrained strength profile for the clay is based on T-Bar testing from the Run 1 centrifuge test as described in Section 3.8.
[4]The clay soil consolidation parameters are based on laboratory consolidation test results (Tessari 2012).
[5]A very small void ratio is used for the sand fill so that the unit weight can be correctly set and incrementally increased during steps of the FLAC analysis. Overall, there is very little volumetric deformation of the sand fill, so it is not necessary to adjust the sand fill unit weight due to small changes in volume and void ratio. Void ratios for other soil layers are estimated based on saturated unit weights and a specific gravity of 2.65 for the clay and 2.67 for the sand (Tessari 2012).

Table 3.2 Preconsolidation Pressures & Initial Pore Pressures

Layer	Top El (ft)	Bottom El (ft)	Pc_{top} (psf)[1]	Pc_{botom} (psf)[1]	Ux_{top} (psf)[2]	Ux_{mid} (psf)[2]	Ux_{bot} (psf)[2]
1 – Soft Clay	0	-10	244	223	0	105	208
2 – Soft Clay	-10	-20	223	348	208	309	408
3 – Soft Clay	-20	-30	348	619	408	500	555
4 – Soft Clay	-30	-40	619	1036	555	580	574
5 – Soft Clay	-40	-50	1036	1599	574	542	485
6 – Soft Clay	-50	-60	1599	2308	485	402	294
7 – Soft Clay	-60	-70	2308	3163	294	160	0

Notes:
[1]The preconsolidation pressure profile was estimated based on soil unit weights, elevations, and the pore pressure measurements from the centrifuge after initial consolidation under the surcharge load. At the end of the initial consolidation phase, the top of the surcharge load was at El 13.5 ft, and it consisted of 3 ft of sand overlaying clay surcharge and clay foundation soil. The saturated and moist unit weight of the sand was assumed to be 100 pcf, and the saturated and moist unit weight of the clay was assumed to be 98 pcf.
[2]The initial excess pore pressure is the excess pore pressure during the "nulling" phase of the Run 2 centrifuge test, and these values are used initially in the numerical model.

Table 3.3 Soil Elastic Properties

Layer	Young's Modulus, E (psf)[1]	Poisson's Ratio, ν[2]
Sand Fill	$1x10^6$	0.29
Sand, Layer 8	$1x10^6$	0.29

Notes:
[1]The value of Young's modulus is an estimate from RPI.
[2]The Poisson's ratio is estimate based on the drained friction angle from Table 1 and $\nu=(1- \sin(\phi'))/(2- \sin(\phi'))$ from Duncan et al. (2007).

Table 3.4 Structural Material Properties

Layer	Effective Width x Effective Length (in)[1]	Area (in^2)	Moment of Inertia (in^4)	Unit Weight (pcf)[2]	Young's Modulus (psi)	Poisson's Ratio, ν
Aluminum T-wall	-	-	-	168	$4.17x10^6$	0.155
Brass Piles	12.6 x 19.7	47.6	1780	0	$1.50x10^7$	-

Notes:
[1]The effective width accounts for the presence of the strain gauges and wires along the instrumented piles that were used to measure pile bending moments in the centrifuge.
[2]The actual unit weight of the piles is 532 pcf. However, in the FLAC analysis the piles were assumed to be weightless because any bending due to self-weight was zeroed out during the centrifuge nulling phase.

Table 3.5 Final Pore Pressure Distribution

Elevation (ft)	Pore Pressure (psf)
0	0
-20	1300
-37	2550
-53	3310
-70	4368

Note:
In the Run 2 centrifuge test, the final pore pressure distribution measured after consolidation under the sand fill to El 15 ft was very similar to the final pore pressure distribution after consolidation under the sand fill to El 25 ft. Therefore, the same final pore pressure was used in the numerical model during placement of both the 15-ft and 25-ft sand fill increments. The pore pressure distribution is close to hydrostatic, but the pore pressures are slightly higher towards the center of the clay layer since the clay foundation soils did not fully consolidate in the centrifuge under the 15-ft or 25-ft sand fill increments.

3.4 MVN FLAC Model and Centrifuge Test Results

This section shows the results of the MVN FLAC model and also presents a comparison of the Run 2 MVN FLAC model and centrifuge test results. These results are then used to explain the related events and predictions that can be based on these results.

3.4.1 Results of MVN FLAC Model

The results of the MVN FLAC model show that large settlements produce corresponding large bending moments in the piles. This result was expected and confirms the centrifuge test. It is interesting to look at the effect of the piles in the embankment and the effect the piles have on the stress levels and the displacements. The piles produce a significant shielding effect on the soil between the piles as seen in the vertical effective stress and horizontal effective stress contours as seen in Figures 3.3 and 3.4 (compression stresses are negative in the FLAC model). This effect is more pronounced in the 25 ft increment in the vertical effective stress and horizontal effective stress contours (Figures 3.5 and 3.6). The difference in the degree of shielding between the 15 ft and 25 ft fill increments is most likely due to how the fill was placed. The 15 ft fill embankment between the piles is placed at the same time as the piles so the clay foundation has not yet had a chance to consolidate from this fill placement. Therefore significant amounts of stress are still being placed on the soil which the piles can not affect. For the 25 ft fill increment, most of the new fill is being placed outside the pile area and the piles are able to shield the foundation in between to a greater degree. This is useful to note as any subsequent soil sampling that is done in the area would not be accurate across the width of the embankment. The soil in between the piles would be expected to be softer and less consolidated than the soil immediately outside the piles.

The piles produce high stress concentrations in their immediate vicinity due being in the path of the soil settlement for the pile foundation. This in turn causes high axial loads and bending moments. These are discussed further in section 3.4.2.

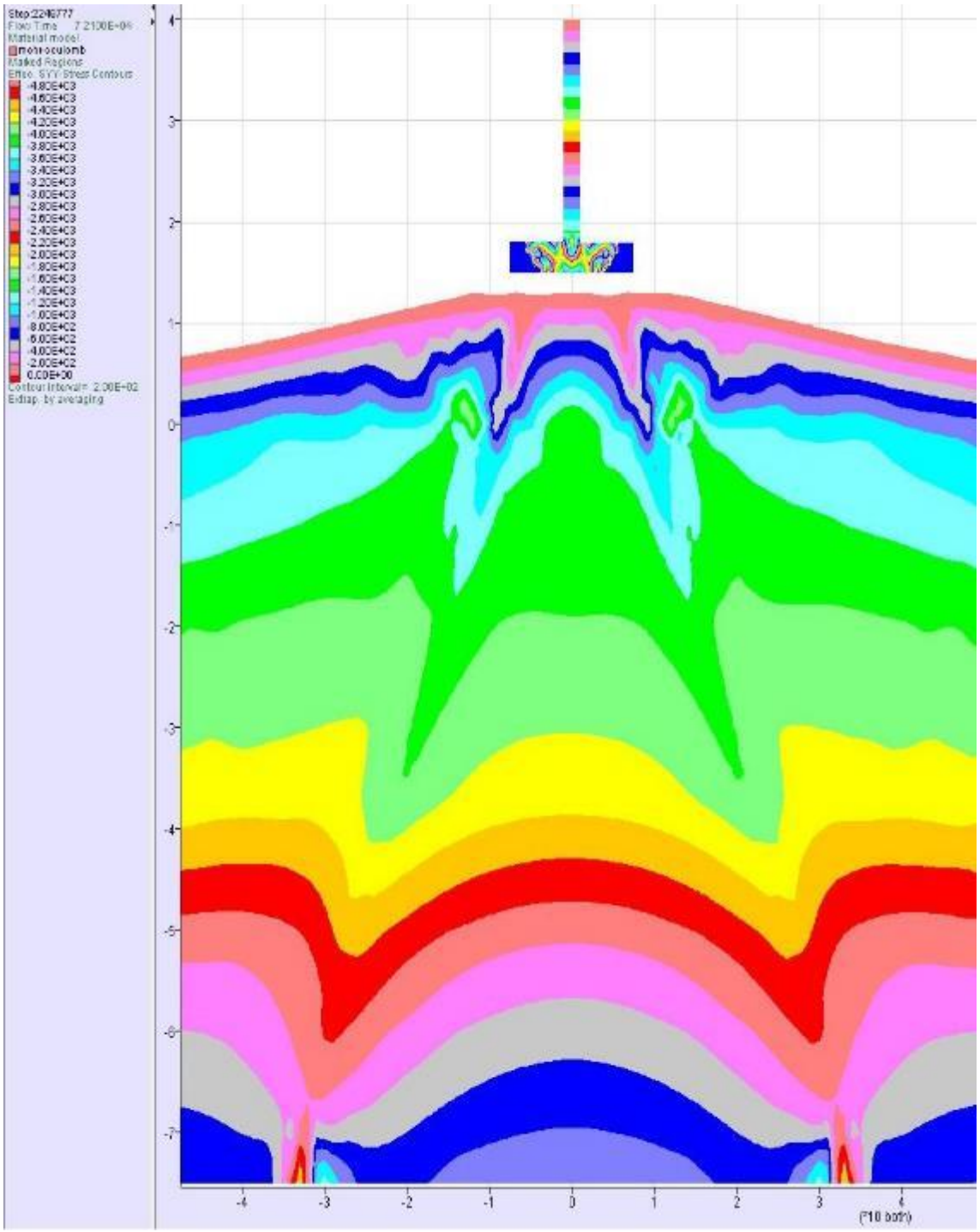

Figure 3.3 Vertical Effective Stress Contours

Notes: 15’ increment. Axis Units - ft.; Stress - psf

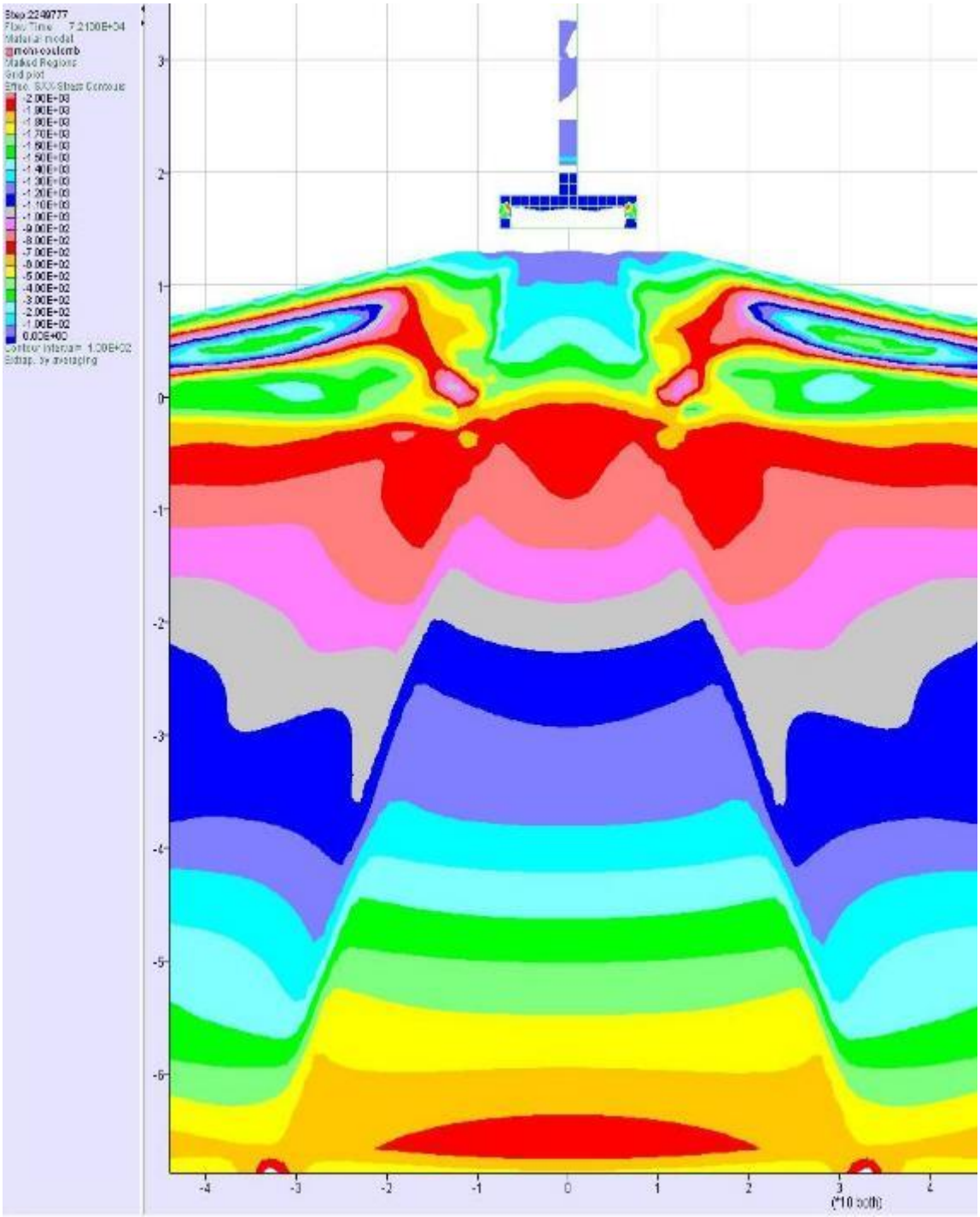

Figure 3.4 Horizontal Effective Stress Contours

Notes: 15’ increment. Axis Units - ft.; Stress - psf

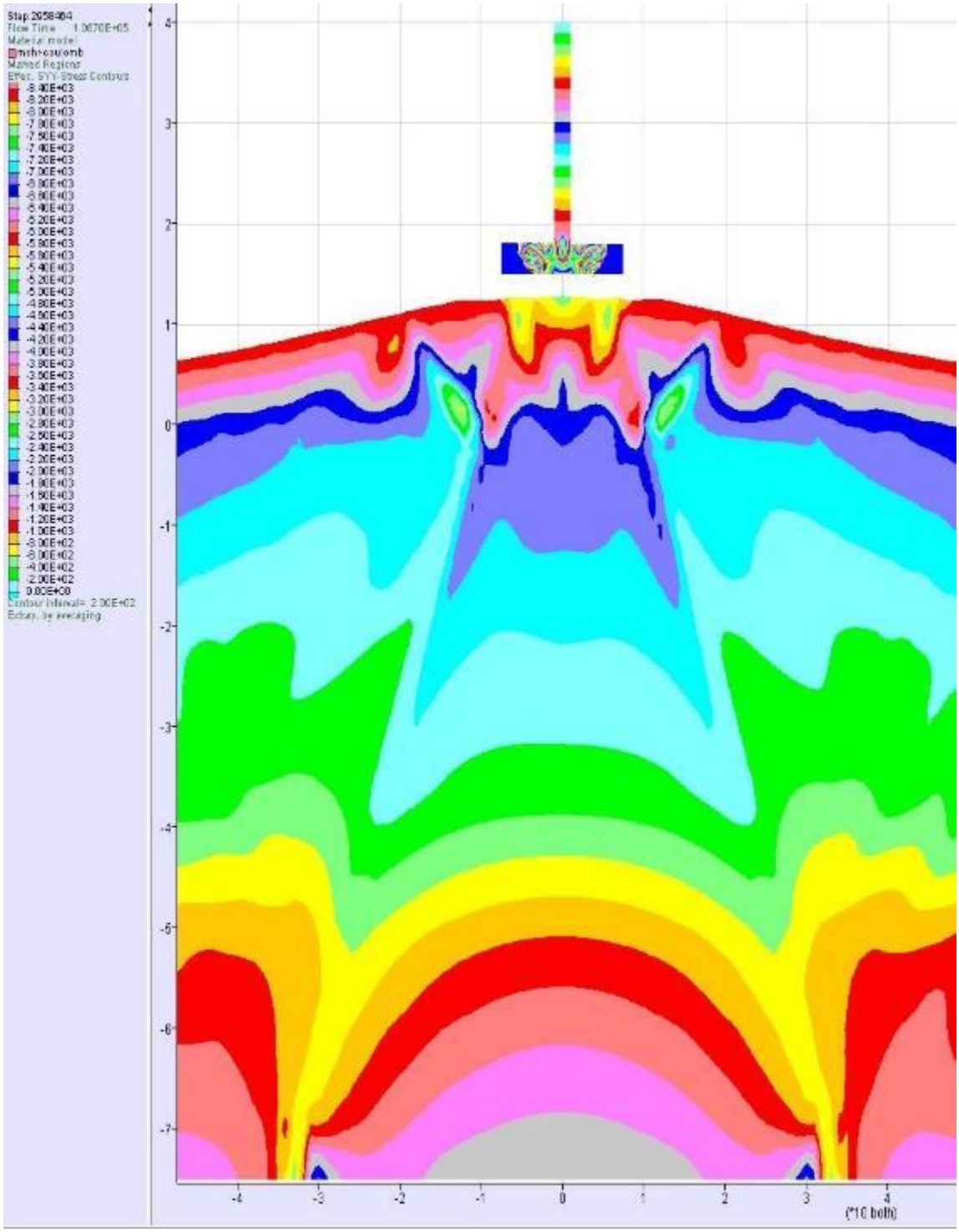

Figure 3.5 Vertical Effective Stress Contours

Notes: 25’ increment. Axis Units - ft.; Stress - psf

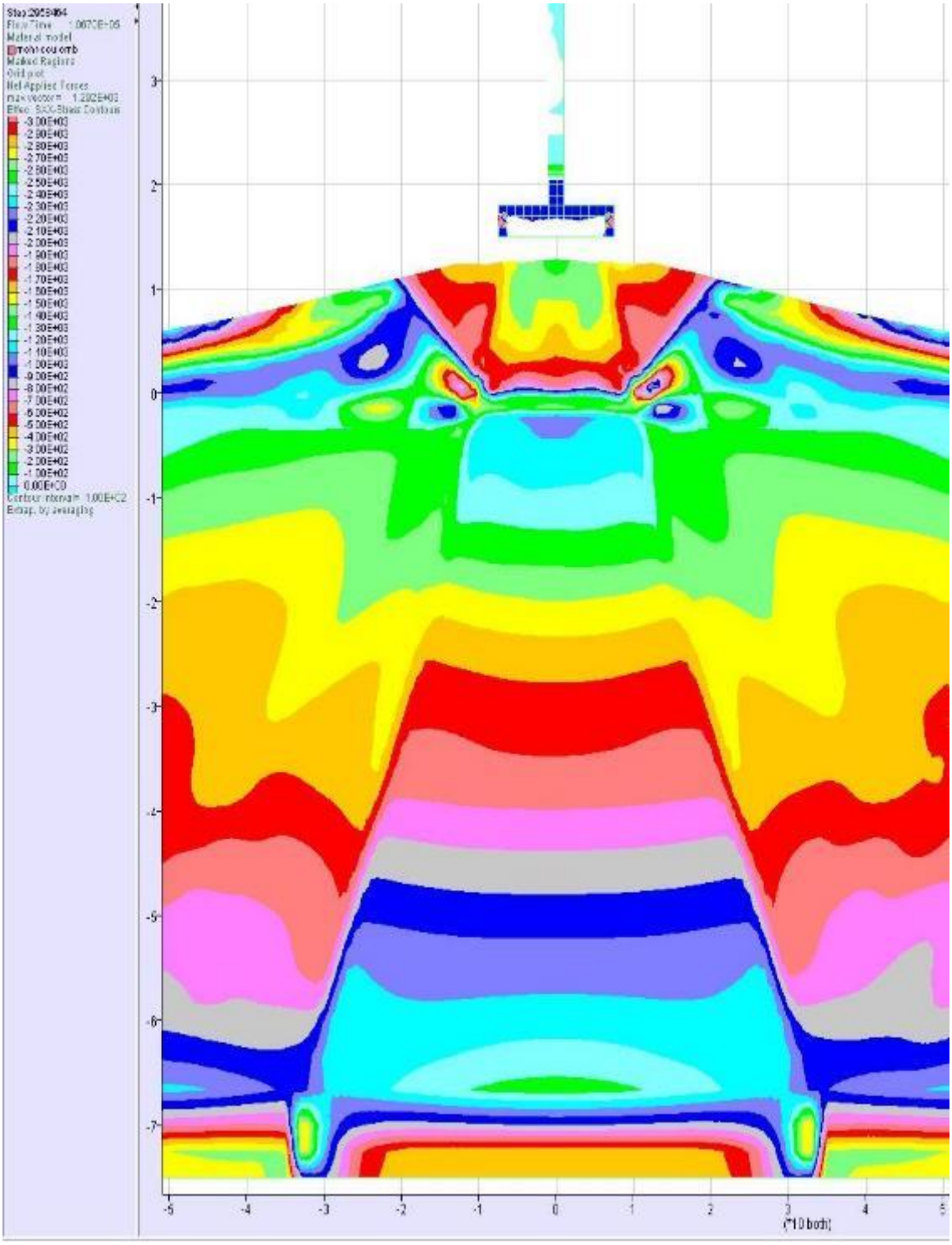

Figure 3.6 Horizontal Effective Stress Contours

Notes: 25’ increment (Axis Units - ft. ; Stress - psf)

The shielding effect of the pile is noticed in the vertical displacements as seen in Figures 3.7 and 3.8. The displacements on the outside of the piles are greater than the displacements on the inside of the piles. This is expected since the stresses are directly related to the displacement. The shielding effect is not total, however, and some soil displaces into between the piles as seen in Figures 3.9 and 3.10. This is expected otherwise the fill on the inside of the pile sections would be much higher than outside of it. Some "stretching" of the soil zones do occur in the model but this does not seem to be significant.

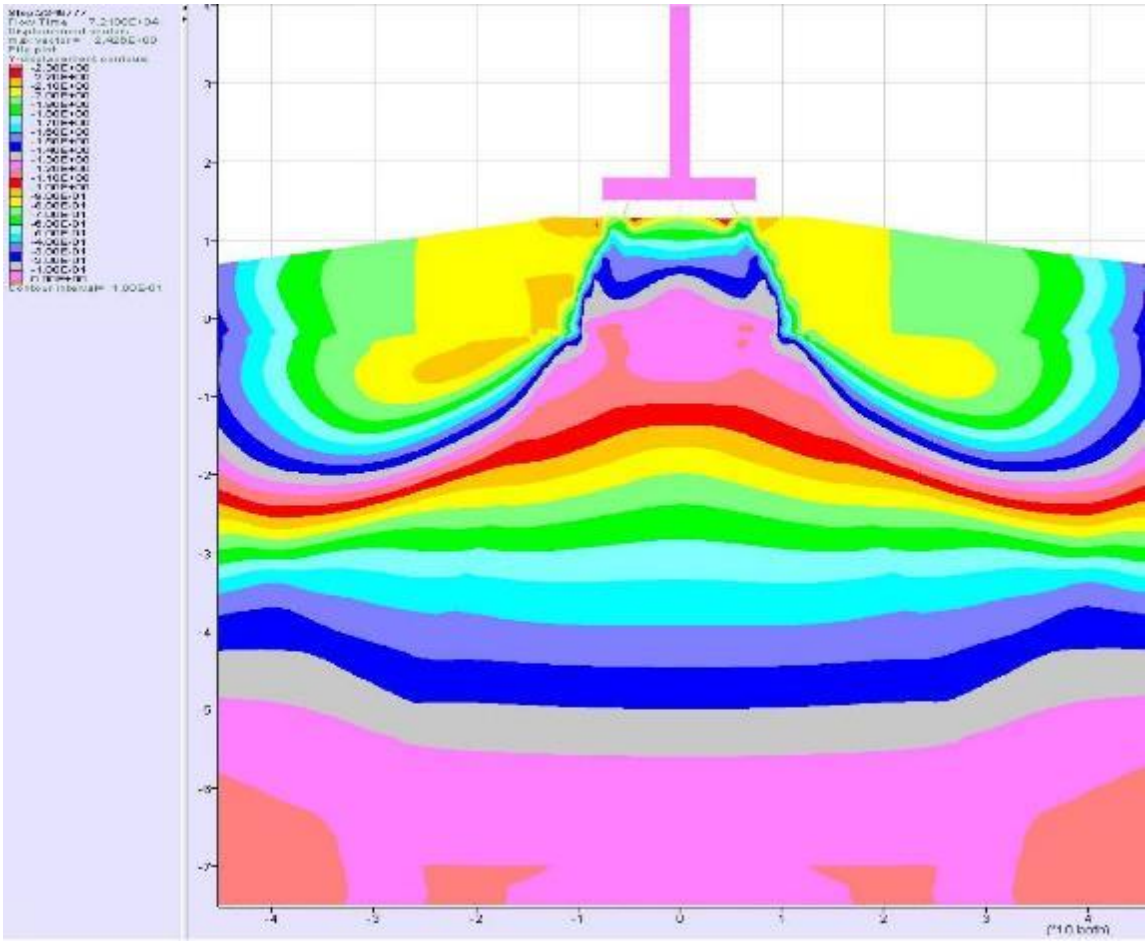

Figure 3.7 Vertical Displacements

Notes: 15’ fill increment. Axis Units – ft; Displacement - ft

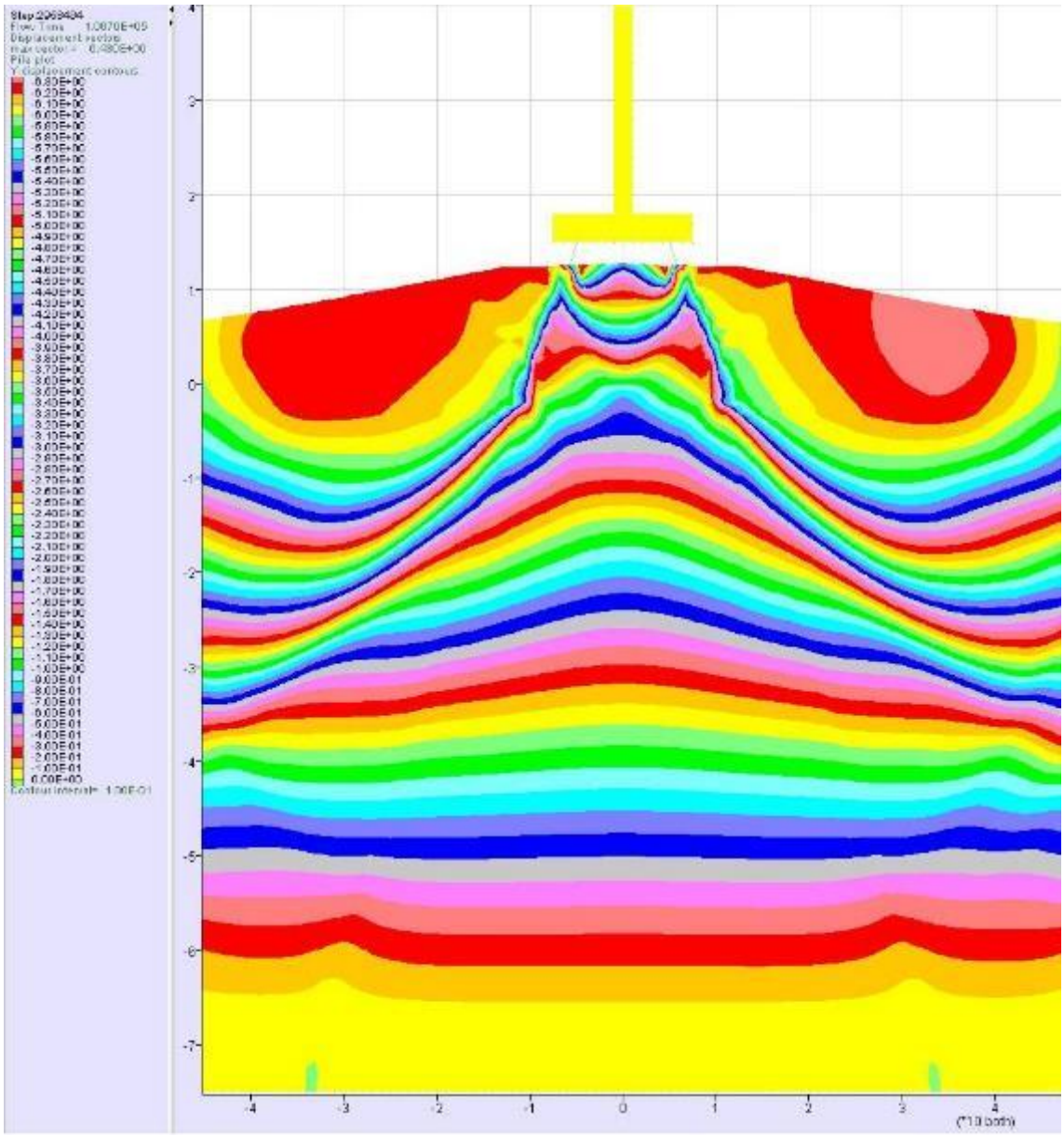

Figure 3.8 Vertical Displacements

Notes: 25’ fill increment. Axis Units – ft; Displacement - ft

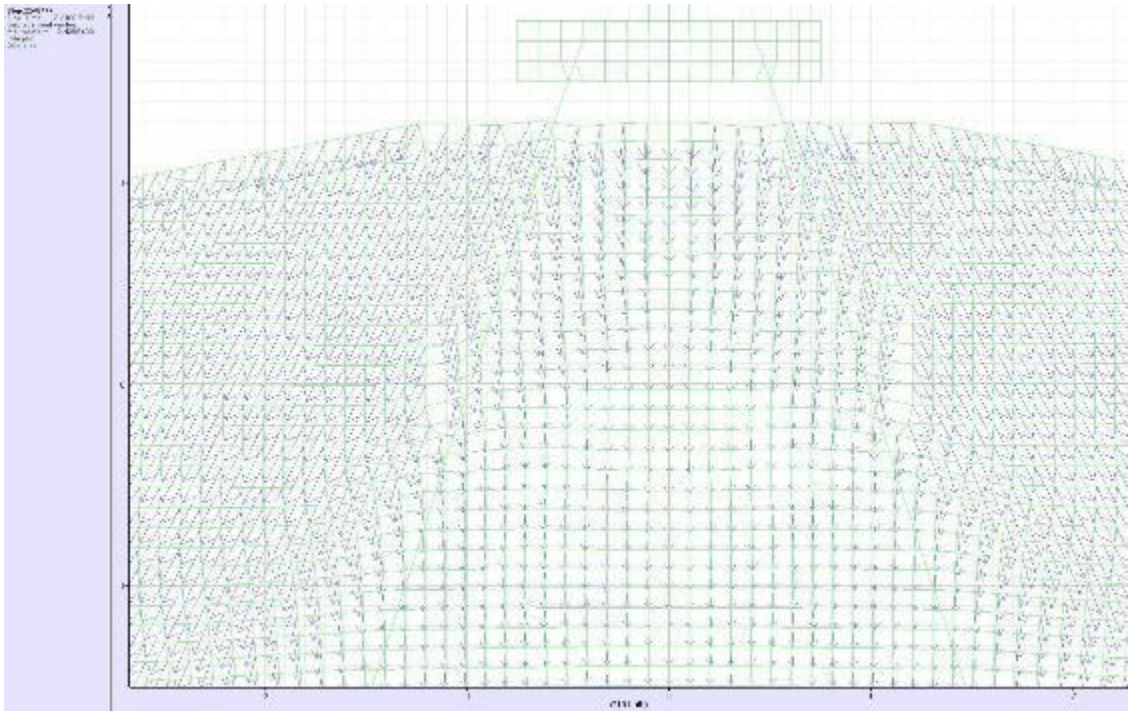

Figure 3.9 15’ fill Displacement Vectors

Notes: Axis Units – ft; Displacement - ft

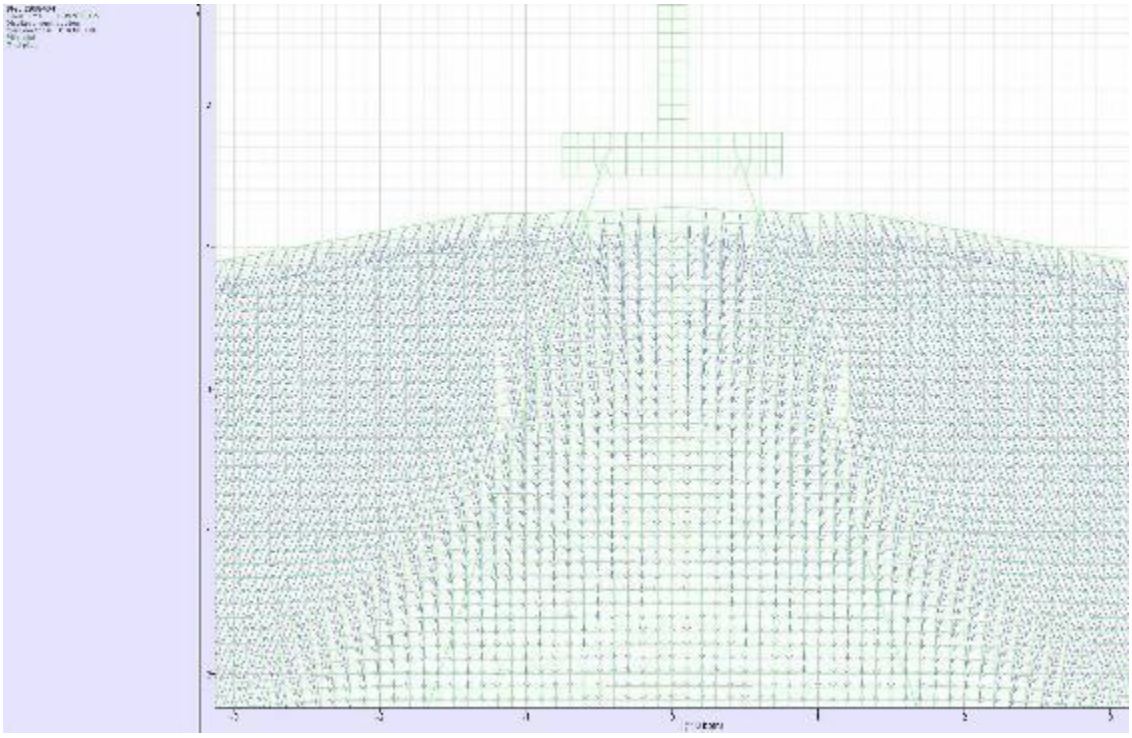

Figure 3.10 25’ fill increment Displacement Vectors

Notes: Axis Units – ft; Displacement - ft

3.4.2 Comparison of MVN FLAC Model and Centrifuge Test Results

3.4.2.1 Settlement of the Clay Foundation Soils

Figure 3.11 shows a comparison of the settlements predicted by the MVN FLAC model and as measured during the centrifuge test after consolidation under the 15-ft and 25-ft fill loading increments. The locations of S1 and S2 are the same as the ones in the VT Model. The settlements predicted by the MVN FLAC model are lower than the settlements measured in the centrifuge tests. This can be explained by MVN’s modeling procedure. MVN’s model solves the stresses in small strain mode with a set pore water pressure than converts the difference in stresses to an excess pore water pressure. The model resets the velocities and displacements and then consolidates the model. This zero

outs the values for the displacements that happened due to deformation caused by loading and not by consolidation settlement. This would by necessity result in lower displacements than seen in the centrifuge but does not result in lower bending stresses in the piles. The bending stresses that were developed by the model in small strain mode are still in the piles and are not zeroed out. So the moments that are caused by the displacement of the soil not caused by settlement are still in the model. Therefore when the settlement occurs then there is additional moment added due to the settlement and not deformation due to fill loading.

This issue is mainly significant only during the 15' fill increment case. For the 25' fill increment, significant settlement and consolidation has already taken place so the addition of the 25' fill increment does not produce the same amount of deformations as the 15' fill increment. This can be seen in the change in the settlement values for the MVN FLAC model between the 15' increment and the 25' increment. The value for S1 changes by 3.03' for the MVN FLAC model and 3.2' for the centrifuge test. The value for S2 changes by 2.79' for the MVN FLAC model and by 2.0' for the centrifuge test. This indicates that the MVN FLAC model is correctly predicting the consolidation settlement. This is useful because in most situations the amount of deformation that will be caused by fill placement will be small compared to the settlement that the fill placement can cause.

It should be noted that neither of these settlement locations are beneath the T-wall base. This is significant as the most convenient place to take settlement readings in an actual situation would be in the area immediately adjacent to the T-wall and to observe any gaps that would form between the T-wall base and the levee embankment. This area

was not measured during the centrifuge test and no comparisons between the predicted settlement and the actual settlement is able to be made.

3.4.2.2 Bending Moments in the Piles

Figures 3.12 and 3.13 show comparisons of the pile bending moments predicted by the MVN FLAC model and as measured during the centrifuge test after consolidation under the 15-ft and 25-ft fill loading increments, respectively. The bending moments predicted by the FLAC model are in reasonably good agreement with the flood side bending moments measured in the centrifuge test. The protected side bending moments do not match due to experimental error during the centrifuge test as the wall and loading is symmetrical and should result in symmetrical moments like is shown in FLAC. More gages were present in the centrifuge test piles but did not record data most likely due to damage that occurred during the construction and consolidation of the centrifuge test.

The bending moments in both the centrifuge and FLAC model are very high but that is expected from the high amount of settlement that is produced by the fill loading with the 15' increment being 5510 in-kips and the 25' increment being 9600 in-kips. The pile batters are also not steep in order that the piles would generate high bending moments during the centrifuge test. High settlement induced bending moments were desired to reduce the any other causes of bending moments. This would help isolate the settlement induced bending moments, making it easier to analyze and develop models to replicate.

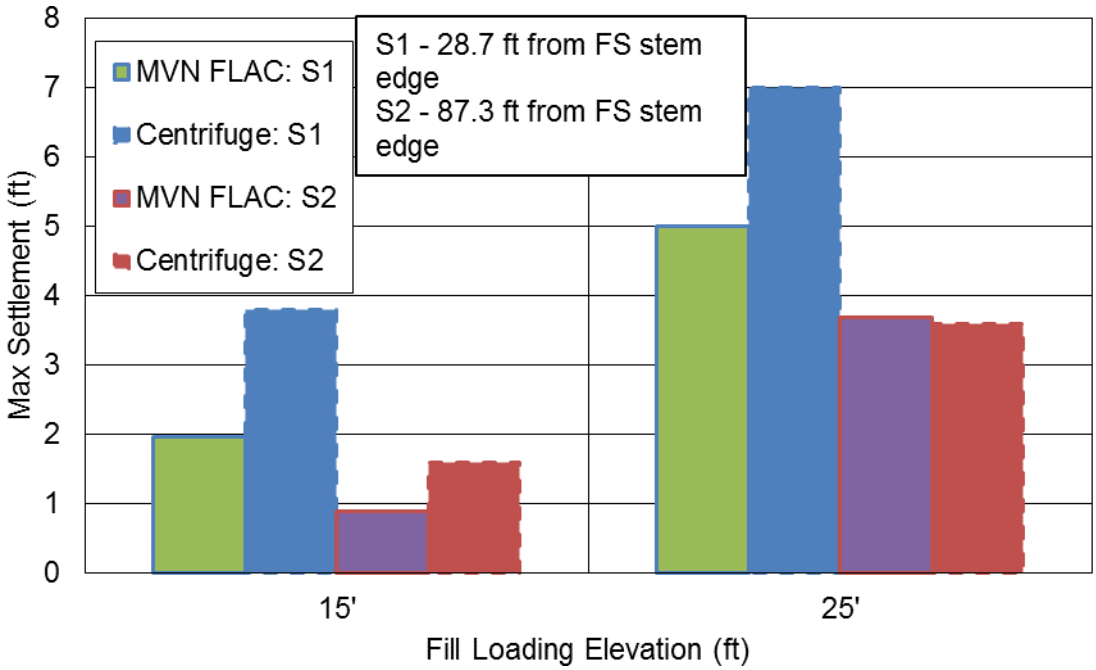

Figure 3.11 Maximum Settlement of Foundation Soil

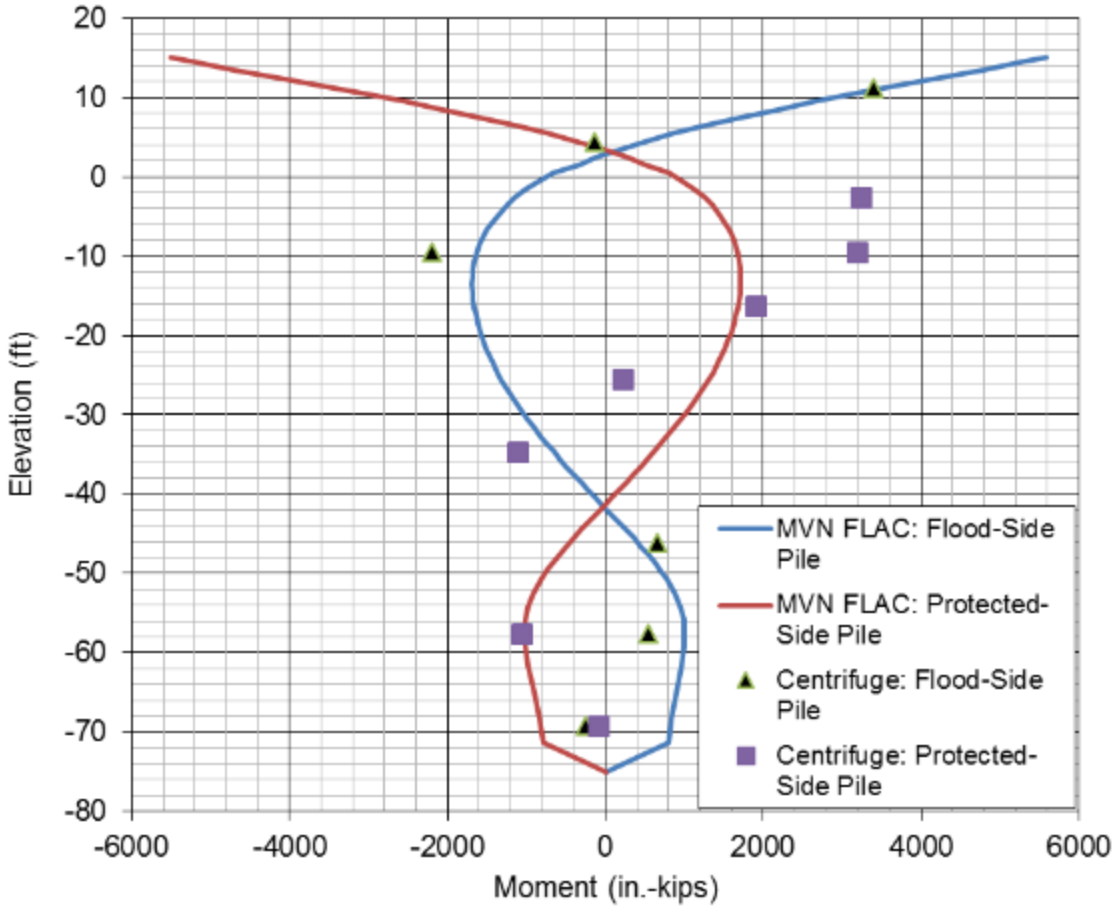

Figure 3.12 Bending Moments In Piles 15’

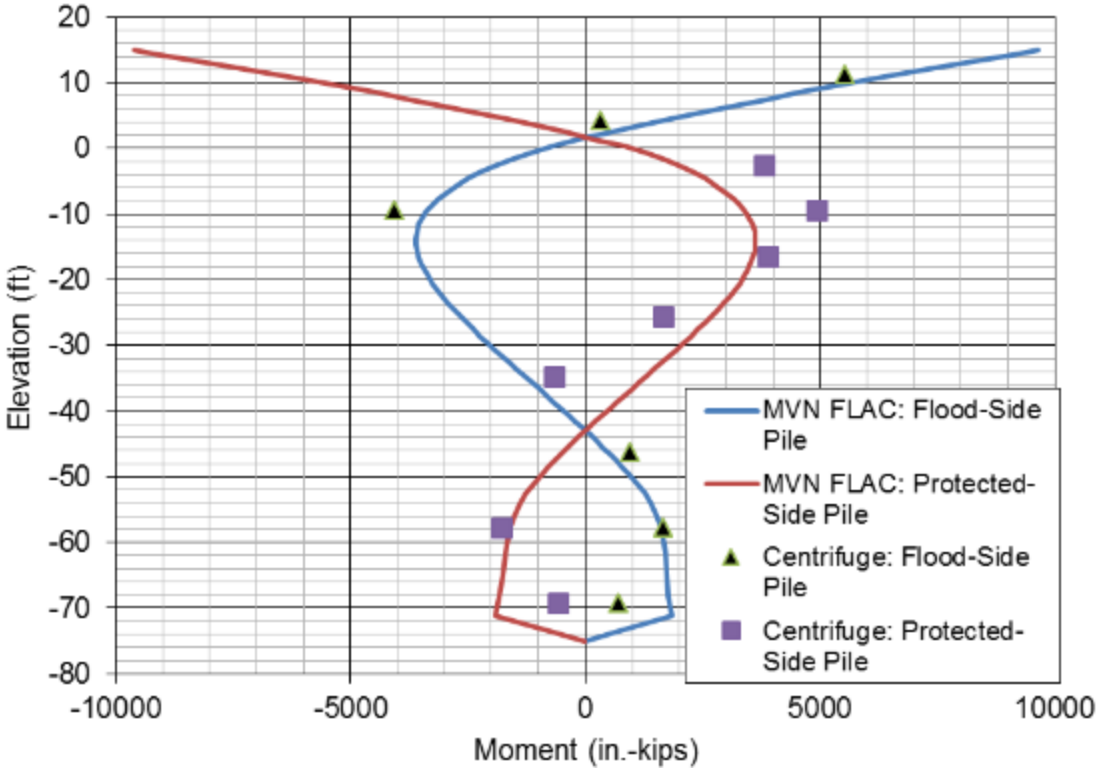

Figure 3.13 Bending Moments In Piles 25’

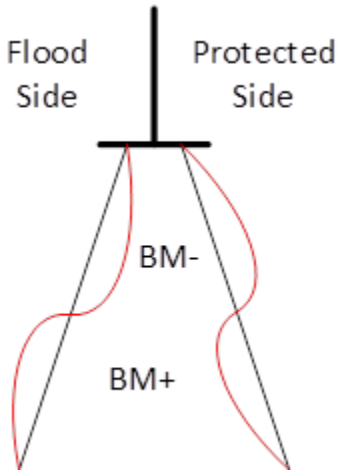

Figure 3.14 Bending Moment Sign Convention

CHAPTER IV

COMPARISON BETWEEN VT FLAC MODEL, MVN FLAC MODEL AND CENTRIFUGE RESULTS

4.1 Differences between the Models

The VT FLAC model and the MVN model give similar answers to each other. The VT FLAC Run 2 model is detailed in other papers (Reeb et al. 2015) and will also be part of a dissertation in the future by Virginia Tech. VT has also used this modeling approach on other similar jobs within the New Orleans Area (Reeb et al 2014). The main differences between the two models are the approach to stepping down the pore pressures, the use of an equivalent load for the 25 ft fill increment, and the shear and normal coupling springs. These differences are what contribute to the difference in the calculated moments.

The method of stepping down the pore pressures is most likely the biggest and most important difference between the two models. The manual stepping down method that the VT model uses is much less computationally intensive then the uncoupled approach used by the MVN model. The soil movements and bending moments that are produced by the two methods should be theoretically identical; however, the different procedures of applying the pore water pressure reduction in FLAC results in a process that creates differences in the final bending moments. The MVN model has to apply a high strength to the soil and gradually steps this down as the pore water dissipates to keep

the model stable while the VT model is able to avoid this issue by never letting the pore water pressure grow to a value that would destabilize the strength of the model. For the development of future models the VT method should be the recommended method as it produces similar results with significantly less running time.

The use of the equivalent forces versus fill placement will have a small difference which will most likely result in a higher bending moment compared to the fill placement method in the VT model. The equivalent force method is much easier to use and has less numerical issues that result from the use of the forces compared to the fill placement method. The equivalent force method is also able to place fill beneath the T-wall base which the fill placement cannot do. The actual fill placement would result in the load becoming more spread out as the fill settles. However, the inaccuracy should be minor and would not cause an significant difference in the results. The fill placement method also results in the model superficially resembling the actual field conditions.

The difference between the shear and normal coupling springs is very minor and probably only contributes a small amount to the difference in bending moments between the two models. VT uses a slightly different procedure in calculating the shear and normal coupling springs but the calculated values are very close to each in magnitude.

4.2 Comparison of the Two Models with the Centrifuge Results

As can be seen in Figures 4.1 - 4.3 the models and centrifuge tests have a reasonable correlation with each other in terms of bending moments. The VT model has a good correlation with the settlement sensors. The MVN model predicts a lower settlement but this explained by the modeling procedure as discussed in Section 3.4.2.

The MVN model predicts a slightly higher bending moment at the top of the pile than the VT model or the centrifuge tests. The difference is minor, however, and is not seen as being significantly different. The difference in bending moments is less than 10% for the 15' fill increment and is only 15.5% for the 25' fill increment.

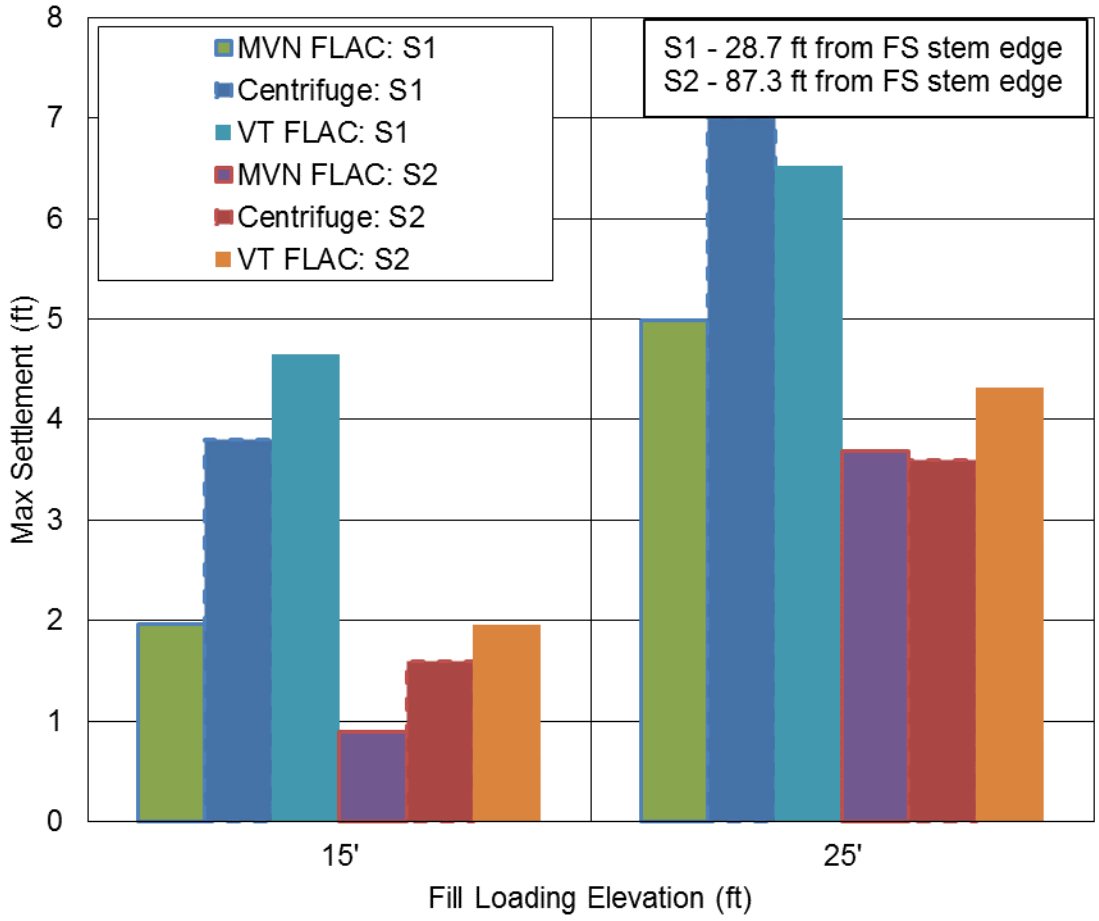

Figure 4.1 Maximum Settlements

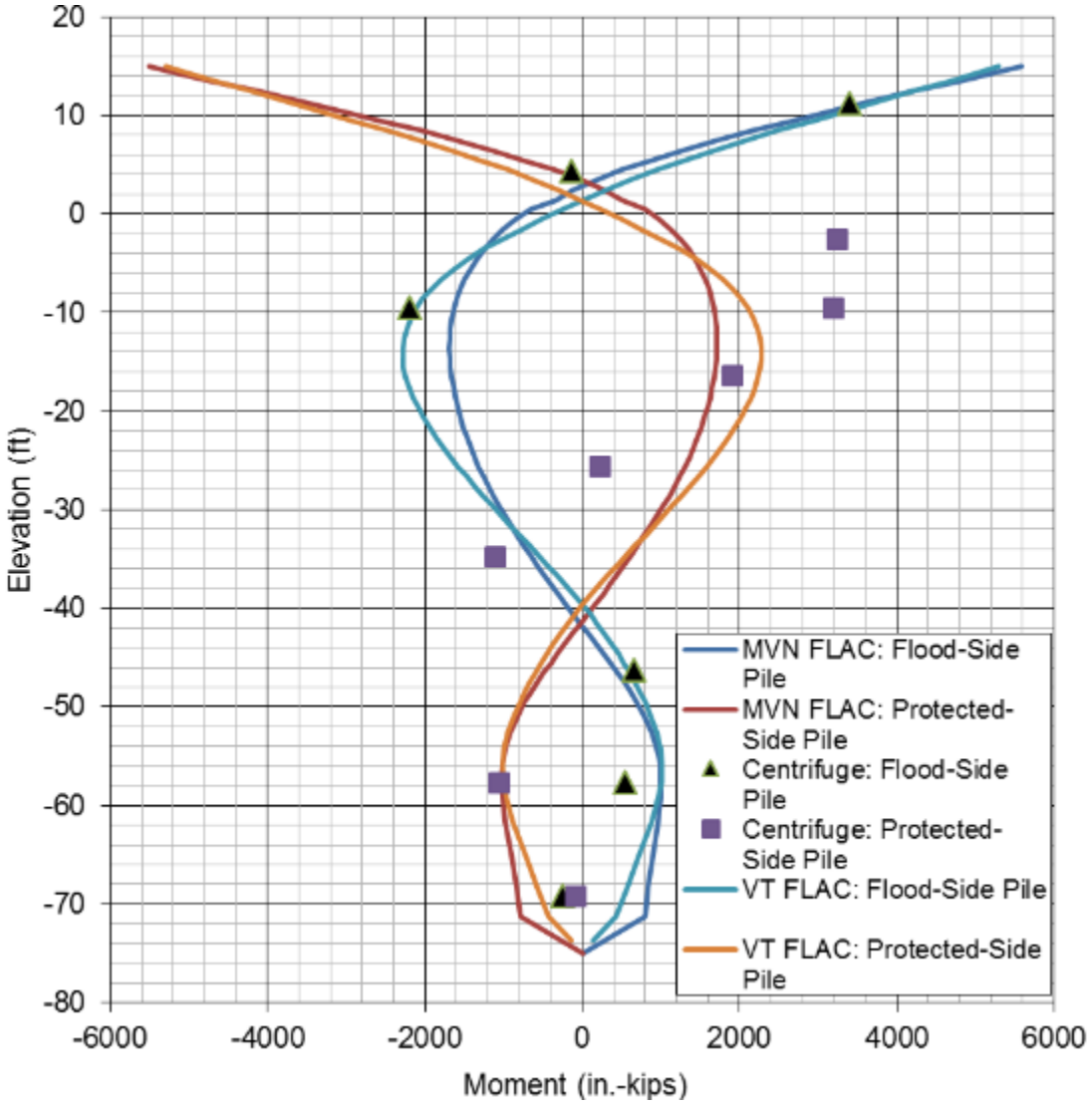

Figure 4.2 15’ Bending Moments

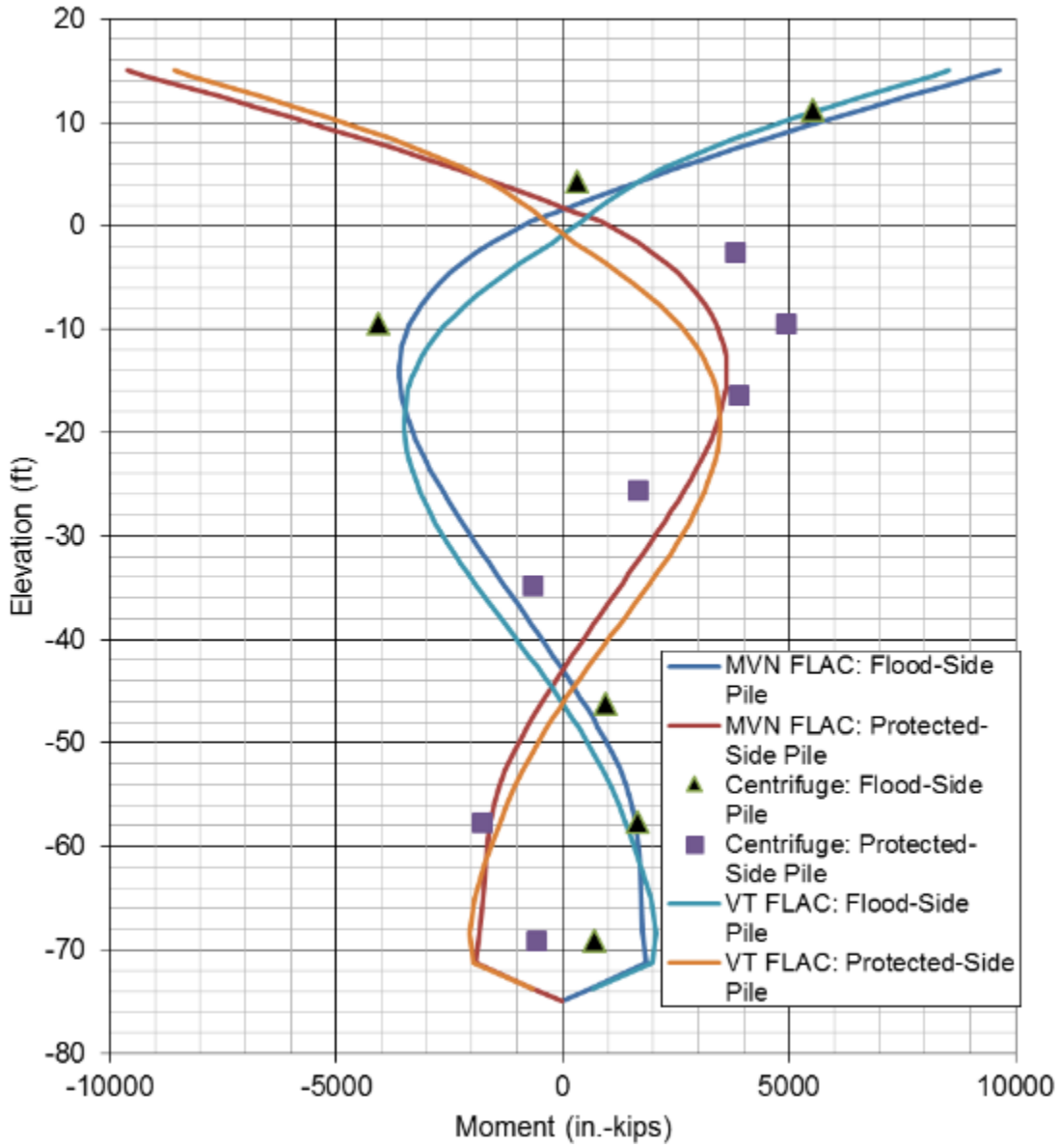

Figure 4.3 25' Bending Moments

4.3 Discussion and Conclusions Based on the Results

As is shown in both the centrifuge and FLAC models, the SIBM can be very large. Plastic deformation, pile buckling, or even pile rupture are possible depending on the magnitude of the bending moments. Neither the centrifuge nor the FLAC models

investigated what would occur if a plastic hinge were to form in the model and how this would affect the calculated bending moment. However, the formation of a plastic hinge is not desirable in most designs and most T-walls are not designed to have permanent deformations. Therefore significant structural pile capacity should be reserved for any SIBM or the settlement should be eliminated with either a preload or ground improvement techniques such as jet grouting.

Neither the centrifuge nor the MVN and VT numerical modeling included flood loading but based on historical experience and the literature reviewed (Won et al. 2011, Varuso 2010, Isenhower et al. 2014) it can be said that the bending moment in the flood side pile will go down due to flood loading while the bending moment in the protected side pile will increase. This is also true for the axial loads as well. The reasons for this are that the flood side pile will go into tension while the protected side pile will go farther into compression. After flood loading the bending moment in both piles should return to calculated SIBM unless plastic deformation occurred during flood loading. The SIBM itself will always be present in the piles and does not seem to decrease or be relieved with time based on the centrifuge test data (Appendix A). This needs to be taken into account for any design work and should be treated in a manner similar to the dead load.

As mentioned earlier, the centrifuge run was designed to produce large bending moments so an idealized cross-section of a large clay was used. In reality, many times clay layers are interspersed with sand and silt layers that can have the clay layers on either side of them consolidate. A stiff continuous sand or silt layer near the surface may act as a lateral support between the two piles. These layers may also result in a settlement distribution throughout the foundation that is significantly different than what

was used in the FLAC models. This would change the calculated bending moments' magnitude and distribution. This is a limitation of the current models and centrifuge runs. However, significant parametric analysis can be performed with the current models.

CHAPTER V

PARAMETRIC ANALYSIS

5.1 Different Parameters

The centrifuge case is a specific case of a T-wall in an embankment, however, there are many different configurations that can take place even in this scenario. A designer may want to use pinned connections for the pile to the T-wall structure versus fixed supports as was used in the centrifuge. The designer may want to use different batters. The shallower the batter, the higher the lateral load resistance will be, conversely, this will logically result in a higher bending moment as the length of the moment arm would increase. To account for this the designer may want to use piles with greater moment capacity. Trying to perform all these various parametric studies would be costly to perform in the centrifuge test but can be accomplished easily with small changes to the numerical model. The MVN numerical model was used to perform these different parametric analyses and the results are presented below. Only one parameter is changed for each case.

5.2 Pinned vs. Fixed Connections

Many different designs utilize pinned connections instead of fixed connections for various reasons. Several numerical models have been developed to represent the effects of settlement and/or flood loading on pile-supported T-walls and were reviewed for this

thesis (Isenhower et al. 2014, McGuire et al. 2012, LCR&A 2011, Won et al. 2011, Varuso 2010). However, all the models which addressed settlement show the pile connection as a pinned connection and the author could not find a model that had a fixed connection at the pile head. Also several of the models have 3 rows of piles which will change the bending moment distribution (Isenhower et al. 2014, LCR&A 2011). The author could not find a comparison between pinned and fixed pile heads in the literature and how this would affect the bending moment generated by settlement. This section shows the drastic impact that having assuming a fixed or pinned connection will have on any particular design.

The MVN model compared the pinned vs. fixed connection for the 15' and 25' fill case. The results are shown in Figures 5.1 and 5.2. The fixed connection for the 15' fill increment resulted in a maximum bending moment in the protected side pile (the wall and loading is symmetrical) that was 5,510 kip-inches while the pinned connection had a maximum value of 2,725 kip-inches. This is a reduction of 50.5%. Therefore, by solely changing the fixity between the pile head and the base of the T-wall, the calculated bending moment was cut by more than half of what it was for the fixed connection. This is a very significant change in the calculated bending moments. Also it should be noted that the second highest peak in the fixed model is still substantial with a moment of 1717 in-kips, being 37% less than the maximum from the pinned case. For the lower half of the pile the moments are roughly equivalent to each other and are smaller than the upper peaks.

For the 25' fill increment, the fixed connection resulted in a maximum bending moment in the protected side pile that was 9,602 kip-inches while the pinned connection

had a maximum value of 4,319 kip-inches. This is a reduction of 55%. This is a slightly greater reduction than the 15' increment. As in the case of the 15' fill increment mention, the second highest peak in the fixed model is still substantial with a moment of 3627 in-kips, being only 16% less than the maximum from the pinned case. The higher settlement resulted in the difference being less between the second fixed moment and the maximum pinned moment. This suggests the gap may be wider at lower settlements and smaller at higher settlements, however, the gap between the maximum bending moments is getting greater. Further research with additional settlement points is needed before this can be said definitely.

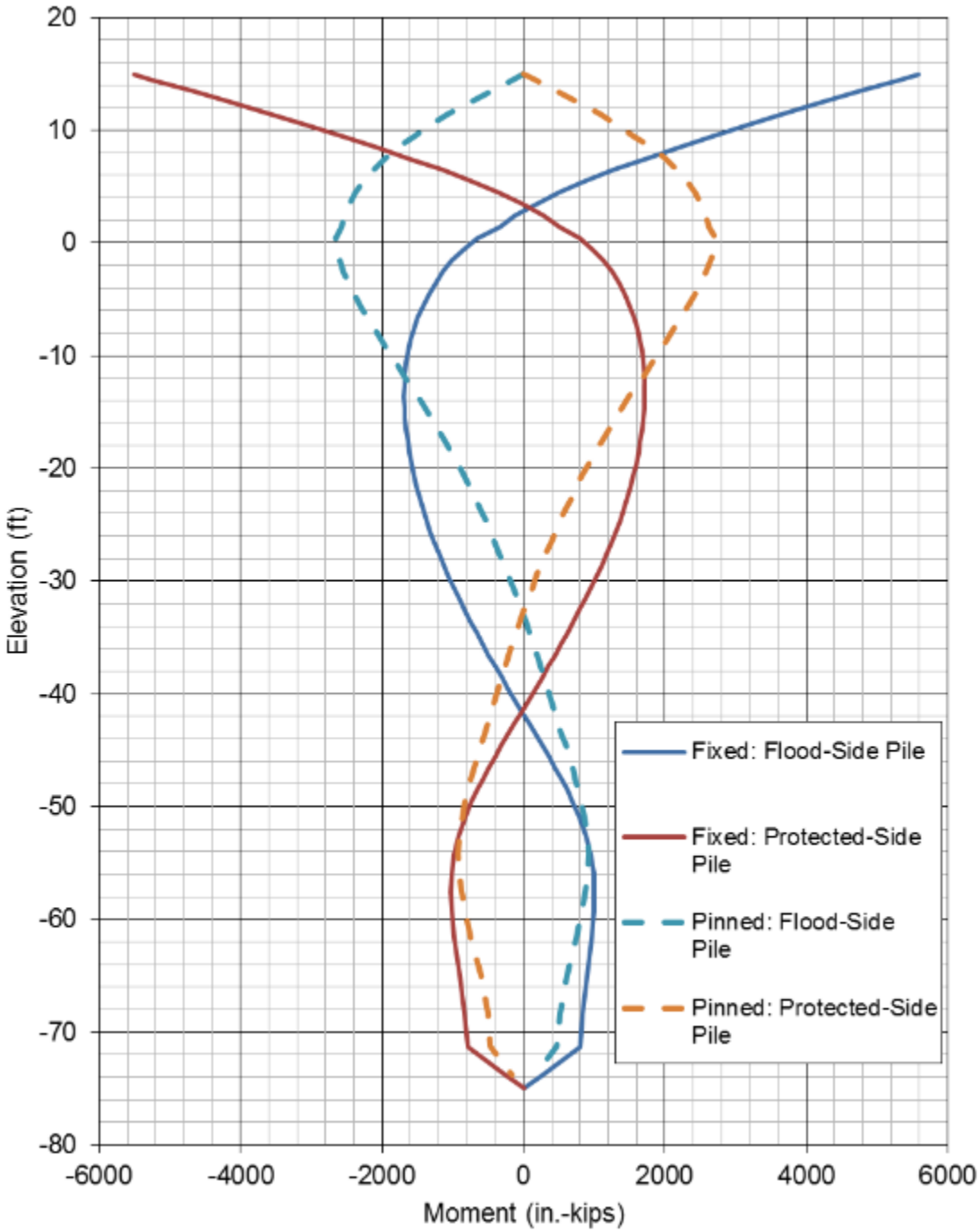

Figure 5.1 15’ Pinned Vs. Fixed Moments

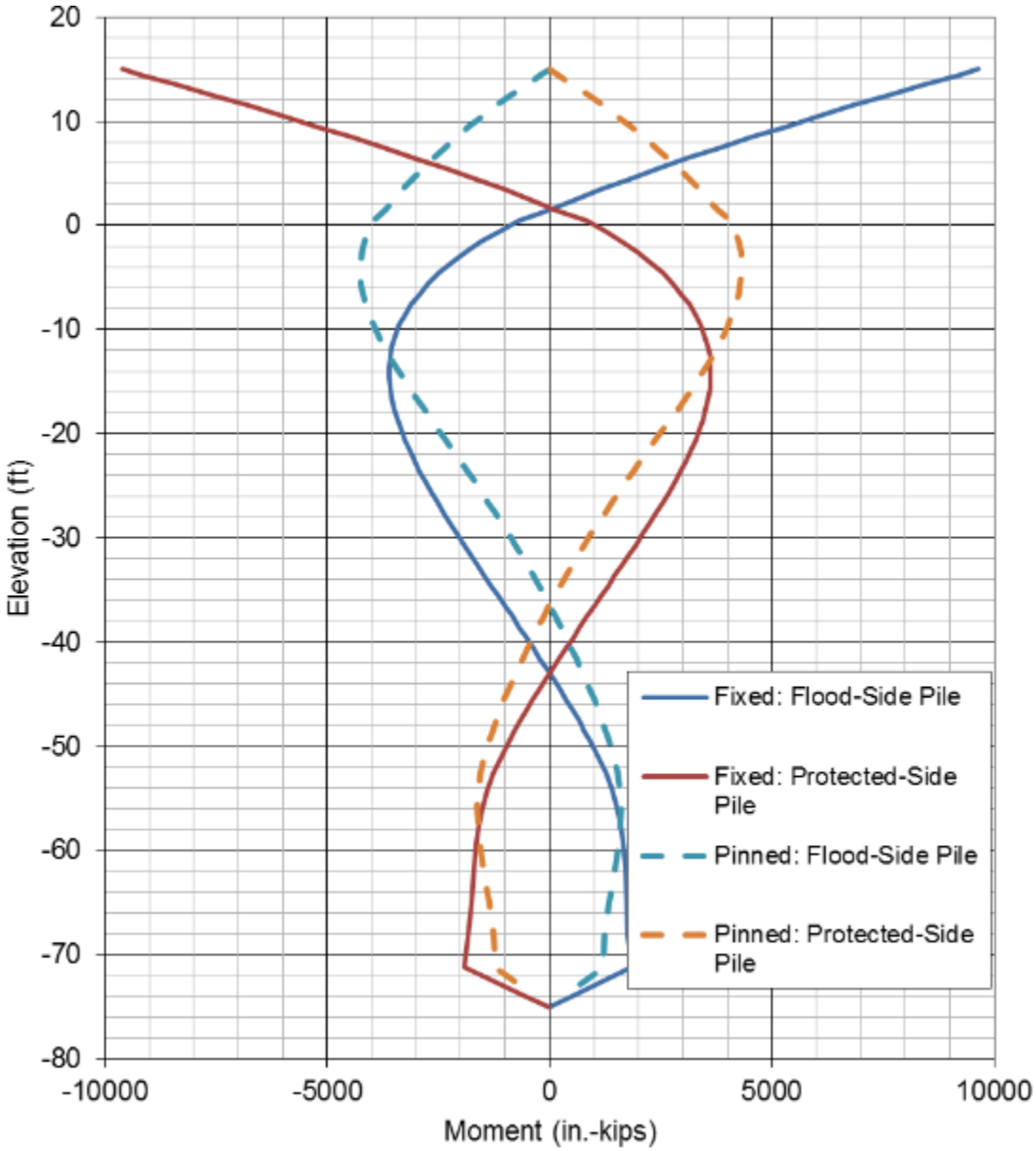

Figure 5.2 25’ Pinned Vs. Fixed Moments

Axial forces need to be taken into account during the design as well as bending moments. This load is due to the weight of the wall plus drag load from the settlement. The drag load can be significant and needs to be taken into account during the design (Fellenius 2014). The fixed connection results in higher axial forces compared to the

pinned connection (Figures 5.3 and 5.4). For the 15' increment, the axial load at the top of the fixed pile was 57.1 kips while the pinned pile had an axial load of 50.3 kips. This is an increase of 12.9% from the pinned case to the fixed case. For the 25' increment, the axial load at the top of the fixed pile was 63.7 kips while the pinned pile had an axial load of 50.9 kips. This is an increase of 20% from the pinned case to the fixed case. This is an interesting result as the fixed case axial load increased at a much higher rate for the higher settlement case compared to the almost negligible increase for the pinned case. For both cases, the axial load increased as the depth increased until bottom of the profile. This is an expected result as the drag load should increase until there is no settlement greater than the settlement of the structure (i.e. the neutral plane).

The critical case for the axial load differs for the fixed and pinned cases. The most critical load for the fixed case is at the top of the pile where the bending moment is its greatest while the most critical case for the pinned connection is farther down for both fill increments. This is an important design feature to remember when designing the pile foundations.

The pile deflections are important to note. The pinned pile deflects 100 to 300% more than the fixed pile as shown in Figures 5.5 and 5.6. This is expected as a pinned pile connection would be expected to have greater deflections at the pile head compared to the fixed as the fixed pile head has a restraint against rotation. The difference in deflection between the two cases decreases deeper along the pile length.

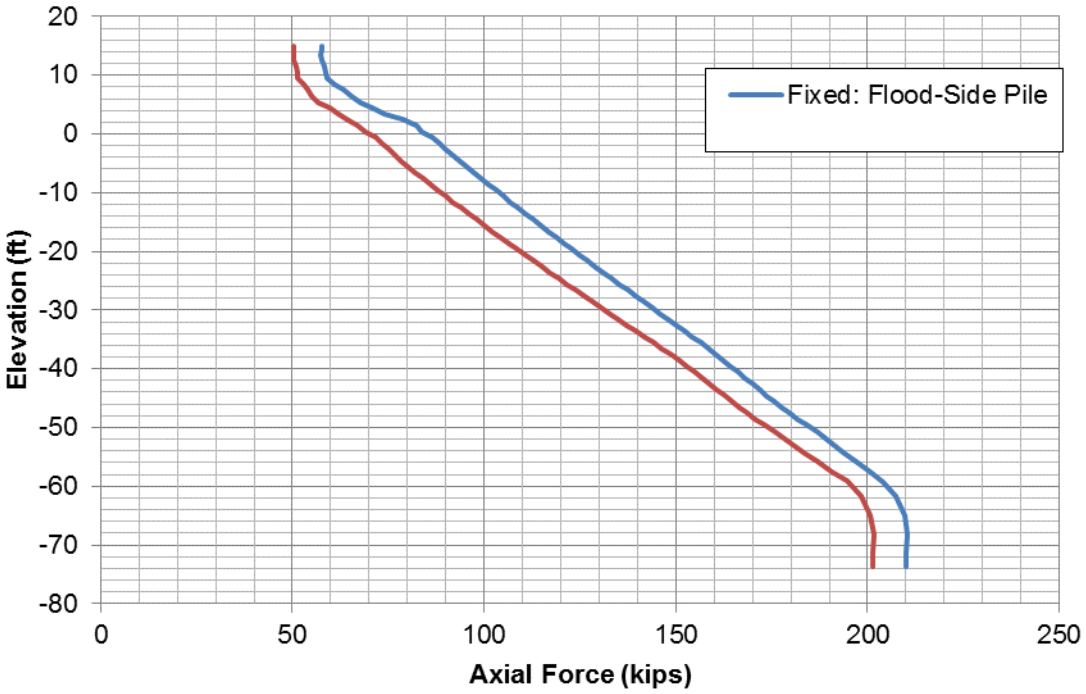

Figure 5.3 15’ Pinned Vs. Fixed Axial Forces

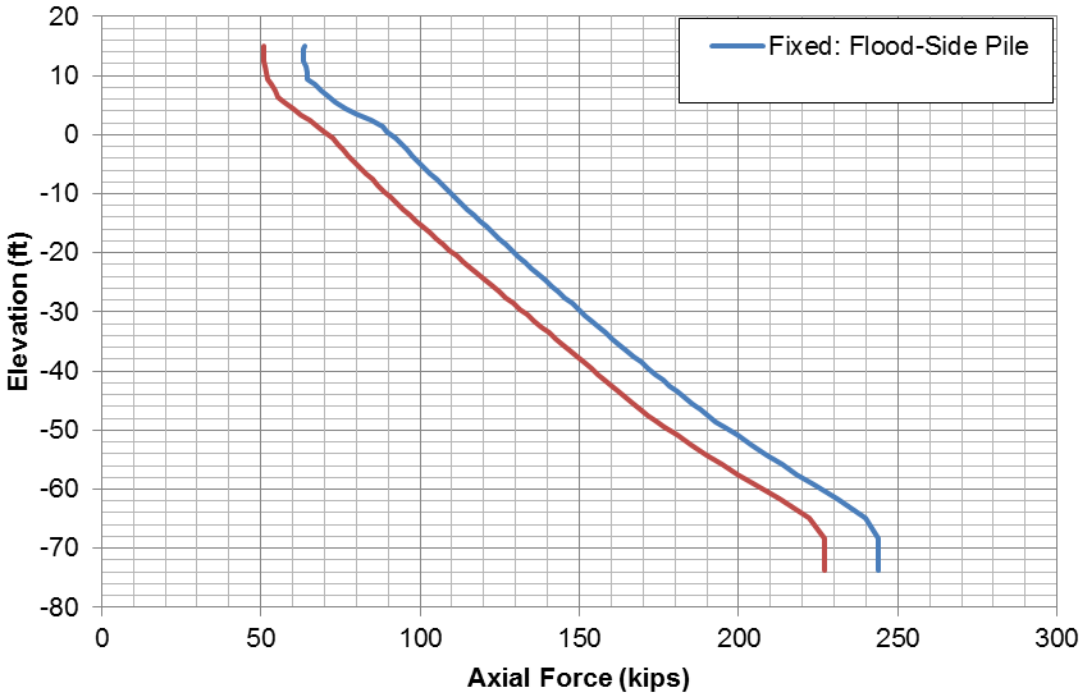

Figure 5.4 25’ Pinned Vs. Fixed Axial Forces

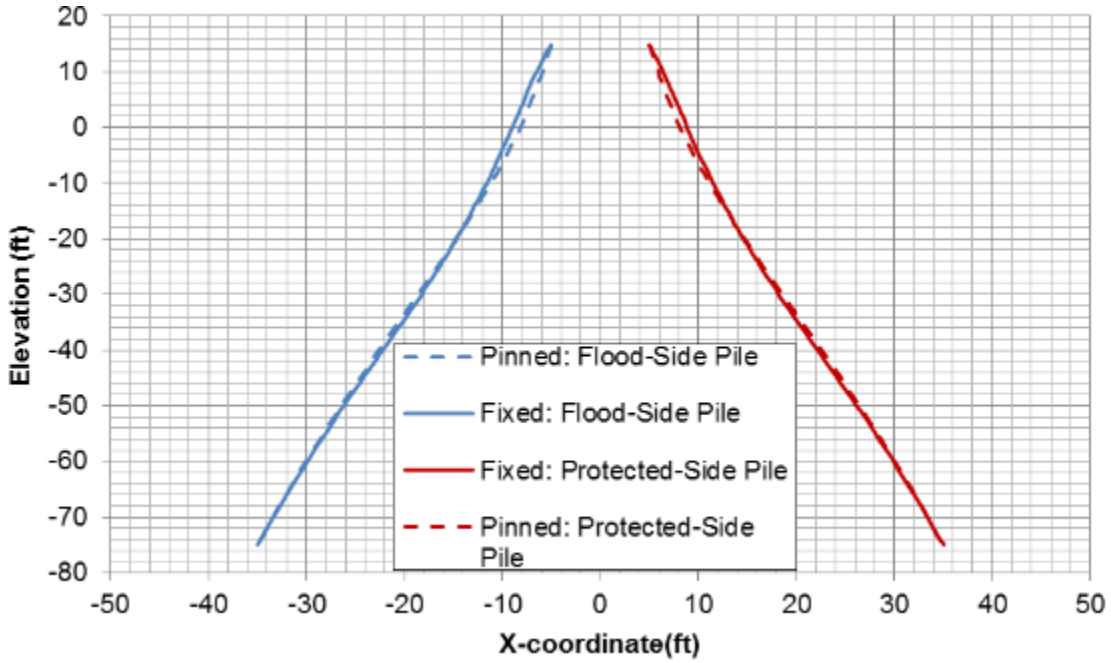

Figure 5.5 15’ Pinned Vs. Fixed Deflected Shape

Notes: Deflection 5x Magnified

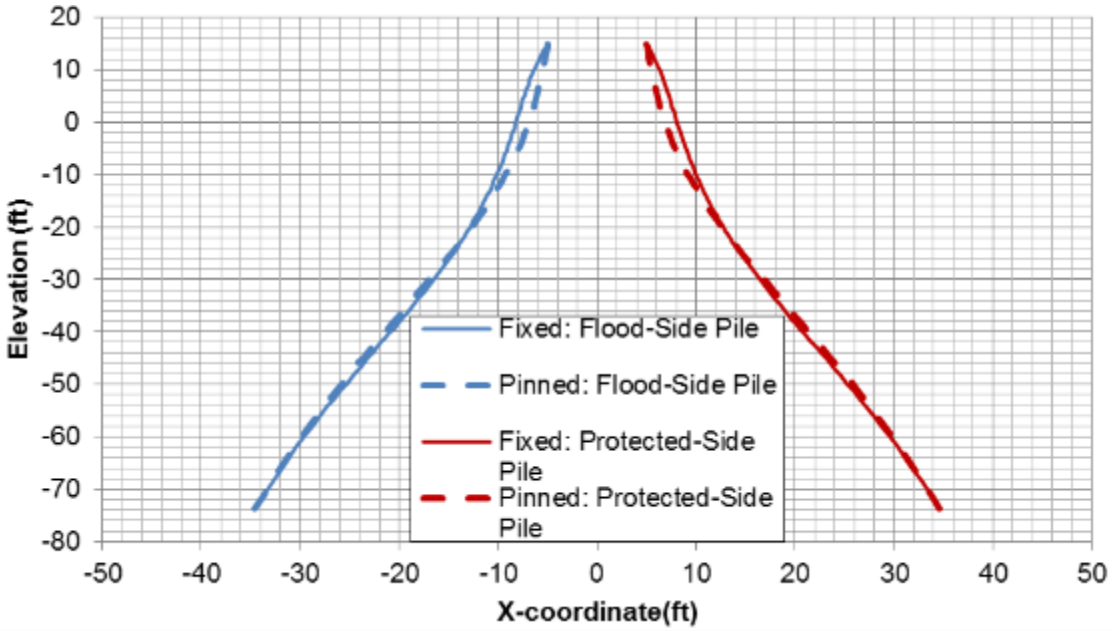

Figure 5.6 25' Pinned Vs. Fixed Deflected Shape

Notes: Deflection 5x Magnified

The additional moment restraint at the top of the pile is to blame for the increase in both axial load and bending moments from the pinned case to the fixed case. The moment restraint will produce lower lateral deflections during loading and will increase stresses in the pile and also allow bending moments developed in the piles to be transmitted into the slab. This can have important implications on the steel reinforcement used in the slab designs.

The difference in results due to pile head fixity is an important phenomenon that any designer needs to take into account whenever designing pile foundations as not only does the maximum bending moment due to settlement change location within the pile but it is drastically increased as well for fixed connections. If there is damage or corrosion at the pile head (most likely location) then these issues could be compounded. The fact the secondary peak of the fixed case is almost as large as the maximum pinned case bending

moment is also very significant. This is important if the designer tries to weld stiffening plates or use a composite section to compensate for the bending moment at the top of the pile and does not account for the large stresses generated further down in the pile.

The ability to be able to get an actual pinned connection is also in doubt. According to some research, even low embedment depths with reinforcing steel will produce pile head connections closer to fixed then pinned (Rollins, & Stenlund 2010). Consequently, if the designer assumes a pinned head connection, they may drastically underestimate the SIBM. It is recommended, based on the results in this section, that the designer always assumes a fixed head connection as this will be the most conservative case.

5.3 Effect of Different Batters

There are many different reasons that designer will choose different batters such as pile interference issues, increase in lateral capacity, and avoiding underground obstructions. Logically, the steeper the batter the lower the settlement induced bending moment. Pile batters of 1H:1.5V, 1H:2V, 1H:2.5V, 1H:4V, and 1H:6V were compared to the batter of the MVN FLAC model which was 1H:3V. All the batters go to the same depth. The results are shown in Figures 5.7 and 5.8. Only the protected side pile is shown for clarity, however, as previously noted, the bending moments are symmetrical about the wall. As expected the bending moment increases as the batter becomes more horizontal. Figure 5.9 show the maximum bending moment versus the batter angle for the 15' fill increment and 25' fill increment. A linear trendline was chosen with only a small error in curve fitting. The bending moment was set to be 0 at a batter angle of 0° (i.e. a vertical pile). This is useful as a designer may want to compute the bending

moment for one pile batter then draw a line through the origin and the designer may only have a small error in the calculated bending moment. This has only been validated for fixed pile head connections and may not be applicable for pinned pile head connections.

The different batters will result in different observed settlements due to the shielding effect being spread out over a different area. These effects may be substantial for the larger pile batters, however, the overall usefulness of this obervation is marginal. Most designers would not consider this fact when designing foundations as the predicted ground surface settlement is less important to the structure than the stresses in the piles.

Kohno et al. (2010) shows the results of centrifuge tests and suggested equations for calculating the bending moments for different batters. However, these equations and the centrifuge test indicate a settlement induced bending moment greater than 0 for a batter angle of 0°. This at first seems to be incongruous, as no bending moment should be created when there is no lateral load being placed on the piles. Analysis of the centrifuge test that was performed indicates that the vertical pile was placed in a foundation with battered piles and all the piles had a fixed head connection. The centrifuge test then applied loading to cause the settlement. Bending moments from the other piles were most likely translated into the vertical pile through the fixed connections.

This has important implications as a designer may want to use multiple batters for each side of the structure in their design. As stated earlier in Section 4.3, flood loading should decrease the bending moment in the flood side pile and increase it in the protected side pile. Therefore a designer may choose to use a steep protected side pile batter to reduce the SIBM in that pile while using a shallower flood side pile batter to increase lateral capacity counting on the flood loading to unload the flood side batter pile.

However, the protected side pile may get a SIBM greater than intended due to a load transfer between the two piles. The designer must calculate the bending moments as a system and not as individual piles if the piles and non-flood loading are not symmetrical about the wall.

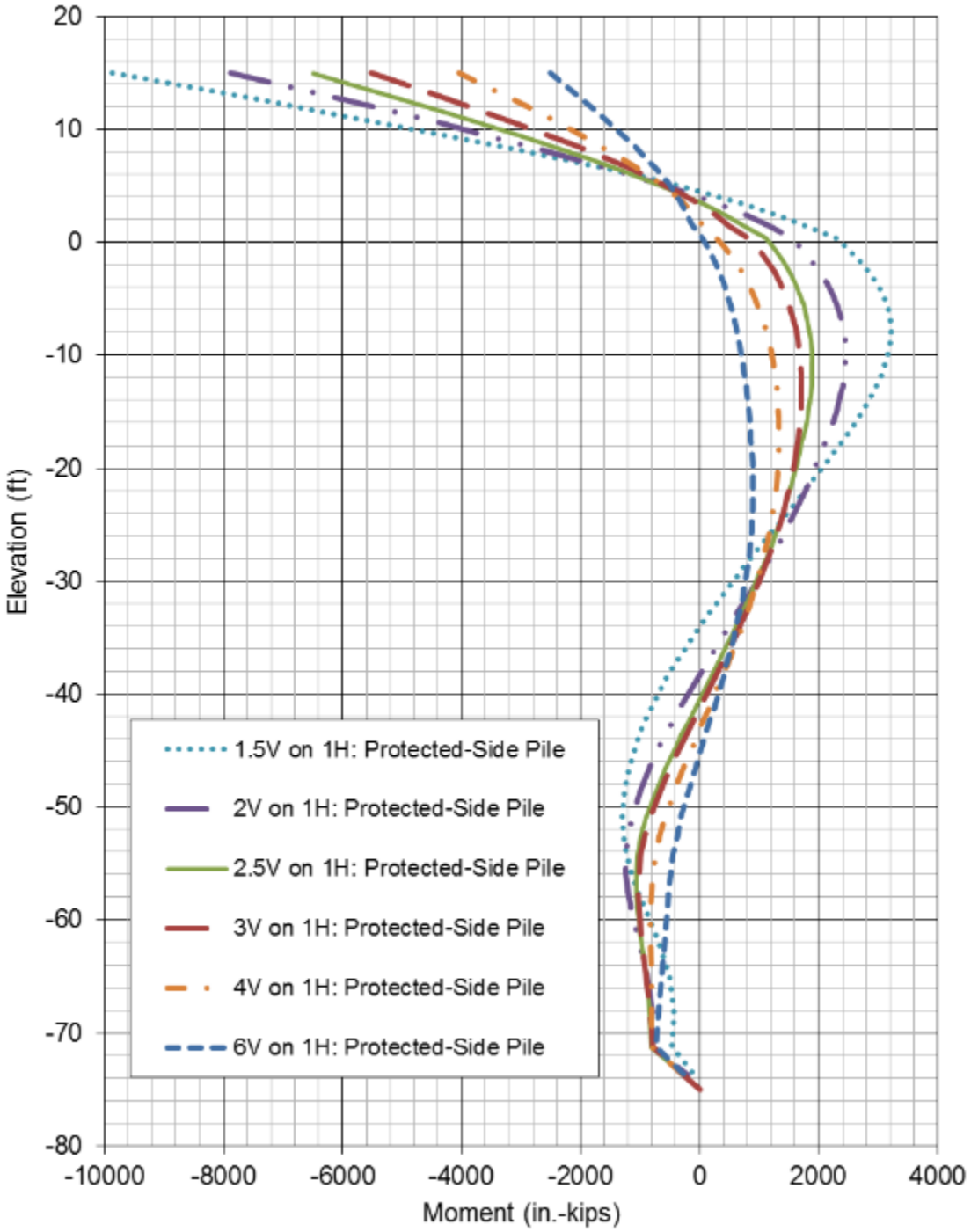

Figure 5.7 Protected Side Moments 15’

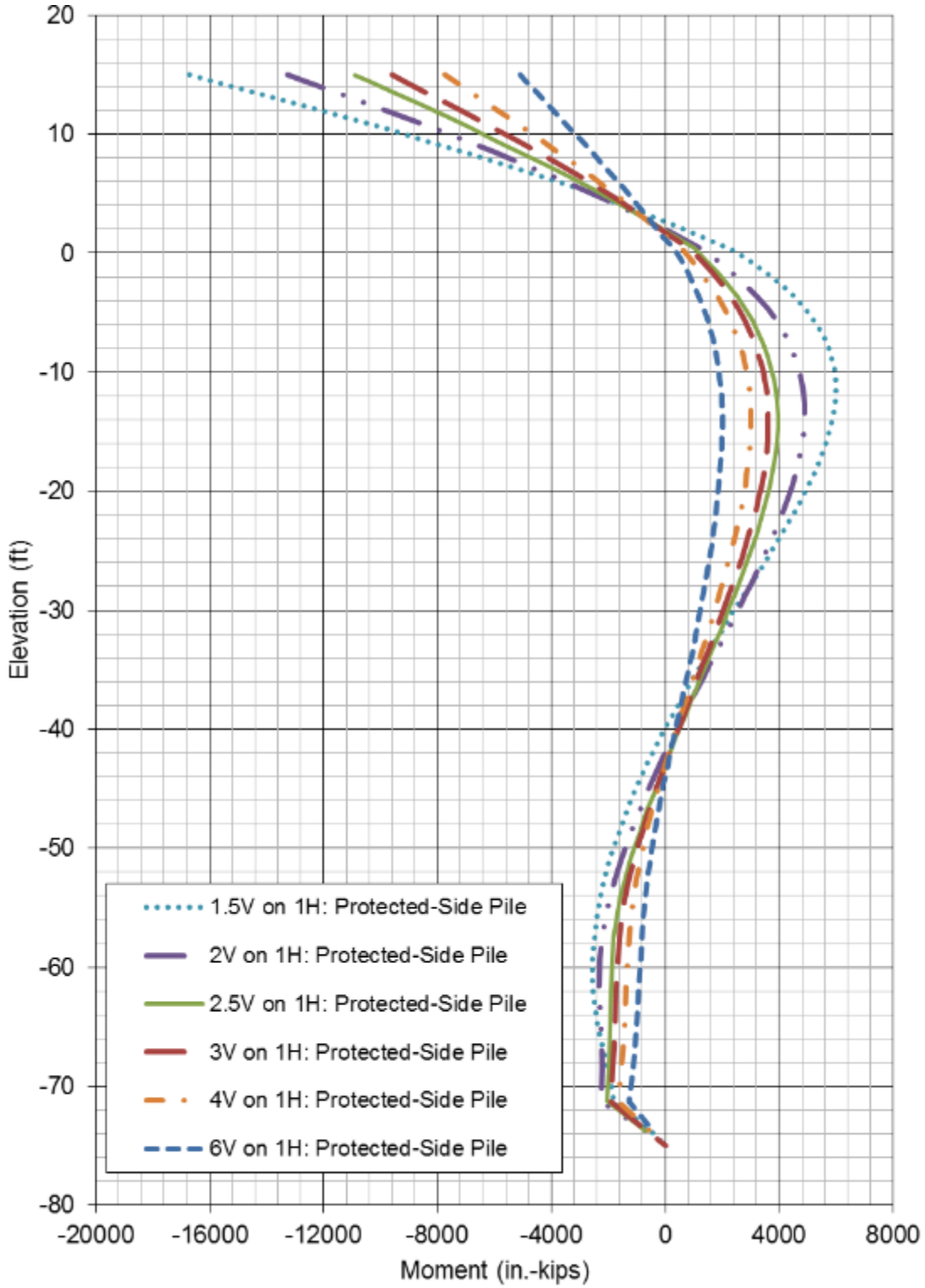

Figure 5.8 Protected Side Moments 25’

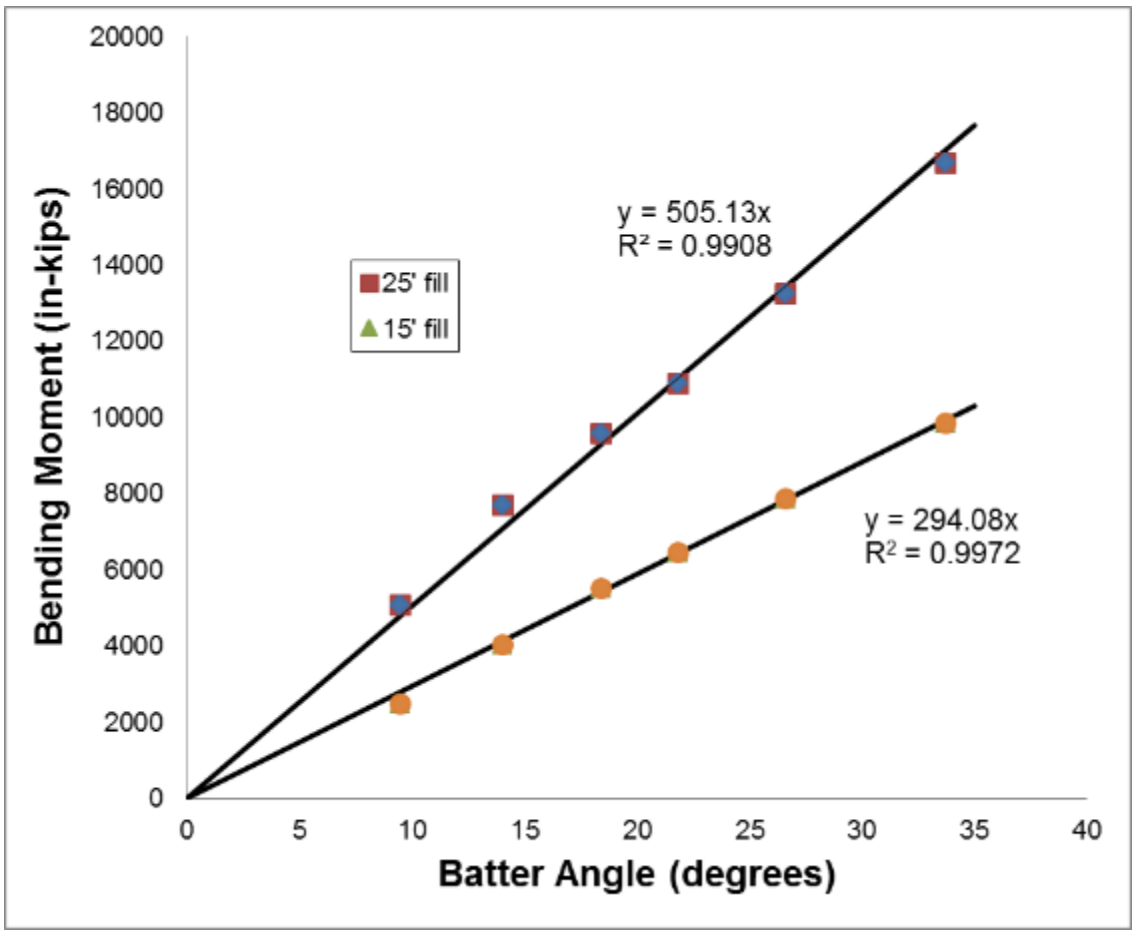

Figure 5.9 Maximum Moments versus Batter Angle

5.4 Effect of Stiffer Piles

To compensate for the calculated settlement induced bending moment a designer may use thicker piles to increase his capacity without changing the other aspects of the design. To simulate this, the piles in the MVN FLAC model had the second moment of inertia I increased by 30%, which is roughly equivalent of going from a 14x73 H-pile section to a 14x89 H-pile. Another model was also performed that had the second moment of inertia I increased by 60% above the original value. No other changes to the pile were made and no changes to the axial pile capacity were made.

As is shown in the Figures 5.10 and 5.11, the stiffer pile sections increase the bending moment that is developed in the piles. This can be attributed to the stiffer piles attracting more load and to also deflecting less in the course of loading. For the 15' fill increment, the bending moment increased by 7% from 5510 in-kips to 5910 in-kips for the 30% stiffer pile and by 19.8% from 5510 in-kips to 6598.4 in-kips for the 60% stiffer pile. For the 25' fill increment, the bending moment increased by 11% from 9600 in-kips to 10640 in-kips for the 30% stiffer pile and by 24% from 9600 in-kips to 11870 in-kips for the 60% stiffer pile. This does not seem to follow a linear pattern which suggests that as the stiffness of the pile goes up the pile will have increasingly higher bending moments. It is unlikely that the bending moments will ever exceed the increased capacity so these seem to be adequate tradeoffs. Therefore, a designer should be able to utilize stiffer piles to increase bending moment capacity but needs to insure that they take into account the increase in loading as well. This model did not look into what would happen if a composite section was used for the top half of the pile or welding stiffener plates to add additional capacity.

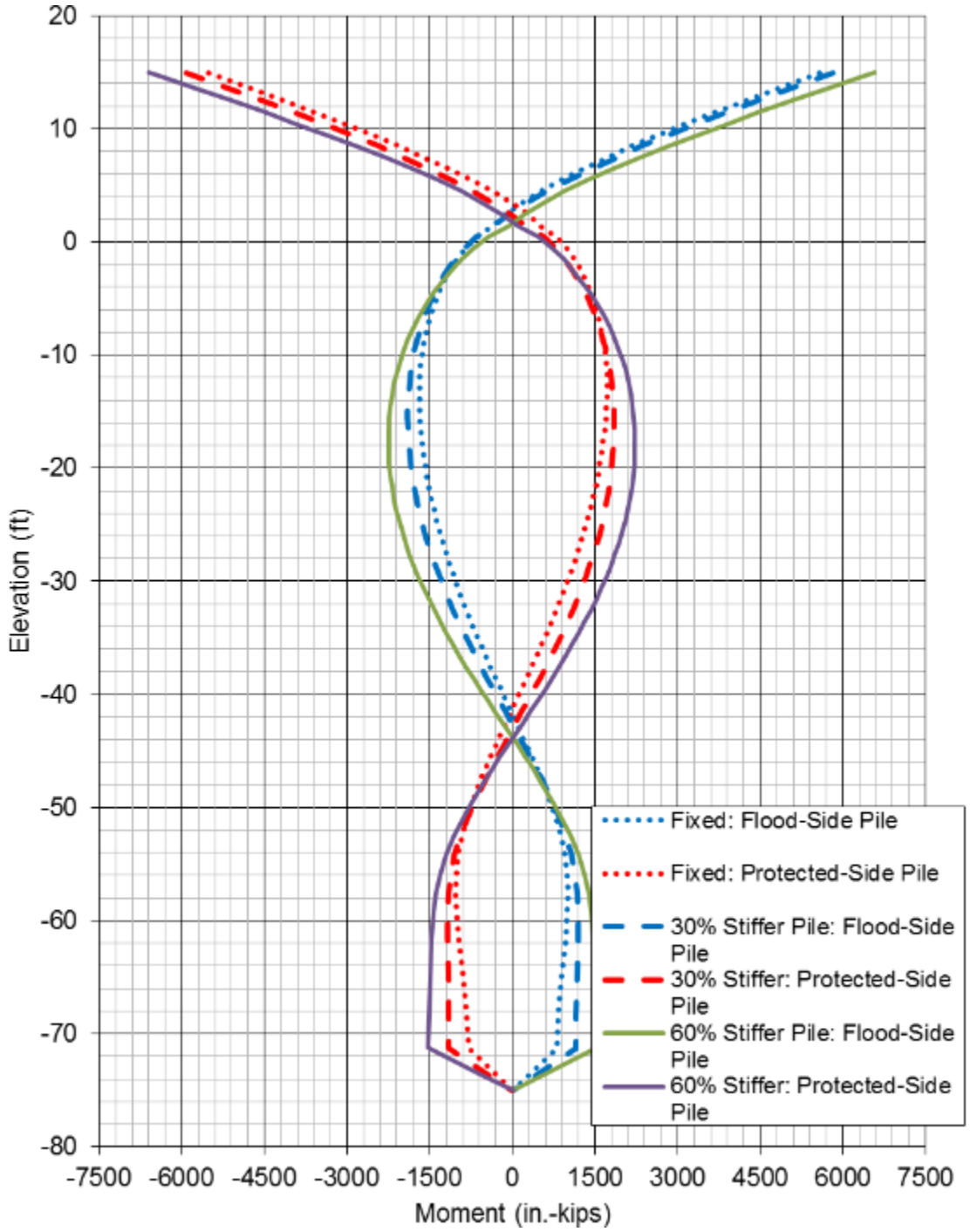

Figure 5.10 15’ Stiffer Piles Moments

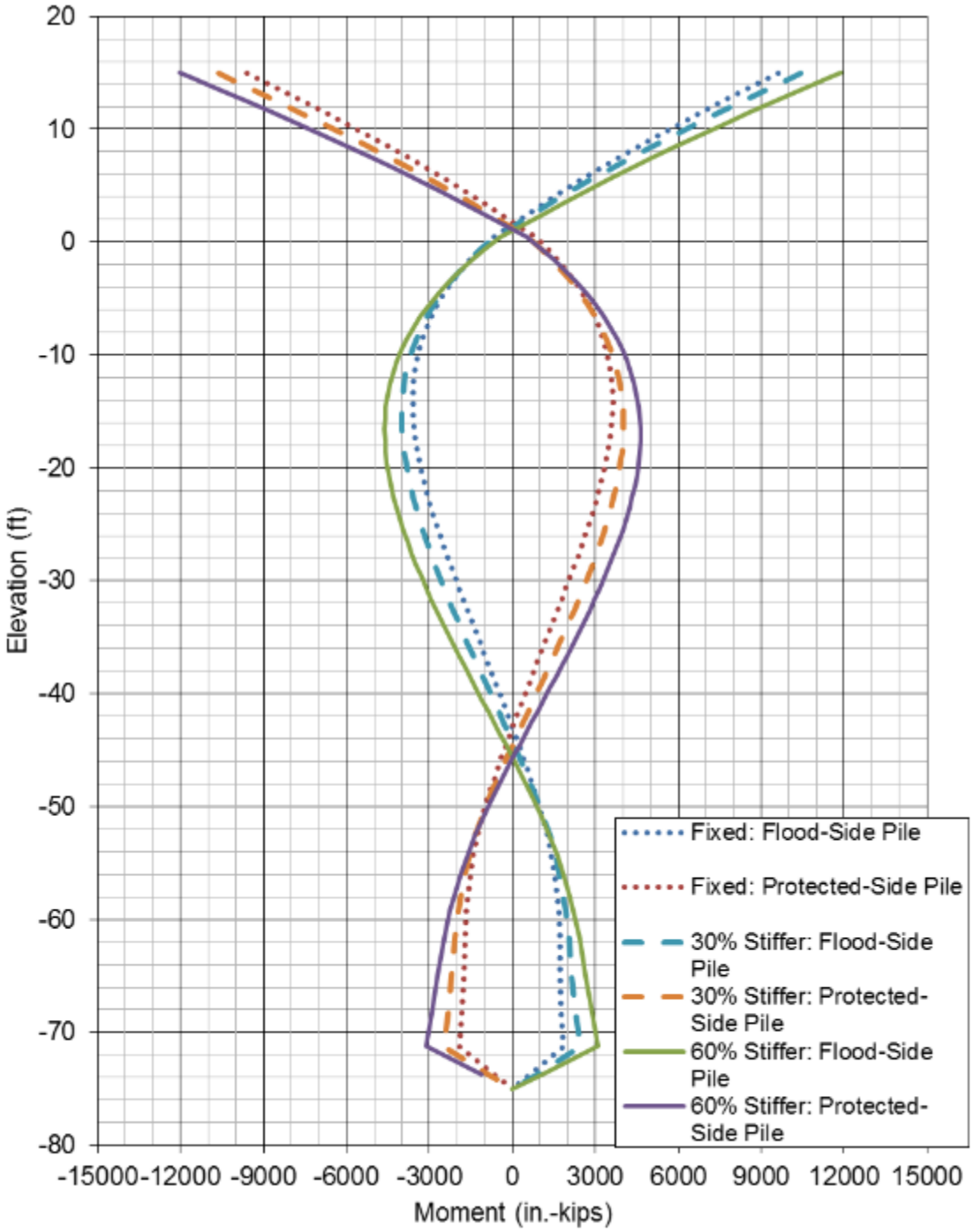

Figure 5.11 25’ Stiffer Piles Moments

CHAPTER VI

COMPARISON WITH USACE LE METHOD

6.1 Comparison of Different Methods

Over the years there have been many different methods developed over the years to evaluate settlement induced bending moments. The earliest method that was found was done by Sato et al. (1970) but as this method was only presented in Japanese, it did not seem to get much attention in other countries. Several other methods have been proposed over the years each with various strengths and weaknesses (Broms and Fredriksson1976; Shibata et al. 1982; Takahashi 1985; Sawaguchi 1989; Rao et al. 1994; Hance and Stremlau 2009; Hance and Stremlau 2009; Templeton 2009; Kohno 2010). USACE decided in 2009 to mandate a consistent method for the use in evaluation of settlement induced bending moments in the New Orleans area. In January 2010, Virginia Tech was contracted to do three things: review the existing methods used and published, evaluate the existing methods, and recommend changes to an existing method for use on projects in the New Orleans area. After the review and evaluation, none of the existing methods were determined to be "sufficiently validated or detailed enough" (McGuire et al. 2012). A detailed and useful breakdown and evaluation of the methods that Virginia Tech reviewed is in Appendix A of the USACE LE Method report (McGuire et al. 2012). Consequently, Virginia Tech, in conjunction with USACE, developed a method using the commercially available LPILE software, developed by

Ensoft, Inc. The method is relatively easy to use and can be performed in a reasonable amount of time compared to numerical methods.

6.2 Overview of the USACE LE Method

The USACE LE Method has become the standard method which USACE MVN uses to evaluate settlement induced bending moments in battered piles despite its limitations. The method has the user perform a settlement analysis using any valid method at a point on the ground surface equivalent to 25% of the piles length. The user has to transform both the piles and the subsurface layers based on the pile batter. The settlements are then converted using a formula to expected soil movements with a pile in place. The soil layers, soil movements, and pile properties are input into the LPILE program. The program gives a bending moment distribution versus depth, however, only the maximum bending moment should be used and not the location.

The current USACE LE Method has many limitations and assumptions with the biggest one being that it was designed for only pinned connection which is how the vast majority of floodwalls in the New Orleans area were designed. It is also only calibrated for piles that are battered at 3V:1H. It was also designed using version 5 of the LPILE software and the current version 7 made several changes that required an adjustment to the method to keep results consistent. There is also a limit to the amount of settlement that the method is applicable for, mainly due to the conversion equations being polynomial. For higher settlements the conversion equations produce numbers that are not realistic. There are many other limitations and assumptions to this method and are listed in the LPILE report (McGuire et al. 2012 pg 6-10).

6.3 USACE LE Method Results

The USACE LE Method was performed for the centrifuge case using version 7 of LPILE and Settle3d with the Boussinesq method. The settlement numbers from the Settle3d output correlate very well with the settle predicted by the FLAC model. The USACE LE Method results can be compared to the MVN FLAC pinned results which are also discussed in Section 5.2. The comparison between the methods is shown in Figures 6.1 and 6.2. As can be seen in the figures, the USACE LE Method does a good job predicting the maximum bending moment for the 15' fill increment but is very conservative for the 25' fill increment. The USACE LE Method's 15' increment produces a maximum bending moment of 2,990 in-kips which is only 12% higher than the maximum bending moment of 2,670 in-kips produced by the MVN FLAC model. The USACE LE Method's 25' increment produces a maximum bending moment of 7,870 in-kips which is 85% higher than the MVN FLAC model's maximum bending moment of 4260 in-kips.

The data suggests that the USACE LE Method is a good method for moderate amounts of settlement as experienced in the 15' fill case but should not be used for the more extreme amounts of settlement such as the 25' fill case. This is stated in the USACE LE Method report, with the limit in the report being 30 inches for the case of battered piles within a levee embankment. It was still performed, however, to show what would happen if the method were used for higher settlements. Also, as stated previously, the bending shape from the USACE LE Method does not match what was computed using the FLAC model and only the maximum bending moment should be used for the USACE LE Method and not the shape of the curve.

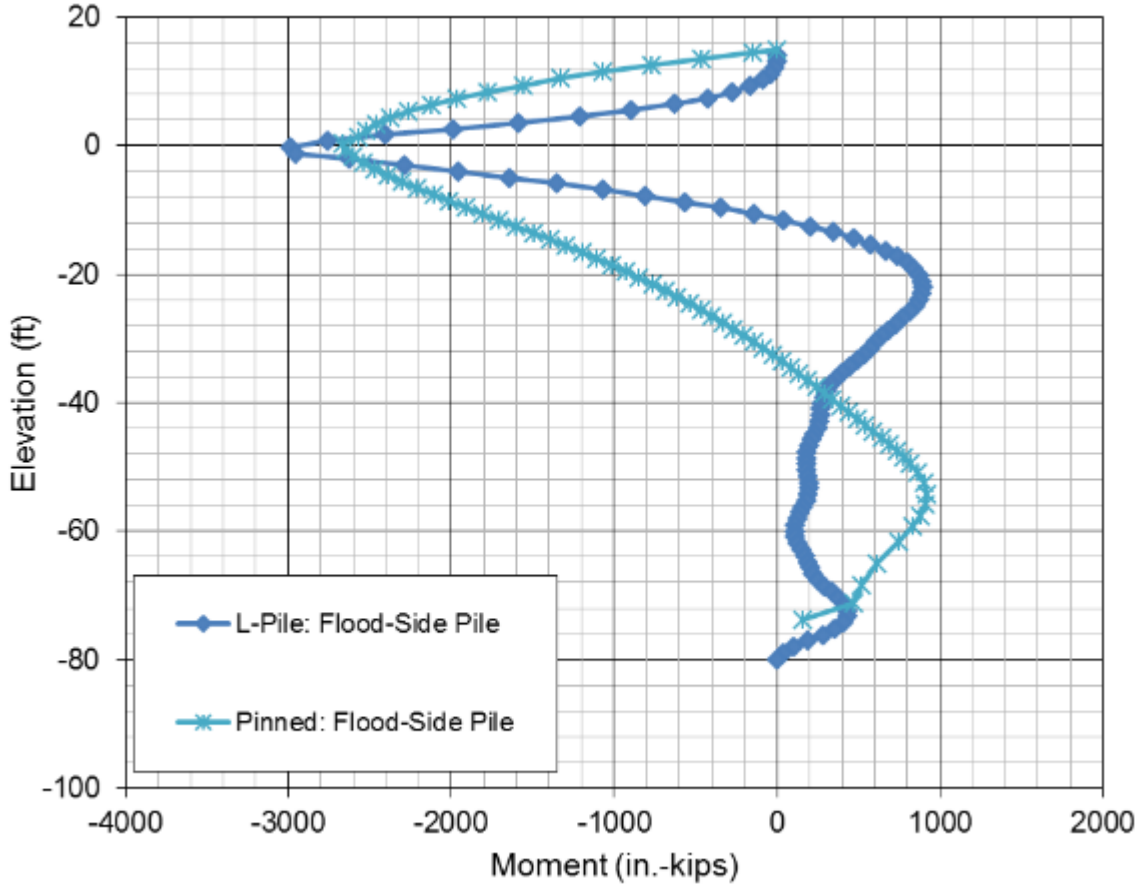

Figure 6.1 15’ Moment FLAC Vs. USACE LE

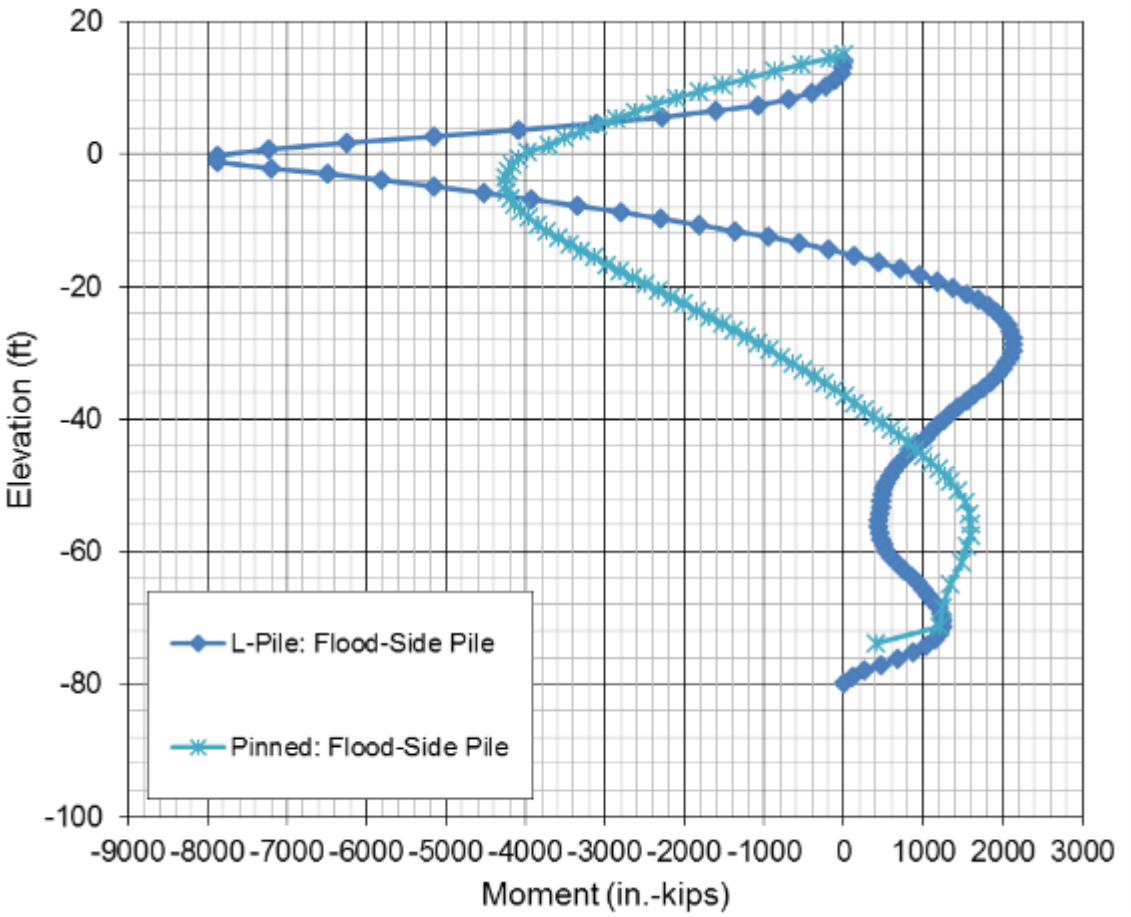

Figure 6.2 25' Moment FLAC Vs. USACE LE

6.4 LPILE Fixed Case

As stated earlier, the USACE LE Method was explicitly created to deal with piles with a pinned pile head connection. However, in many cases a designer may wish to use the method on a fixed pile head case. There are currently two ways to simulate a fixed head condition in LPILE version 7. One method applies a shear and slope at the pile head while letting the pile head be allowed to displace. This method is compared to the FLAC model in Figure 6.3. As shown in the figure, the USACE LE Method will not produce accurate or even conservative results for this case if all that is done is change the

fixity. The other method is to set the displacement and slope at the pile head. Doing this for the 15' fill increment resulted in a bending moment greater than 60,000 in-kips which is far outside the bounds of reasonable answers. Any designer should not use the current method and just change the settings in LPILE for a fixed pile head. Much further research and adjustment to the current method is needed before it can be applied to a fixed pile head case.

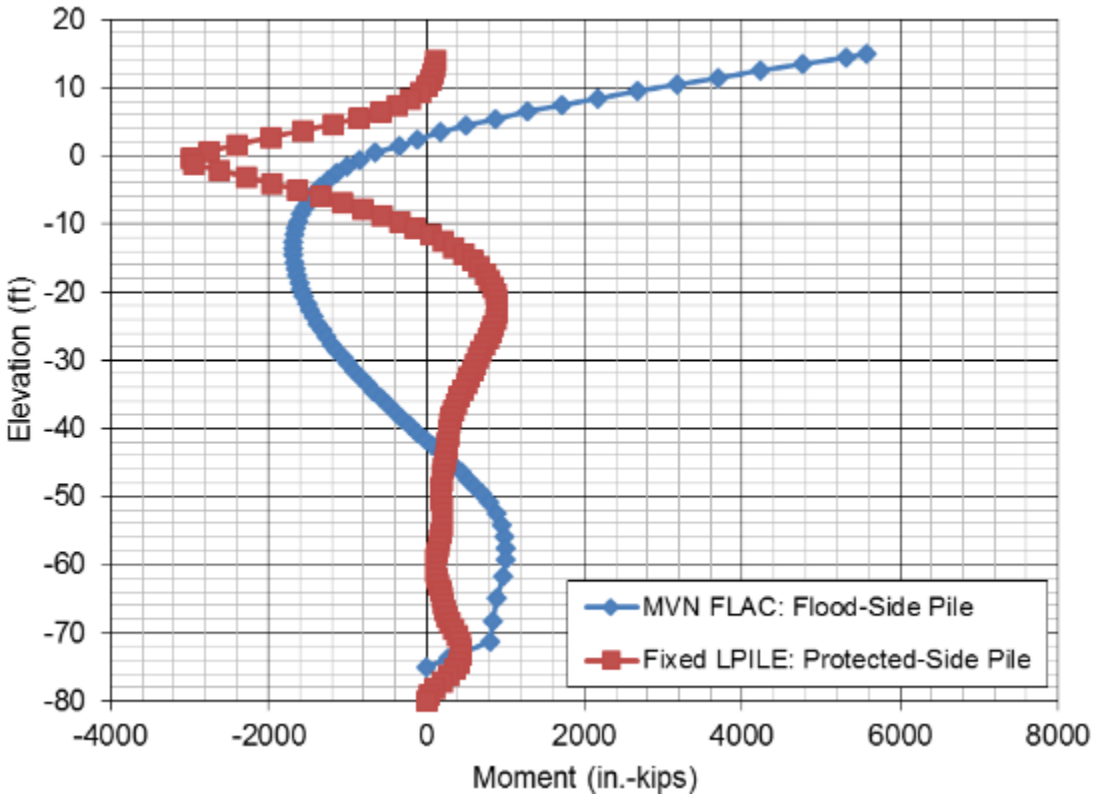

Figure 6.3 15' Fixed LPILE Vs. USACE LE

A superior way to calculate the maximum bending moment for the fixed case using the USACE LE Method may be to calculate the bending moment for the pinned case and multiply that number by a value of 2.5 to 3.0. This would result in a bending

moment higher than the results shown in the centrifuge test but should be a conservative way of calculating the bending moment. This would not give any information beyond the maximum bending moment though the maximum bending moment from the pinned case could be used to approximate the secondary fixed peak.

CHAPTER VII

CONCLUSION & RECOMMENDATIONS

7.1 Conclusions

Both the MVN and Virginia Tech modeling approaches predict bending moments that are in reasonable agreement with the measured values from the centrifuge test, and this provides validation for the modeling approaches. Therefore, these approaches can be used for parametric studies. Pile fixity makes an enormous difference in the computed bending moment and its location. This can have huge implications for any design. Designers should assume a fixed connection for any design that has settlement induced bending moments. Changes in the batter pile angle can be reasonably approximated as having a linear change in the bending moment. Stiffer piles will produce higher bending moments but this is easily offset by the increase in capacity. The current USACE LE Method produces maximum bending moments that are in reasonable agreement with the computed bending moments in the FLAC model as long as the limitations in the USACE LE Method are heeded. Making changes to the USACE LE Method without proper validation can result in either extremely conservative answers or very unconservative answers.

7.2 Recommendations for Further Research

Further research is needed, and is underway with Virginia Tech and USACE, for different wall and levee geometries, pile spacing, additional rows of piles, and asymmetrical loading. Additional case histories should be obtained or created to show bending moments in real world situations. Updates and expansions to the USACE LE Method should be performed to eliminate many of its limitations especially pile fixity.

REFERENCES

Almeida, M. S. S., & Parry, R. H. G. (1984). Penetrometer apparatus for use in centrifuge during flight. *Proceedings of Symposium on Application of Centrifuge Modelling to Geotechnical Design*, Manchester, pp. 47-66.

Broms, B., and Fredericksson, A. (1976). "Failure of pile-supported structures caused by settlements." Proceedings of the 6th European Conference on Soil Mechanics and Foundation Engineering, 383-386.

Dong, W, Schwanz, N (Not Dated). "Finite Element Soil-Pile-Interaction Analysis of Floodwall in Soft Clay". http://www.gerwick.com/topmenu/aboutgerwick/technicalpapers/Pages/technicalpapers.aspx 2014

Duncan, J. M. and Bursey, A. (2007), "Soil and Rock Modulus Correlations for Geotechnical Engineering." Center for Geotechnical Practice and Research, Virginia Tech, Blacksburg, VA, p. 88.

Fellenius, B.H. (2014), Basics of Foundation Design. Electronic Edition, www.Fellenius.net, 410 p.

FHWA (1993). Report No. FHWA-SA-91-048

Garnier, J. & Gaudin, C. (2007). ISSMGE TC2 Scaling Laws Catalogue. Retrieved from http://www.tc104.group.shef.ac.uk/

Hance, J., and Stremlau, T. (2009). "Lateral load on piles subjected to downdrag." Internal document, Eustis Engineering, Metairie, Louisiana.

Isenhower, W., Vasquez, L., and Wang, S. (2014). "Analysis of Settlement-Induced Bending Moments in Battered Piles." *From Soil Behavior Fundamentals to Innovations in Geotechnical Engineering*: 497-511.

Itasca (2011), *FLAC Fast Lagrangian Analysis of Continua*. Minneapolis, Minnesota: Itasca Consulting Group.

Kohno, T., Tanaka, H., Shirato, M., Nakatani, S. (2010). "Evaluation of Bending Load in Batter Piles Set in Soft Clay." 26th US - Japan Bridge Engineering Workshop. New Orleans, LA.

Lymon C. Reese & Associates (2011). “Evaluation of Bending in Batter Piles due to Settlement.” *Report prepared for FFEB Joint Venture, LLC.* Lymon C. Reese & Associates, Austin, TX.

Matlock, H. (1970), “Correlation for design of laterally loaded piles in soft clays.” *Proc. 2nd OTC Conference*, Houston, TX, Vol. 1: 557-559.

McGuire, M., Filz, G., Navin, M., Hokens, K., (2012). LPILE Method For Evaluating Bending Moments In Batter Piles Due To Ground Settlement For Pile-Supported Floodwalls In New Orleans And Vicinity. US Army Corps of Engineers.

Randolph, M. F., & Houlsby, G. T. (1984). The limiting pressure on a circular pile loaded laterally in cohesive soil. *Geotechnique*, *34*(4), 613-623.

Randolph, M. F., & Andersen, K. H. (2006). Numerical analysis of T-bar penetration in soft clay. *International Journal of Geomechanics*, *6*(6), 411-420.

Reeb, A. B., Filz, G. M., and Volk, J. C. (2014). “Numerical modeling of a pile-supported T-wall structure for hurricane protection.” *Proc., 8th European Conf. on Numerical Methods in Geotech. Engrg.*, CRC Press/Balkema, Leiden, The Netherlands, Vol. 2: 927-932.

Reese, L. C., Cox, W. R. and Koop, F. D. (1974), “Analysis of laterally loaded piles in sand.” *Proc. of the Annual Offshore Technology Conference*, Houston, TX, Vol. 2: 473-483.

Rao, S. N., Murthy, T. V. B. S. S., and Veeresh, C. (1994). "Induced bending moments in batter piles in settling soils." *Soils and Foundations*, 34(1), 127-133.

Rollins, K., Stenlund, T. (2010). “Laterally Loaded Pile Cap Connections”. Utah Department of Transportation Research Division

Sato, S., Akai, K., Funahashi, T. (1970). "Study on methods to calculate negative skin friction and bending in a batter pile." Laboratory Report of Japan Road Corporation, pp. 31-49 (*in Japanese*).

Sato, S., Iwashita, F., and Ohmori, H. (1987). "The calculation method on the bending moment of a batter pile induced by ground settlement." *Soils and Foundations*, 27(2), 75-84 *(in Japanese)*.

Sawaguchi, M. (1989). "Prediction of bending moment of a batter pile in subsiding ground." *Soils and Foundations*, 29(4), 120-126.

Shibata, T., Sekiguchi, H., and Yukitomo, H. (1982). "Model test and analysis of negative friction acting on piles." *Soils and Foundations*, 22(2), 29-39.

Stremlau, T., and Hance, J. (2009). "Lateral loads on piles." Internal document, Eustis Engineering, Metairie, Louisiana.

Stewart, D. P., & Randolph, M. F. (1991). A new site investigation tool for the centrifuge. *Centrifuge 91 (eds. Ko and McLean),* Balkema, Rotterdam, pp. 531-538.

Takahashi, K. (1985). "Bending of a batter pile due to ground settlement." *Soils and Foundations*, 25(4), 75-91.

Taylor, R. N. (1994). *Geotechnical Centrifuge Technology*. CRC, London.

Templeton, A. E. (2009). "Settlement and settlement induced stress." Burns Cooley Dennis, Inc., Ridgeland, Mississippi, pp. 49.

Tessari, A. (2007). *Measuring primary and secondary wave velocities on a geotechnical centrifuge using bender elements*. Master's Thesis, Rensselaer Polytechnic Institute, Troy, NY.

Tessari, A., Sasanakul, I., & Abdoun, T. (2010). Advanced sensing in geotechnical centrifuge models. *Proceedings of the International Conference on Physical Modeling in Geotechnics*. Zurich, Switzerland, pp. 395-400.

Tessari, A. (2012), *Centrifuge Modeling of the Effects of Natural Hazards on Pile-Founded Concrete Floodwalls.* PhD Dissertation, Rensselaer Polytechnic Institute, Troy, NY.

Varuso, R. (2010). "Influence of Unstable Soil Movement on Pile-Founded Concrete Floodwalls and a Resulting Design Methodology." Ph.D. thesis, Louisiana State University, Baton Rouge, LA.

White, D. W. D., Gaudin, C. G. C., Boylan, N. B. N., & Zhou, H. Z. H. (2010). Interpretation of T-bar penetrometer tests at shallow embedment and in very soft soils. *Canadian Geotechnical Journal*, *47*(2), 218-229.

Won, J., Adhikari, S., Song, C., Cheng, A., and Al-Ostaz, A. (2011). "Evaluation of a T-Wall Section in New Orleans Considering 3D Soil-Structure Interaction." J. Geotech. Geoenviron. Eng., 137(8), 731–742.

APPENDIX A

RUN 2 CENTRIFUGE DATA

Data for the run 2 centrifuge was received from Rensselaer Polytechnic Institute (RPI) in two separate files and is included as a single supplemental file.

The filename of the supplemental file is Centrifuge_Data_Run_2.pdf.

The supplemental file is a PDF and can be viewed using any standard PDF software.

The data was received on 8/22/2013 and 9/5/2013.